LINKING LARGE SCALE MONITORING AND SPATIALLY EXPLICIT CAPTURE–RECAPTURE MODELS TO IDENTIFY FACTORS SHAPING LARGE CARNIVORE DENSITIES: CASE STUDY OF THE AMERICAN BLACK BEAR IN ONTARIO, CANADA

A Thesis Submitted to the Committee of Graduate Studies in Partial Fulfillment of the Requirements for the Degree of Master of Science in the Faculty of Arts and Science

TRENT UNIVERSITY

Peterborough, Ontario, Canada

Environmental and Life Science M.Sc. Graduate Program

January 2023

ABSTRACT

Linking large scale monitoring and spatially explicit capture–recapture models to identify factors shaping large carnivore densities: case study of the American black bear in Ontario, Canada

Brynn Andrea McLellan

Understanding the spatial ecology of large carnivores in increasingly complex, multi-use landscapes is critical for effective conservation and management. Complementary to this need are robust monitoring and statistical techniques to understand the effect of bottom-up and top-down processes on wildlife population densities. However, for wide-ranging species, such knowledge is often hindered by difficulties in conducting studies over large spatial extents to fully capture the range of processes influencing populations. This thesis addresses research gaps in the above themes in the context of the American black bear (*Ursus americanus*) in the multi-use landscape of Ontario, Canada.

First, I assess the performance of a widely adopted statistical modelling technique – spatially explicit capture-recapture (SECR) – for estimating densities of large carnivores (Chapter 2). Using simulations, I demonstrate that while SECR models are generally robust to unmodeled spatial and sex-based variation in populations, ignoring high levels of this variation can lead to bias with consequences for management and conservation.

In Chapter 3, I investigate fine-scale drivers of black bear population density within study areas and forest regions by applying SECR models to a large-scale, multi-year black bear spatial capture-recapture dataset. To identify more generalizable patterns, in Chapter 4 I then assess patterns of black bear density across the province and within forest regions as a function of coarse landscape-level factors using the same datasets and assess the trade-offs between three

different modeling techniques. Environmental variables were important drivers of black bear density across the province, while anthropogenic variables were more important in structuring finer-scale space use within study areas. Within forest regions these variables acted as both bottom-up and top-down processes that were consistent with ecological influences on black bear foods and intensity of human influences on the species' avoidance of developed habitats.

Collectively, this thesis highlights the opportunities and challenges of working across multiple scales and over expansive landscapes within a SECR framework. Specifically, the multi-scale approach of this thesis allows for robust inference of the mechanisms structuring fine and broad scale patterns in black bear densities and offers insight to the relative influence of top-down and bottom-up forces in driving these patterns. Taken together, this thesis provides an approach for monitoring large carnivore population dynamics that can be leveraged for the species conservation and management in increasingly human-modified landscapes.

Keywords: animal abundance, black bear, capture-recapture, carnivore, density estimation, landscape heterogeneity, spatially explicit capture–recapture, statistical ecology, wildlife management

Preface

This thesis is based on data collected from the Ministry of Natural Resources and Forestry (MNRF) long-term black bear monitoring program. Research staff from the Wildlife Research and Monitoring Section designed and established sampling arrays for trap locations and field sampling was conducted by MNRF staff across 26 districts. Genetic analyses were performed by the MNRF DNA lab personnel. Access to these datasets were provided by my supervisor, Joe Northrup (MNRF, Trent University), and Eric Howe (MNRF).

The data chapters presented in the body of this thesis (Chapters 2 - 4) are formatted as manuscripts for submission to peer-reviewed journals. Conceptualization of research questions and analytical approaches was developed with Joe Northrup and Eric Howe, with input from my committee members Justina Ray (Wildlife Conservation Society Canada, adjunct professor Trent University) and Adam Ford (University of British Columbia). Because of the collaborative nature of the study, I use the term 'we' in the data chapters. However, I was responsible for all major areas of data analysis and wrote original drafts of all data chapters with guidance and input from co-authors, as identified below. The introduction and general discussion of this thesis (Chapters 1 and 5) are my original work, with suggestions and edits from Joe Northrup.

Chapter 2

Authors: Brynn McLellan (BM), Eric Howe (EH), Joe Northrup (JN), Robby Marrotte (RM).

BM, EH and JN conceptualized research ideas and designed the methodology. BM conducted data analysis and wrote the original manuscript, with JN, EH and RM providing guidance with analysis and interpreting results. All authors and JR provided manuscript suggestions and edits.

Chapter 3

Authors: Brynn McLellan (BM), Eric Howe (EH), Joe Northrup (JN)

All authors conceptualized research ideas and designed the methodology. BM conducted data analysis and wrote the original manuscript, with JN and EH providing guidance with analysis and interpreting results and manuscript edits.

Chapter 4

Authors: Brynn McLellan (BM), Eric Howe (EH), Joe Northrup (JN)

All authors conceptualized research ideas and designed the methodology. BM conducted data analysis and wrote the original manuscript, with JN and EH providing guidance with analysis and interpreting results and JN providing manuscript edits.

Acknowledgments

Foremost, I want to acknowledge my supervisor, Joe Northrup, for this incredible opportunity, for fostering my interest in quantitative ecology, and for providing me with the support and encouragement to grow as a student and researcher. Thank you for always being available at a moment's notice despite your chaotic schedule and for your enduring patience and flexibility as I navigated the academic world and field seasons during the pandemic. I also extend my appreciation to my committee members, Adam Ford and Justina Ray, for your thoughtful input and guidance throughout this project.

This thesis uses data collected as part of the much larger Ministry of Natural Resources and Forestry (MNRF) long-term black bear monitoring program, of which I am most grateful for those who laid the foundation of this project. In particular, Eric Howe, thank you for your invaluable assistance working with these datasets and SECR models, graciously sharing code, and patiently helping me troubleshoot models. To the Northrup Lab, I have been fortunate to have been inspired by such an exceptional cohort. Special thanks to Robby Marrotte, I would still be waiting for my models to run without your help getting serial farms running on Compute Canada, and to the black bear team (Derek Potter, Eric, Joe, Noah Wightman, Robby, Shilah LeFeuvre) for the weekly meetings that shaped many ideas presented in this thesis.

A special thanks to Garth Mowat and the 2021 South Grizzly Bear Project field team (Jonathan Van Elslander, Stew Clow, Laura Smit, and Taylor Wilson) for adopting me for the field season. From sharing your wealth of grizzly bear knowledge and the opportunity to capture my first grizzly; it was such a privilege, and a dream come true, to spend a summer at the flathead cabin. Many thanks to Grant MacHutchon for your hospitality in Nelson and for trusting my backcountry driving skills when I did not.

This project would not be possible without the countless personnel at the MNRF and the DNA lab who conducted field work and genetic analysis. Funding was provided by the Natural Sciences & Engineering Research Council of Canada – Master's and the Queen Elizabeth II Graduate Scholarship in Science and Technology.

Finally, many thanks to those that started and supported me throughout this process. Kristen Walker, who was instrumental in starting me down this path and encouraged me to take a risk out of my undergraduate. To my parents, for the opportunity to grow up in the Rocky Mountains, instilling a lifetime of passion for the outdoors, and your unwavering support and encouragement to pursue my interests. Jessy Lee, for helping me through the sticky spots, celebrating the little things, and everything in between. And lastly, Kathryn, for being there every step of the way.

Table of Contents

List of Tables

List of Figures

Chapter 1: General introduction

1.1 Challenges of contemporary carnivore management and conservation

Humans have become one of the primary drivers of changes in ecological systems, with far-reaching impacts to global biodiversity, ecosystem functioning and human well-being (Ripple et al. 2014, Newbold et al. 2015). The rapidly expanding human footprint, coupled with changing environmental conditions driven by climate change, pose ongoing threats to all species, but large terrestrial mammalian carnivores face particular challenges (hereafter, carnivores; Ripple et al. 2014, Tilman et al. 2017, Su et al. 2018, Ashrafzadeh et al. 2022). Carnivores are vulnerable to the cumulative effects of these stressors because these species tend to have low densities, slow reproductive rates and wide-range behaviors that often brings them into conflict with people (Cardillo et al. 2004). As a result, many carnivores have experienced historical range contractions and population declines associated with habitat loss and degradation, persecution, utilization, and depletion of prey (Ceballos and Ehrlich 2002, Laliberte and Ripple 2004). Consequently, understanding how humans and carnivores can coexist in shared landscapes has become an increasing focus of research and goal of many carnivore management and conservation programs (Lozano et al. 2019, Treves and Karanth 2003).

Challenges of carnivore conservation and management arise in part due to polarizing societal perspectives towards these species. Carnivores are often revered for their economic, cultural, and aesthetic value, yet can be simultaneously feared due to the threats they can pose to human safety and livelihoods (Ripple et al. 2014). Moreover, these species exert widespread influences on the structure and functioning of terrestrial ecosystem (Beschta and Ripple 2009) and can be viewed as umbrella species due to their large space requirements. Thus, due to their importance in conserving biodiversity as well as being charismatic animals, many carnivores have become a

symbol for wildlife conservation (Karanth and Chellam 2009). To that end, the persistence of carnivore populations in human-modified landscapes remains one of the most pressing and challenging issues facing contemporary ecologists, wildlife managers, and policy makers (Lute et al. 2018, Lamb et al. 2020).

This thesis is guided by two research areas in ecology that are central to addressing challenges of conserving and managing carnivores. The first is the use of increasingly sophisticated analytical methods for estimating wildlife population abundance and distribution, and the second is the application of these methods to understand how wildlife populations respond to human modification of landscapes and changing environmental conditions. I address these overarching themes within the context of a large bodied terrestrial mammal, the American black bear (*Ursus americanus*), in the multi-use landscape of Ontario, Canada. In this first chapter, I provide an overview of these themes as they relate to the study context and present the objectives and hypotheses that frame my research. Then I introduce the three data chapters that comprise the body of this thesis, followed by a description of the general modeling approach used in all data chapters.

1.2 Pattern and scale in the study of population ecology

Quantifying spatial variation in population density forms one of the foundations of ecology (Brown 1984, Lamb et al. 2019). Identifying how many individuals of a species occur within an area is fundamental to understanding species-habitat relationships (Fretwell and Lucas 1969), population dynamics (Turchin 2001) and patterns of dispersal (Travis and Murrell 1999) among numerous other processes. As a result, while quantifying population density provides valuable insight into ecological processes and patterns it also structures the primary evidence required for

many large-scale carnivore management and conservation programs (Royle et al. 2004, Burton et al. 2015, Tourani 2021, Jones 2011).

The distribution and abundance of species are largely influenced by species habitat requirements and tolerances (Brown 1984). Subsequently, landscape ecology frames spatial heterogeneity as a key factor shaping variation in ecological processes (e.g., movement, habitat use and selection, vital rates) that gives rise to spatial patterns in population density (Turner 1989, Turner 2005, Scheiner and Willig 2008). In turn, wherever heterogeneity exists, it necessitates the consideration of the theme of spatial scale (hereafter, scale), because how we understand heterogeneity is fundamentally dependent on the scale at which it is measured (Wiens 1989). Levin's seminal paper "The problem of pattern and scale in ecology" (1992) provided a launching point of ecological thinking on the concept of scale. When considering scale, extent is the size of the study area, grain is the area surrounding a point over which a process is measured, and resolution is the minimum mapping unit of data that reflects how finely a covariate is measured. Compared to resolution which is typically restricted to the minimum pixel size in the available data, grain is up to the analyst and can be calculated across continuous space as a buffer or radius around a sample point based on the biology of the study species or data-driven through model selection methods (Wiens 1989, Wheatley and Johnson 2009, Northrup et al. 2021).

Despite the wide-spread recognition that the scale of an analysis has profound implications on the understanding of ecological processes, there remains considerable ambiguity on its application (Hobbs 2003). Ecological processes may operate across multiple scales, and therefore what may appear to be important at one scale may not be at another (Turner 1989). Thus, it is increasingly recognized that all ecological studies are scale-sensitive and decisions made to address management and conservation challenges must consider the scale at which data

are collected and synthesized (Turner 1989, Ciarniello et al. 2007, Toews et al. 2017). The issue of scale is particularly important when interpreting single estimates of population density; both spatial and temporal scales interact such that current and past habitat conditions and human relationships with carnivores shape carnivore abundance and distribution (Boulanger et al. 2018). Consequently, identifying the most appropriate scale at which to conduct ecological research and how to best translate information across scales remains an ongoing challenge (Schneider 2001, Wu 2004). To this end, spatial heterogeneity and scale are interrelated concepts that are perceived as both challenging and unifying concepts in ecology (Levin 1992, Toews et al. 2017).

Management of carnivores and their habitats occurs across a variety of scales and often over large landscapes. For example, designation of protected areas for wide-ranging carnivores often occurs at broader extents whereas matters related to human access or sport harvest can occur more locally. Consequently, understanding ecological processes requires a multi-scale characterization of spatial patterns across large landscapes (Wiens 1989, Wu et al. 2000, Towes et al. 2017). However, despite the theoretical and applied importance, understanding how different factors shape ecological patterns remains poorly understood, in part because studying interactions among multiple drivers and scales remains challenging (Turner 2005). This is particularly true for carnivore research as the species are notoriously difficult to monitor due to their low and variable densities and detectability, paired with wide-ranging movements and home-ranges that cover large landscapes (MacKenzie et al. 2005).

1.3 Bottom-up and top-down influences on carnivores

How animals distribute themselves across their range – that is, second-order selection (Johnson 1980) – is assumed to relate to the ecological requirements of a species and the spatial scale at which important factors regulating and limiting populations occur (Brown 1984,

Duquette et al. 2017). Despite being some of the most widely studied species, there remains considerable challenges in measuring and identifying the key factors influencing carnivore population densities. One school of thought holds animal population limitation by top-down mortality to be the most important process determining population abundance, whereas others consider regulation via bottom-up food resources as the primary process (Hunter and Price 1992). While often treated as mutually exclusive, bottom-up and top-down factors are most likely to operate simultaneously, with the relative strength of their effects varying across landscapes and scales (Hunter and Price 1992, Nielsen et al. 2017). Moreover, as humans continue to transform natural landscapes on a global scale, modification of habitat can increase or decrease important food resources while concurrently exposing populations to a mosaic of human mortality risks such as roads, hunting, and human-wildlife conflict (Treves and Karanth 2003, Laufenberg et al. 2018). To that end, understanding the relationship between bottom-up and top-down factors and large carnivore density across scales and over large landscapes is critical for predicting ecological outcomes and informing conservation and management (Schoen 1990).

1.4 Estimating carnivore population size and distribution: classic and contemporary techniques

The ability to estimate carnivore abundance and distribution has improved with the advent and application of non-invasive sampling methods. In particular, non-invasive genetic sampling and camera traps, coupled with advances in ecological statistical techniques, have markedly improved our ability to study and monitor elusive species (Lewis et al. 2018). For decades, capture-recapture (CR) methods represented one of the most common approaches to estimate animal population size and formed the foundation of ecological statistics as applied to population

ecology (Royle et al. 2014). However, a major limitation of classical CR methods is they are inherently non-spatial, accounting for neither the spatial structure nor the ecological processes that give rise to the distribution of animal detections or the spatial nature of the sampling (Royle et al. 2013, Royle et al. 2018). It was not until spatially explicit capture-recapture (herein referred to as SECR; Efford 2004, Royle et al. 2014) methods were developed that many of these issues were resolved. By making ecological processes – including density, movement, and space use of individuals – explicit in the model, SECR unifies fundamental concepts of population and landscape ecology and provides a means of modeling wildlife distribution in space, as well as investigating the drivers of this distribution, with direct implications for conservation and management (Royle et al. 2014). However, while SECR models and non-invasive sampling methods represent an unparalleled opportunity to quantify population patterns in a widespread manner, there still remains limited SECR studies conducted across broad landscapes (> 10 000 km^2; Tourani 2021), which introduces substantial challenges to applying SECR methods.

1.5 Focal species: black bears in Ontario, Canada

The American black bear in North America typifies the challenges facing carnivore management and coexistence. Black bears influence ecosystem dynamics (Enders et al. 2012, Levi et al. 2020), are integrated into the culture of many Indigenous peoples (Hallowell 1926) and provide economic benefits through ecotourism and harvest (Poulin et al. 2003). Further, although black bears may be characterized as a charismatic species that represents a symbol of wilderness, they are also often persecuted due to their tendency to damage property and come into conflict with humans and livestock (Poulin et al. 2003, Hagani et al. 2021). Moreover, as a popular game animal, black bears are subject to highly publicized and politically charged debates

surrounding hunting regulations (Poulin et al. 2003). Lastly, as with many large carnivores, black bears range widely and are elusive, making population estimation and monitoring challenging.

Black bears are found throughout most of Ontario Canada, although densities are lower in the northern boreal (Herrero 1972, Poulin et al. 2003). They are characterized by low-densities, wide-ranging behaviours, and slow reproductive rates that make them vulnerable to the cumulative effects of human persecution and changing habitats conditions (Kolenosky 1990, Obbard and Howe 2008). Thus, the species' population dynamics are largely driven by inter-related bottom-up and top-down factors. As with many large mammals, humans can be the predominate top-down pressure influencing black bear survival, directly through hunting or vehicle collisions or indirectly through human-wildlife conflict (Hebblewhite et al. 2003, Gantchoff et al. 2020). In Ontario, black bears are subject to substantial harvest and regularly come into conflict with people (Kolenosky 1986, Obbard et al. 2014, Obbard et al. 2017; Northrup et al. *in press*). Further, as a species that depends on accumulated fat stores during winter hibernation and for reproduction, their demographic rates are subject to bottom-up processes including the availability, quality, and diversity of food sources (Kolenosky 1990, McLaughlin et al. 1994, Costello et al. 2003). Main food sources for Ontario black bears include vegetation and hard and soft mast, primarily found in uneven-aged mixed coniferous and deciduous forests (Romain et al. 2013).

Bottom-up and top-down process are tightly linked, with human interference and alteration of habitats (i.e., land-use conversion, habitat loss and fragmentation) being a primary factor influencing bear behaviour and space usage directly and indirectly. For instance, timber harvest or wildfires can improve bear habitat by creating open early successional forests that act as important foraging grounds or can degrade and render habitat unavailable to bears (Brodeur et al.

2008, Romain et al. 2013). Further, forestry often creates extensive road networks that can provide high quality vegetation for bears (Mosnier et al. 2008); however, such benefits can be offset by increased human activity associated with roads and subsequently higher rates of bear mortality (McLellan 1989, Proctor et al. 2019). Moreover, human settlements and agriculture can provide areas of supplemental food, paradoxically attracting bears to areas of higher mortality risks that may results in population sinks (McLaughlin et al. 1994, Baruch-Mordo et al. 2014, Laufenberg et al. 2018, Penteriani et al. 2019).

Ontario black bears are managed as a game species by the Ministry of Natural Resources and Forestry (MNRF). Management of black bear populations and their habitat involves different spatial scales due to the species' expansive geographical range coupled with wide-ranging individual movements (Schoen 1990). Population management occurs at the Wildlife Management Unit (WMU) level (Newton and Obbard 2018) where non-invasive genetic spatial capture-recapture surveys have been used to estimate abundance and density in most huntable WMUs since 2004 (Figure 1.1; Obbard et al. 2010, Howe et al. 2013, Newton and Obbard 2018). Curvilinear arrays of approximately 40 baited barbed-wire hair corrals (Woods et al. 1999) have been used to sample black bears in the spring and early summer. From 2017 to 2019, a total of 78 study areas were sampled with different areas sampled each year. These population surveys are ongoing, with estimates contributing to district management decisions (Newton and Obbard 2018). Comparatively, habitat management occurs indirectly through application of forest management guidelines at the landscape and stand or site levels for the provision of a variety of wildlife species (OMNRF 2009).

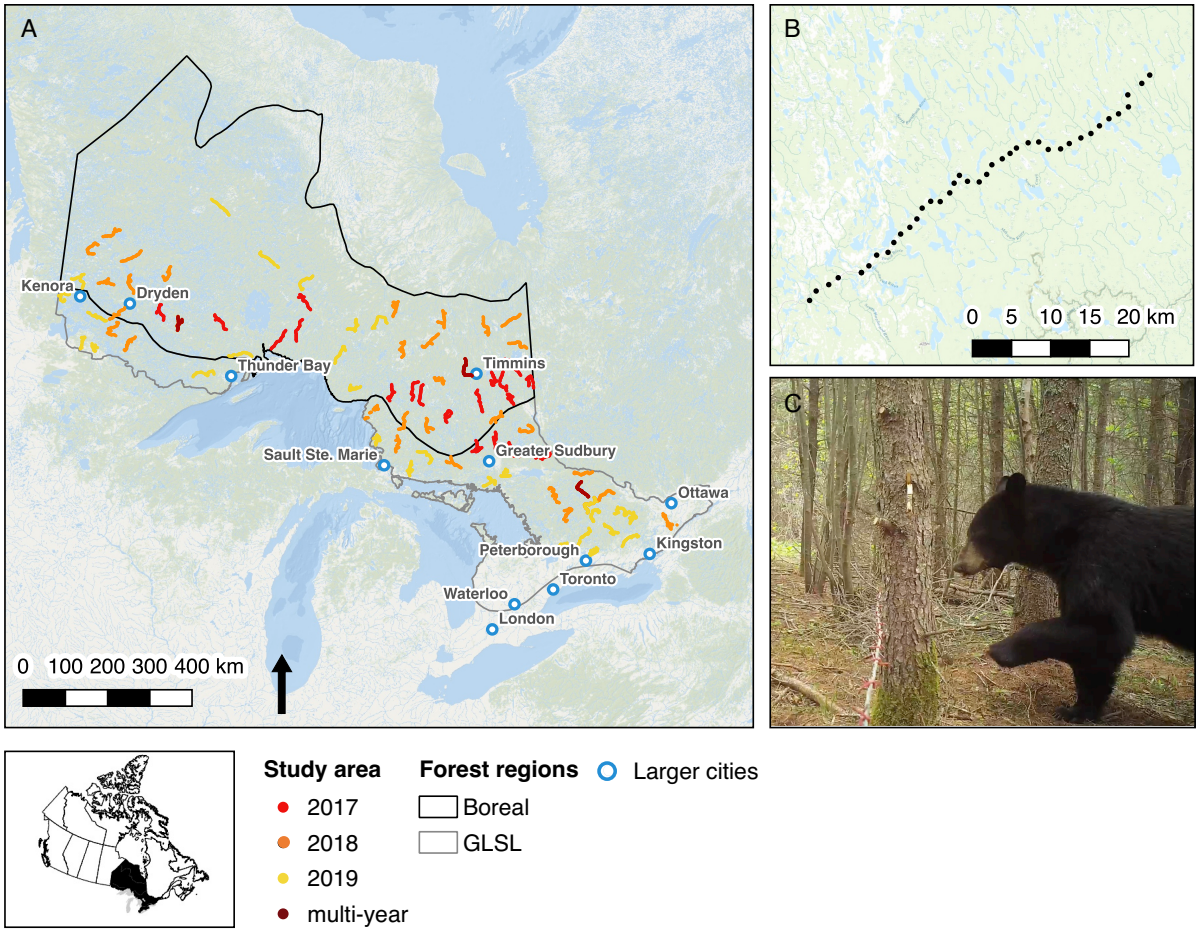

Figure 1.1. Location of traplines of baited barbed wire hair corrals across the Great Lakes – St Lawrence (GLSL) and boreal forest regions (Rowe 1972) in Ontario, Canada where black bear hair samples were collected between 2017 - 2019. At the scale in Figure A, traplines appear as thin lines. Black points in Figure B represent baited barbed wire corrals. Figure C shows a black bear at a corral.

1.6 Research objectives, hypotheses and predictions, and thesis structure

The MNRF surveys constitute one of the largest datasets available for understanding the factors influencing carnivore density and have been collected across an expansive, continuous geographical area over several years. The climatic and land-use patterns in Ontario – with higher habitat fragmentation and human densities in the South compared to the North and gradient in productivity increasing from the West to the East – reflect general trends in black bear habitat observed across the continent. As such, the Ontario black bear population and MNRF surveys represent an ideal study system to produce an integrated picture of the underlying forces shaping variation in carnivore densities across spatial extents previously unattainable.

In this thesis I leverage the MNRF surveys and SECR models to address two research objectives:

1. Evaluate the ability of SECR modeling methods to provide robust and unbiased density estimates for large scale surveys of carnivores
2. Identify key bottom-up and top-down factors, and the relative influence of these factors, driving spatial variation in black bear densities across Ontario

A multiple competing hypothesis framework is used to address the second objective. Specific hypotheses and predictions for the second objective are outlined in Table 1.1 and Figure 1.2.

1.6.1 Thesis structure

The core of this thesis consists of three data chapters (Chapters 2 to 4) presented as a collection of manuscripts formatted for submission to a peer-reviewed journal, followed by general conclusions and discussion (Chapter 5). All chapters (Chapters 1 - 5) have a joint list of references and appendices, found at the end of the thesis.

Chapter 2 addresses the first research objective by using simulations to assess the consequences of unmodeled heterogeneity on the performance of SECR models and model selection via information theoretic criteria. Insight from these simulations inform the modeling structure in the following data chapters. Chapters 3 and 4 address the second research objective, where the former assesses factors shaping density at a finer extent and the latter at a broader extent. In Chapter 3, I seek to understand how environmental and anthropogenic factors influence local variation in black bear distribution. I apply SECR models to the MNRF survey datasets to assess the influence of fine-grained spatial covariates representing natural productivity and human disturbances on black bear distribution within each study area and across two forest regions. Then, in Chapter 4 I take a broader-scale approach and examine the influence of coarse-grained landscape level factors representing bottom-up and top-down factors on black bear density across the province and forest regions, as well as assess the trade-offs between three different modeling techniques. Chapter 5 consists of general conclusions where results are synthesized and contextualized within the broader field of literature, research strengths and limitations are highlighted, and applications to management are suggested.

1.7 Spatially explicit capture–recapture (SECR) model framework

Throughout this thesis, the broader modeling framework that I employ is spatially explicit capture-recapture (SECR; Royle et al. 2014). While I briefly outline the general modeling approach in the following section to provide context for this thesis, there are numerous extensions and modifications that I detail, where applied, in the following chapters.

This model is a hierarchical model that uses spatial-detection histories of animals to account for spatial variation in probability of detection across a landscape. The model is composed of two sub-models, a detection model and state model. The detection model describes

the probability of detecting an animal at each detector as a function of distance from the centroid of the space that an animal occupies during the period in which detectors are active, known as an animal's activity center. Animals have highest probability of detection at their activity center, with declining probability as the distance from the activity center increases. The state model then estimates the distribution of activity centers with a region of interest which can be used to estimate of density.

Within a sampling occasion, baited barbed-wire hair corrals (hereafter, detectors) can detect multiple bears but cannot distinguish between multiple visits of the same individual; such detectors are referred to as 'proximity detectors' in SECR. If individual i is detected at detector j at least once during sampling occasion k, then the detection history for that individual is $y_{ijk} = 1$ and if the individual is not detected $y_{ijk} = 0$. For the basic SECR model, the encounter frequencies y_{ijk} follows a Bernoulli distribution such that

$$y_{ijk} \sim \text{Bernoulli}(p_{ijk}).$$

The probability of detecting individual i at detector j is p_{ijk} and is modeled using an encounter model proportional to the Gaussian probability density function, or half-normal detection function, such that

$$p_{ijk} = p_0 e^{-\alpha_1 d_{ij}} ,$$

For a Gaussian model $\alpha_1 = (1/2\sigma^2)$ and p_0 is the baseline detection probability at distance zero. The spatial parameter σ describes the rate at which detection probability declines as a function of Euclidean distance $d_{ij} = d(x_j, s_j)^2$ between and individuals activity center s_i and the detector location x_j. As follows, σ can be interpreted as a detection range which is proportional to an animal's space use when activity centers are static, home ranges are symmetric and animals use space within home ranges independently (Dunpont et al. 2021, Royle et al. 2014). The parameter

p_0 can further be modeled as a function of individual, detector and time level covariates thought to influence encounter probability as follows:

$$\text{logit}(p_{0,ijk}) = \alpha_0 + \alpha_2 X_{ijk}.$$

where α_2 is the coefficient to estimate and X_{ijk} is some covariate that potentially varies by the individual i, detector j, or occasion k, for example, whether an individual has been captured at a trap previously.

Within the detection model, the detector locations x_j are known but the activity centers s_i are latent variables. Accordingly, the state model describes the distribution of unobserved locations of activity centers s_i within the state space $\mathcal{S}$. The state model can be formulated as a homogeneous Poisson point process where activity centers are distributed randomly across the area of the state space $\mathcal{S}$. An inhomogeneous point process can also be used in which the intensity parameter is modeled as a function of spatially referenced covariates (often habitat features) and a vector of regression coefficients β. In other words, using a Poisson log-linear regression framework,

$$N_c \sim \text{Poisson}(\phi_c)$$

$$\log(\phi_c) = \beta_0 + \sum_{v=1}^{v} \beta_v X_v$$

where N_c is the number of bear activity centers s_i in the landscape pixel c and ϕ_c is the expected number of activity centers in the pixel c given the covariate values at c. There are v number of covariates X_v with corresponding regression coefficients β_v , and β_0 is the intercept. This inhomogeneous Poisson point process allows variation in density with variation in spatial covariates. The final model can be fit using marginal likelihood (Borchers and Efford 2008) where the latent variables are removed from the likelihood by integration or Bayesian analysis by

Markov chain Monte Carlo (Royle and Young 2008) where the activity centers are directly estimated alongside other variables and unknown parameters.

Table 1.1. Multiple-hypothesis framework for comparing bottom-up and top-down factors shaping black bear density. Rows represent anthropogenic and environmental factors. Columns represent hypotheses about if a factor acts as a bottom-up (BU) and/or top-down (TD) process, the direction of effect (i.e., if a factor positively [+] or negatively [–] influences density), the mechanisms underlying each factor (HCM = human-caused mortality; D = human disturbance [human/livestock access and presence]; R = resource availability [food, habitat, shelter]), and black bear literature to support predictions. Figure 1 illustrates predictions in schematic diagram.

Category	Factor	Hypothesis	Prediction			References
			Mechanism	Description	Effect	
Anthropogenic	Harvest	TD	HCM; D	Source of mortality[2]; provides human access to bear habitat; contributes to displacement	– [1]	[1] Loosen et al. 2013 [2] Gantchoff et al. 2020
	Roads	TD	HCM; D	Cause of animal-vehicle collisions[5]; barrier to movement; provides human access to habitat contributing to landscape fragmentation and elevated human-bear interactions and mortality[4]	– [3]	[3] Humm et al. 2017 [4] McFadden-Hiller et al. 2016 [5] Hostetler et al. 2009
		BU	R	Roads can act as travel pathways; source of herbaceous food in areas adjacent to roads[6]	+ [3]	[3] Humm et al. 2017 [6] Poulin et al. 2003
	Human settlement	TD	HCM; D	Human presence associated with elevated human-bear conflicts and mortality[5]; creates forest edges that contributes to landscape fragmentation[9]	– [3, 7, 8]	[3] Humm et al. 2017 [7] Welfelt et al. 2019 [8] Laufenberg et al. 2018 [9] Evans et al. 2014 [5] Hostetler et al. 2009
		BU	R	Source of anthropogenic foods[12,10]	+[9, 11]	[10] van Manen et al. 2020 [11] Beckmann and Berger 2003 [12] Lewis et al. 2015 [9] Evans et al. 2014

Table 1.1 (continued).

Category	Factor	Hypothesis	Prediction			References
			Mechanism	Description	Effect	
Anthropogenic	Agriculture	TD	HCM; D	Source of human/livestock conflict; bears avoid agricultural areas frequented by humans[4, 13, 14]	–	[13] Jones and Pelton 2003 [14] Zeller et al. 2019 [4] McFadden-Hiller et al. 2016
		BU	R	Cultivated crops, apiaries and livestock can act as supplemental food source[6, 13, 14, 15]	+	[13] Jones & Pelton 2003 [14] Zeller et al. 2019 [6] Poulin et al. 2003 [15] Jonker et al. 1998
Productivity	NDVI	BU	R	Related to vegetation greenness and availability of mast-producing species[1, 16]	+	[16] Duquette et al. 2017 [1] Loosen et al. 2018
Forest type	Coniferous Deciduous Mixed	BU	R	Black bears select different forest types, often stands with greater abundance and diversity of mast producing species[17, 18]; greater productivity in deciduous GLSL forests than coniferous boreal forests in Ontario[†, 19]	– + +/–	[17] Carter et al. 2010 [18] Zeller et al. 2019 [19] Howe et al. 2013 [15] Potter and Obbard 2017
	Coniferous Deciduous Mixed	TD	D	Increased cover and escape terrain in coniferous forests compared to deciduous forests[20, 21]	+ – +/–	[20] Herrero 1972 [21] Howe et al. 2005

[†] Rowe's (1972) boreal and Great Lakes – St Lawrence (GLSL) forest regions

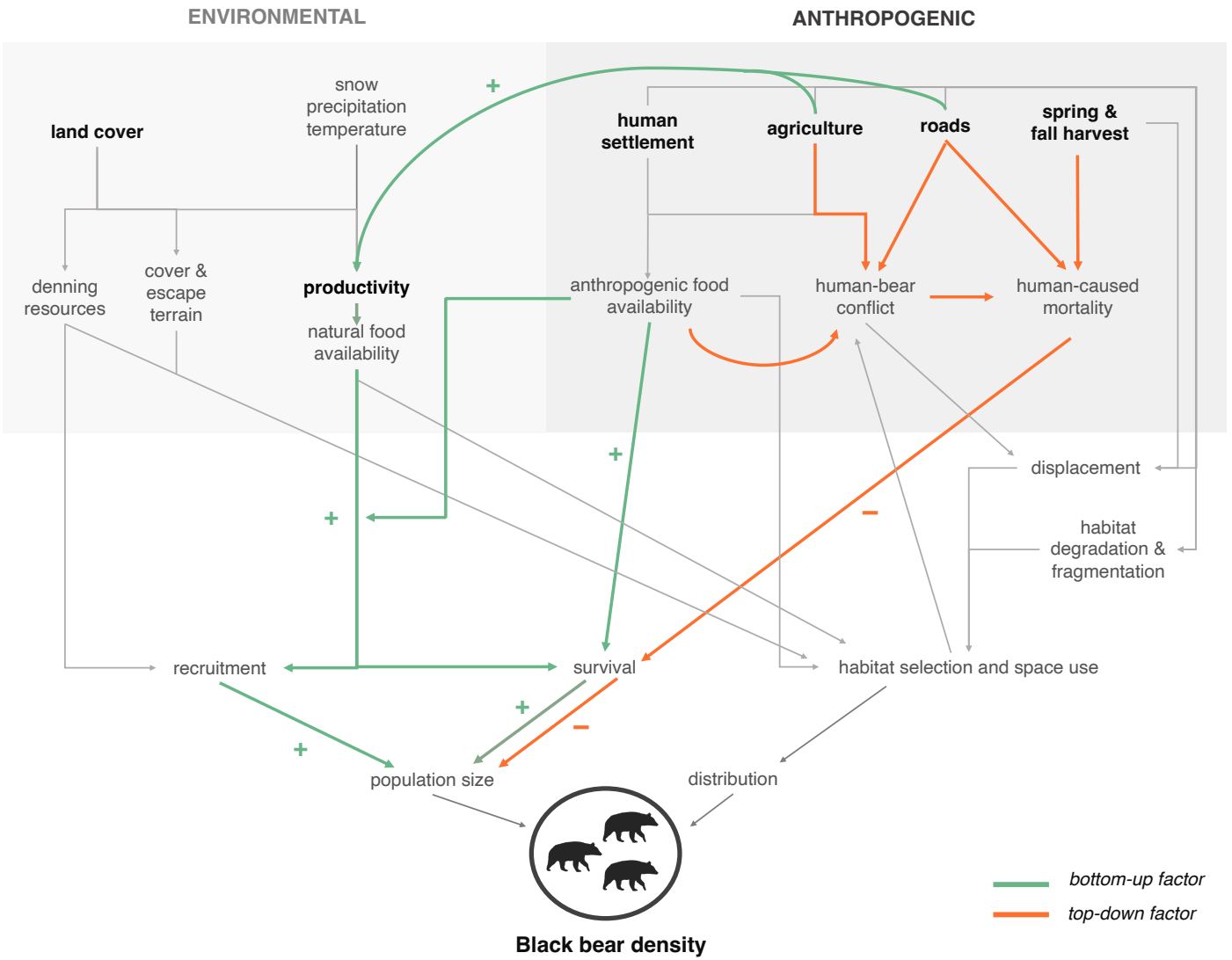

Figure 1.2 Schematic diagram of bottom-up (green lines) and top-down (orange lines) factors hypothesized to shape black bear density. Bold text denotes factors in Table 1.1.

Chapter 2: Accounting for heterogeneous density and detectability in spatially explicit capture-recapture studies of large carnivores

Brynn A. McLellan[1], Eric Howe[2], Robby R. Marrotte[1], Joseph M. Northrup[1,2]

[1]Environmental and Life Sciences Graduate Program, Trent University.

[2]Wildlife Research and Monitoring Section, Ontario Ministry of Natural Resources and Forestry

.

2.1 Abstract

Reliable estimates of population density are fundamental for managing and conserving wildlife. Spatially explicit capture-recapture (SECR) models in combination with information-theoretic model selection criteria are frequently used to estimate population density. Variation in density and detectability are inevitable and, when unmodeled, can lead to erroneous estimates. Despite this knowledge, the performance of SECR models and information-theoretic criteria remain relatively untested for populations with realistic levels of variation in density and detectability. We address this issue using simulations of American black bear (*Ursus americanus*) populations with variable density and detectability between sexes and in space. We first assess the reliability of Akaike Information Criterion adjusted for small sample sizes (AIC_c) to correctly identify the true data generating model or a good approximating model. We then assess the accuracy and precision of density estimates when such a model is selected or not selected. We demonstrate that unmodeled heterogeneity in detection and, more importantly, density, can lead to pronounced bias. However, when a good approximating model is included in the candidate set, AIC_c selects models that include important forms of variation and yield accurate estimates. We encourage researchers and practitioners to consider the impact of unmodeled variation in SECR models when making inferences, and to strive to include covariates likely to be the most influential based on the species biology and ecology in candidate model sets. Doing so can improve the robustness of wildlife density estimation methods that can be leveraged to make more sound conservation and management decisions.

2.2 Introduction

Estimating population density is one of the fundamental goals of population ecology and is necessary for effective management and conservation of wildlife (Royle et al. 2014). With the need for robust population estimates has come the advent and application of innovative data collection methods, such as non-invasive genetic sampling and camera traps (Long et al. 2008), enabling data to be collected at increasingly larger spatial and temporal scales. Alongside this growth in data collection abilities, coupled with increasing computing power, has come rapid development and widespread application of more sophisticated quantitative methods to estimate population density (Lewis et al. 2018). As a result, statistical models have become a pervasive tool in ecology and are an integral component of most contemporary wildlife management and conservation programs. However, with this ever-increasing ability to address more complex research questions with advanced models comes the need to continually assess the robustness of models' assumptions to realistic ecological conditions and sampling processes (Gerber and Parmenter 2015).

While estimating population density is the objective of many wildlife monitoring programs (Burton et al. 2015), identifying factors that give rise to spatial variation in density can have broader relevance and applicability to conservation and management (Fuller et al. 2016). Spatially explicit capture-recapture (SECR; Efford 2004, Borchers and Efford 2008, Royle et al. 2014) methods are well-suited for this purpose. SECR represents an extension of the classical capture-recapture framework (Otis et al. 1987), which ignores locations of capture or detection, by coupling a spatial point process model for the distribution of animals ("density sub-model") with an observation model that describes encounter probability as a function of the distance between a sample location and animals' activity center ("detection sub-model"; Royle et al.

2014). Although relatively recent in the field of statistical ecology, SECR methods have undergone considerable development and have become widely adopted as the standard for quantifying spatial patterns in density where animals are individually identifiable (Dupont et al. 2021).

Reliable information on large carnivore (hereafter, carnivore) population density is important given the species' wide-ranging impacts on ecosystems and their vulnerability to human-induced environmental changes (Ripple et al. 2014). Further, carnivores often come into conflict with people, making them more prone to human-induced population declines (Treves and Karanth 2003, Nyhus 2016). Consequently, carnivores are increasingly subject to intensive conservation and management programs that necessitates accurate population estimates to ensure success.

In practice, however, obtaining unbiased, precise estimates of carnivore density is often challenging because the species tend to range widely over difficult-to-access areas and exhibit low and variable densities and capture probabilities (MacKenzie et al. 2005, Dröge et al. 2020). SECR requires multiple detections of some of the same individuals ("recaptures"), including at different detector locations ("spatial recaptures"), where the number and spatial distribution of recaptures inform the baseline detection probability (g_0) and spatial scale parameter (σ) of the detection sub-model (Borchers and Efford 2008, Royle et al. 2014). Sparse data, in which numbers of recaptures and spatial recaptures are low, have been demonstrated to lead to imprecise and biased estimates (Sollmann et al. 2012, Sun et al. 2014, Clark 2017). Data sparsity is one of the major impediments to successfully implementing SECR studies of carnivores (Nawaz et al. 2021). Moreover, this challenge is further amplified when there are multiple sources of variation in detectability or density, as data must then be sufficient to estimate covariate effects or strata-specific model parameters.

Research to date has addressed the issue of data sparsity through improved survey design and statistical techniques. In recent years, multiple studies on the American black bear (*Ursus americanus*) have contributed to improvements in SECR sampling methods and yielded insight into some aspects of survey design (Sollmann et al. 2012, Sun et al. 2014, Wilton et al. 2014, Clark 2017). Collectively, these studies demonstrate that SECR methods generally perform well provided that the spatial components of survey design (extent, spacing, and configuration of arrays of detectors) are appropriate to the spatial characteristics of different subsets of the sampled population during the sampling period (such as home ranges size and range of individual movements). However, in practice, it can be logistically and financially challenging to conduct field surveys with sufficient spatial coverage and trap spacing for wide-ranging species that exist at low and non-uniform densities (Wilton et al. 2014). In cases when surveys yield insufficient data to estimate model parameters a common approach is to pool data from separate surveys, where models are simultaneously fit with parameters shared across time or space (MacKenzie et al. 2005). This approach has been employed in several SECR studies of bears (*Ursus* spp.; Howe et al. 2013, Azad et al. 2019, McLellan et al. 2019, Welfelt et al. 2019; Schmidt et al. 2022). With sufficiently large datasets, covariates can be included to account for differences in density and detectability to better reflect the actual state of the population (Sollmann et al. 2012).

While aggerating data can enhance precision and power to detect and model some sources of variation in detectability or density (Howe et al. 2013, Azad et al. 2019, Schmidt et al. 2022), this approach may come at the expense of bias (MacKenzie et al. 2005). When carnivores are sampled across broad landscapes, the assumption that detection and density parameters remain constant across space is most often violated. This is likely common for surveys of black bears

where both density and detectability have been documented to vary by sex and across space and time (Howe et al. 2013, Humm et al. 2017, Humm and Clark 2021). Thus, if a misspecified SECR model is fit in the presence of sex and spatial heterogeneity, there is potential to produce biased density estimates. Specifically, unmodeled heterogeneity in detection parameters can produce density point estimates that are negatively biased (Tobler and Powell 2013). However, it is often challenging to account for all potential sources of heterogeneity in SECR models due to small sample sizes relative to the number of parameters and the computational burden of fitting highly parameterized SECR models. An alternative to avoiding bias introduced by model misspecification is to fit separate models to subsets of the data. Yet, this approach is not always practical as it may reduce sample size such that it is impossible to estimate parameters or estimates are too imprecise to be useful for management or conservation (Schmidt et al. 2022). Further, for sparse datasets, as the number of spatial and non-spatial recaptures decreases, estimates of σ are often negatively biased causing overestimation of population size and density (Sun et al. 2014, Clark 2017).

Collectively, the above issues highlight a long-standing issue in statistical ecology: selecting an appropriate model for a dataset (Brewer et al. 2016). Model selection, the purpose of which is to identify models that optimize the trade-off between bias and precision (Burnham and Anderson 2002), is a critical yet challenging component of SECR analyses. For the vast amount of SECR studies on bears that use a frequentist framework, models are selected using Akaike Information Criterion adjusted for small sample sizes (AIC_c; Hurvitch and Tsai 1989) in which the top-ranked model(s) are used for inferences regarding parameter estimates and relationships between variables of interest (examples include Obbard et al. 2010, Morehouse and Boyce 2016, Lamb et al. 2018).

Identifying models that allow for aggregation of survey data to improve precision while still accounting for important sources of heterogeneity to reduce bias is thus an essential consideration for SECR studies on elusive species where pooling data across space or time is common. Yet, few studies have systematically examined the performance of model selection and consequences of misspecification of both the density and detectability sub-models on SECR model performance under realistic levels of sex-based and spatial variation in carnivores.

Here, we assess how unmodeled spatial and sex-based variability in density and detectability influences the performance of SECR models and AIC_c model selection when data are pooled across sampling areas. We do so through simulation, using parameters consistent with non-invasive genetic surveys of black bears. However, the findings are generalizable to any wide-ranging or elusive species, particularly carnivores. We had three primary research questions: (1) How well does AIC_c correctly identify the true data-generating model?; (2) How well does the true data-generating model perform, in terms of accuracy and precision, across a suite of simulations with varying levels of complexity in spatial and sex-based variation in density and detectability?; (3) When AIC_c does not select the data-generating model, what are the implications regarding inferences about population density?

2.3 Methods

2.3.1 Hypothetical study area and sampling design

We simulated a hypothetical study area with a heterogeneous landscape composed of three distinct study areas (Areas A, B, C). These study areas broadly represent habitats in Ontario, Canada, in which black bear density and detectability vary due to differences in habitat quality and human disturbances across the landscape (Obbard et al. 2010, Howe et al. 2013). Although these scenarios are parameterized for black bears in Ontario, gradients in density exist

for most carnivore species. In each study area black bears were sampled using two linear arrays of 40 detectors, where arrays were far enough apart so that no individuals were detected at more than one array. Linear arrays were selected to replicate the curvilinear arrays used for ongoing black bear research and monitoring in Ontario (Obbard et al. 2010, Howe et al. 2013, Howe et al. 2022, Marrotte et al. 2022). Literature recommends an optimal detector spacing to be less than two times the minimum spatial scale of the detection probability function (σ_{min}; Sollmann et al. 2012, Sun et al. 2014) and when g_0 is low to be less than σ_{min} (Efford and Boulanger 2019). Therefore, using our σ_{min} of 2500 m (Table 2.2), detectors were spaced 2000m apart.

2.3.2 Simulation of populations and capture histories

Spatially explicit capture-recapture data were simulated for populations of female and male bears over five sampling occasions, where populations were distributed according to a homogenous Poisson point process within each study area. Populations of both sexes were simulated using a 6601.76 km^2 state space defined as the linear array plus a 27-km buffer; this buffer corresponds to $4\sigma_{max,}$ which is recommended to ensure that animals with activity centers outside the state space have negligible chances of being detected (Efford 2021). While this buffer is excessive for most female black bears, using an area of integration that is too small can positively bias SECR density estimates whereas using an area that is too large does not lead to bias as density estimates reach an asymptote with larger buffer widths (Royle et al. 2014, Efford 2021). Spacing between the grid points of the mask was set at 2.2km to reduce computation time after verifying that increasing resolution had negligible effects on density estimates.

A total of 29 scenarios were created (Table 2.1) by holding model parameters (D, σ, g_0) constant or having them vary by either sex, area, or both sex and area. While carnivore populations are likely to exhibit spatial differences in both g_0 and σ, scenarios where g_0 varied by

area alone would contribute little relevance real-world SECR studies. Thus, to reduce the number of scenarios we varied g_0 by sex alone or combined area and sex. Parameter values for each sampling area (Table 2.2) were selected to be consistent with prior simulation studies for black bears (Table 2.2; Sollmann et al. 2012; Sun et al. 2014, Clark 2017) and to represent reasonable parameter combinations for black bears in Ontario (Obbard et al. 2010, Howe et al. 2013). Area A was simulated with relatively high g_0 and σ and low D (representative of relatively unproductive boreal forests in Ontario; Rowe 1972); Area C was simulated with relatively low g_0 and σ and high D (representative productive Great Lakes – St Lawrence [GLSL] Forest in Eastern Ontario); Area B was simulated with intermediate values. Within areas, males were simulated with higher values of σ and lower values of D and g_0 due to differences in density and detectability between the sexes (Hooker et al. 2015, Humm et al. 2017). For each scenario we generated 1000 populations and corresponding capture-recapture datasets (hereafter, simulations), resulting in 29,000 datasets.

Noticeably, these scenarios were not exhaustive of the entire parameter space. For SECR models a minimum of total 20 recaptures is recommended as the precision of density estimates depends on the number of recaptures in a sample (Efford et al. 2004, Sun et al. 2014). As this work aimed to assess the influence of spatial and sex-based heterogeneity on density estimates, irrespective of the influence of sample size, parameters values were selected to maintain a relatively similar and sufficient number of recaptures across sampling areas while still being biologically realistic for black bears.

Table 2.1. Structure of scenarios where each row details a scenario with varying density (D), detection probability (g_0), and spatial scale (σ) parameters for which 1000 populations and capture histories were generated and a set of 105 candidate SECR model forms were fit. Scenario ID coded by variables corresponding to whether the parameters (D, g_0, σ) were held constant (0) or varied by area (1), sex (2), or both sex and area (3). Last column indicates the approximate true data generating model (M_T) for each scenario.

Scenario ID	**D**	**g_0**	**σ**	**M_T**
000	.	.	.	D(.) g_0(.) σ(.)
001	.	.	area	D(.) g_0(.) σ(area)
023	.	sex	sex and area	D(.) g_0(sex) σ(sex + area)
031	.	sex and area	area	D(.) g_0(sex + area) σ(area)
032	.	sex and area	sex	D(.) g_0(sex + area) σ(sex)
100	area	.	.	D(area) g_0(.) σ(.)
101	area	.	area	D(area) g_0(.) σ(area)
103	area	.	sex and area	D(area) g_0(.) σ(sex + area)
122	area	sex	sex	D(area) g_0(sex) σ(sex)
123	area	sex	sex and area	D(area) g_0(sex) σ(sex + area)
130	area	sex and area	.	D(area) g_0(sex + area) σ(.)
131	area	sex and area	area	D(area) g_0(sex + area) σ(area)
132	area	sex and area	sex	D(area) g_0(sex + area) σ(sex)
133	area	sex and area	sex and area	D(area) g_0(sex + area) σ(sex + area)
203	sex	.	sex and area	D(sex) g_0(.) σ(sex + area)
223	sex	sex	sex and area	D(sex) g_0(sex) σ(sex + area)
230	sex	sex and area	.	D(sex) g_0(sex + area) σ(.)
231	sex	sex and area	area	D(sex) g_0(sex + area) σ(area)
232	sex	sex and area	sex	D(sex) g_0(sex + area) σ(sex)
233	sex	sex and area	sex and area	D(sex) g_0(sex + area) σ(sex + area)
301	sex and area	.	area	D(sex + area) g_0(.) σ(area)
302	sex and area	.	sex	D(sex + area) g_0(.) σ(sex)
320	sex and area	sex	.	D(sex + area) g_0(sex) σ(.)
321	sex and area	sex	area	D(sex + area) g_0(sex) σ(area)
322	sex and area	sex	sex	D(sex + area) g_0(sex) σ(sex)
323	sex and area	sex	sex and area	D(sex + area) g_0(sex) σ(sex + area)
331	sex and area	sex and area	area	D(sex + area) g_0(sex + area) σ(area)
332	sex and area	sex and area	sex	D(sex + area) g_0(sex + area) σ(sex)
333	sex and area	sex and area	sex and area	D(sex + area) g_0(sex + area) σ(sex + area)

Table 2.2. SECR parameter values for density (D), detection probability (g_0) and spatial scale (σ) parameters used for generating black bear populations and capture histories across four groupings where parameters remain constant or vary by sex, area, or sex and area.

Grouping code[†]	**Grouping description**	**Parameter**‡	**Area A**	**Area B**	**Area C**
3	sex and area	D female	0.03	0.06	0.12
		D male	0.02	0.04	0.08
		g_0 female	0.35	0.25	0.15
		g_0 male	0.20	0.15	0.10
		σ female	4500	3500	2500
		σ male	6750	5250	3750
1	area	D	0.025	0.05	0.10
		g_0	0.275	0.200	0.125
		σ	5625	4375	3125
2	sex	D female		0.07	
		D male		0.05	
		g_0 female		0.25	
		g_0 male		0.15	
		σ female		3500	
		σ male		5250	
0	baseline	D		0.06	
		g_0		0.20	
		σ		4375	

[†]grouping code corresponds to scenario ID where variables represent whether parameters D, g_0, and σ vary by either area (1), sex (2), sex and area (3), or are constant (0)

‡σ represented by distance (m) and density (bears/km^2)

2.3.3 SECR model fitting

Data from all three study areas from each simulation were analysed simultaneously; study areas were modeled as sessions in a multi-session analysis that allowed for different degrees of data aggregation between sexes and among areas to estimate parameters. For each scenario, we fit 105 candidate model forms, representing almost all possible additive and interactive combinations of parameters (for a full list of candidate models see Appendix A Section 1: Table A.1.1) by maximizing the full likelihood for proximity detectors and using the half-normal detection probability function. This resulted in 3,045,000 models fit overall that required high computational costs and was prohibitively slow to summarize model outputs. However, there were negligible differences in density estimates derived from model forms with the same structure of covariates for each parameter, but either additive or interactive effects of sex and area (i.e., additive model D~area g_0~area+sex σ~sex; interactive model D~area g_0~area×sex σ~sex). See Appendix A Section 4 for further clarification and comparison of density estimates between additive and interactive models. Consequently, we excluded candidate model forms where covariates on any one of the parameters (D, g_0, σ) included an interaction effect; this resulted in 48 candidate models with only additive effects included in the subsequent analysis and presented in the following results and discussion.

2.3.4 Evaluation of model performance

For each scenario and model form we compared density estimates to the expected values in terms of accuracy (mean percent relative bias [MPRB] and the 95% confidence interval [CI] coverage), precision (mean coefficient of variation [MCV]) and the root-mean-square error (RMSE). A $|\text{MPRB}| \leq 5\%$ was considered an allowable bias (Dupont et al. 2020) and a MCV <

0.2 was considered acceptable for carnivore management (Proctor et al. 2010). A low RMSE represented a good trade-off between low bias and variance (Blanc et al. 2013).

2.3.5 Model selection

AIC_c is one of the most commonly used model selection approaches for SECR studies. ΔAIC_c can be used to rank competing candidate models and is the difference in AIC_c between the top ranked model and other models, where the top ranked model has $\Delta AIC_c = 0$. Burnham and Anderson (2004) suggest that models with $\Delta AIC_c \leq 2$ have substantial support, models with $4 \geq \Delta AIC_c \leq 7$ have considerably less support, and models with $\Delta AIC_c > 10$ have negligible support. For each scenario, the data generating model (M_T) that best approximated the expected parameters was first identified. Then, using the above guidelines, for each scenario we calculated the frequency, out of the 1000 simulations, that M_T was included in the following classes: (1) the top-ranked model ($\Delta AIC_c = 0$); (2) $0 \leq \Delta AIC_c \leq 2$; (3) $2 < \Delta AIC_c \leq 10$; (4) $\Delta AIC_c > 10$.

All simulations were implemented through R 4.0.4 using packages 'secr' version 4.3.3 (Efford 2020a) and 'secrdesign' version 2.5.11 (Efford 2020b). As computation time was prohibitively slow with a stand-alone personal computer, high-performance computing software provided by Compute Canada (computecanada.ca; RRG: hyf-453-ab) was used to simultaneously fit many models.

2.4 Results

Simulations yielded variable numbers of animals, detections, and spatial recaptures across scenarios; see Appendix A Section 2 (Figures A.2.1 and A.2.2) for a summary. All models converged.

2.4.1 Model selection

We first identified the data generating model (M_T) that best approximated the expected parameters for each scenario. Interactions between simulated main effects on D, g_0 and σ were absent or slight (Figure 2.1). In Figure 2.1 the parallel lines for D and σ indicate no interaction between main effects whereas slightly different slopes for g_0 indicate a slight interaction. Thus, for scenarios where either D, g_0, or σ varied by sex and area, M_T with an additive effect between sex and area was considered equivalent to the data generating model for D and σ and a good approximating model for g_0.

Across scenarios, AIC_c reliably identified M_T as having substantial support ($0 \leq \Delta AIC_c \leq 2$) for 71.5% to 100% of the simulations (Table 2.3). M_T was identified as the top-ranked model ($\Delta AIC_c = 0$) for fewer simulations on average (42.6 to 99.9% of the simulations; Table 2.3). The likelihood that AIC_c selected M_T generally increased as the number of parameters in M_T increased (Table 2.3; also see AIC_c weights in Appendix A Section 5: Table A.5.1). In contrast, AIC_c rarely selected M_T as having considerably less or no support (0 to 27.2% of the simulations; Table 2.3).

2.4.2 Performance of the data generating model

Accuracy — For all scenarios, M_T yielded estimates of density with less than 5% |MPRB| (Figure 2.2; Appendix A Section 3: Figure A.3.1). Although still within $\pm$ 5% bias, for both sexes and across areas there was a very slight positive MPRB for scenarios where M_T had constant density (Figure 2.2; Appendix A Section 3: Figure A.3.1). Taking into consideration the remaining scenarios (density varied by sex, area, or sex and area), estimates for females were slightly negatively biased, with the magnitude greater in area A (82.6% of the total scenarios displayed negative MPRB in area A, 79.3% in area B and 72.4% in area C) compared to males where there

was a slight positive MPRB for approximately half of the scenarios (51.7% of the total scenarios displayed positive MPRB for area A, 48.2% for area B and 51.7% for area C; Appendix A Section 3: Figure A.3.1). The variance in percent relative bias (PRB; i.e., the spread of estimates across the 1000 simulations) differed by scenario; scenarios where M_T had constant density had the least variable PRB, while scenarios where M_T had density vary by either area or sex and area displayed more variable PRB (Figure 2.2). Scenarios where density varied by sex had intermediate variation in PRB (Figure 2.2). CI coverage was near nominal across all scenarios (across areas and sexes CI coverage ranged from 93.0% to 96.5%; mean 94.9%); see Appendix A Section 3: Table A.3.1.

Precision — For all scenarios, M_T density estimates had CVs well below 0.2 for both sexes and all areas (CV range 0.033 – 0.106; mean 0.062; Figure 2.3). Estimates were most precise where M_T was simple (number of parameter $K \leq 5$) and density was constant, followed by scenarios where density varied by sex but not among study areas (Figure 2.3). However, for the latter scenarios, there were opposing patterns in MCV between sexes and the CV remained relatively consistent across areas for each sex (Figure 2.3). The remaining scenarios (density varied either by area or by sex and area) were generally characterized by the least precise estimates.

In contrast to bias, the CV and its variation differed across scenarios and between sexes and areas. Across most scenarios, Area B (which had intermediate density) exhibited on average the most precise estimates, followed by Area C (which had the highest density), then area A (with the lowest density). Variability in CV generally increased with increasing magnitude of CV, with Area A displaying the most elevated and variable CV values for scenarios where M_T had density vary by either area or sex and area (Figure 2.3). Further, despite attempts to maintain a similar number of total spatial re-captures across scenarios, this was not always possible due to

the nature of parameter combinations for some scenarios. Consequently, there was an indication of generally higher precision for some scenarios with more recaptures (Appendix A Section 1: Figure A.1.1).

Combined precision and accuracy — RMSE followed a similar pattern to precision, with RMSE slightly higher for most scenarios in which MCV was elevated (Figure 2.4); this pattern was most pronounced for area C. Specifically, area C exhibited the highest variability in RMSE for scenarios where M_T had density vary by area or sex and area, followed by Area B then area A. Similar to precision, for scenarios where M_T had density varying by sex, RMSE was relatively consistent across all areas for each sex and there were opposite patterns in RMSE across these scenarios between males and females (Figure 2.4).

2.4.3 Performance of misspecified SECR models

Accuracy — Across scenarios, the number of candidate model forms with unbiased density estimates ($\leq$ 5% |MPRB|) generally decreased with increasing complexity of M_T (Figure 2.5; also see Appendix A Section 5: Table A.5.1 for the MPRB of the most frequently selected misspecified models for each scenario). For the least complex scenarios (K = 3) where M_T had all constant parameters, incorrectly selecting any one of the 47 mis-specified models had negligible impact on the density estimates (Figure 2.5; further see Appendix A Section 5: Table A.5.1). As a result, for these scenarios, despite AIC_c being less likely to select M_T as the top-ranked model, minimal bias was incurred by selecting a model more complex than M_T.

In contrast, for scenarios with complex M_T ($K \geq 10$), selecting a model other than M_T often yielded biased (> 5% |MPRB|) density estimates (Figure 2.5; Appendix A Section 5: Table A.5.1). More specifically, for misspecified models with > 5% |MPRB|, density was often overestimated for males and underestimated for females (Appendix A Section 5: Table A.5.1).

However, as M_T was most often correctly selected for more complex scenarios when a good approximating model was included in the candidate model set (ranging from 70.3% to 99.9% of the simulations, Table 2.3; also see Appendix A Section 5: Table A.5.1), biased density estimates with > 5% |MPRB| were unlikely.

For scenarios with moderate complexity M_T ($7 \leq K \geq 9$), the number of model forms that produced density estimates with > 5% |MPRB| varied (Appendix A Section 3: Figure A.3.1). However, despite these scenarios having a poor to moderate chance of AIC_c selecting M_T as the top-ranked model (ranging from 55.1% to 75.9% of the simulations; Table 2.3), there were generally minimal consequences on the accuracy of selecting a mis-specified model as in these cases the bias most often remains within $\pm$ 5% (Appendix A Section 5: Table A.5.1).

Combined precision and accuracy — The chances of misspecifying imprecise and inaccurate models generally displayed similar trends to those of M_T, with models with higher bias usually characterized by higher MCV and RMSE for both sexes, and vice versa (Appendix A Section 5: Table A.5.1). However, this pattern was not always consistent; for some scenarios, there were minimal changes in MCV and RMSE across candidate model forms (Appendix A Section 5: Table A.5.1). Further, for misspecified models where bias was exceptionally large (> 15% |MPRB|), variances were typically underestimated; this was most apparent for scenarios with more complex M_T (Appendix A Section 5: Table A.5.1).

Table 2.3. The percent, out of 1000 simulations, that the approximate true data generating model (M_T) in each scenario was identified as the top AIC_c ranked model ($\Delta AIC_c = 0$), having substantial support ($0 \leq \Delta AIC_c \leq 2$), considerably less support ($2 < \Delta AIC_c \leq 10$) or no support ($\Delta AIC_c > 10$). Scenarios are coded by variables corresponding to whether the model parameters (D, g_0, σ) vary by area (1), sex (2), sex and area (3), or are constant (0). ΔAIC_c is the difference between the focal model and the top ranked model and K is the number of parameters in M_T.

	Scenario									
	000	**001**	**100**	**023**	**032**	**101**	**122**	**203**	**230**	**302**
K	3	5	5	7	7	7	7	7	7	7
$\Delta AIC_c = 0$	42.6	48.7	51.2	61.8	61.8	58.8	55.1	66.6	64.5	67.6
$0 \leq \Delta AIC_c \leq 2$	71.5	76.2	79.8	84	87	84	75.2	87.3	86	86.7
$2 < \Delta AIC_c \leq 10$	27.2	23.1	19.8	15.4	12.3	15.7	12.5	12.3	13.7	13.2
$\Delta AIC_c > 10$	1.3	0.7	0.4	0.6	0.7	0.3	12.3	0.4	0.3	0.1
	Scenario									
	320	**031**	**103**	**130**	**223**	**232**	**301**	**322**	**123**	**132**
K	7	8	8	8	8	8	8	8	9	9
$\Delta AIC_c = 0$	63.0	58.5	67.1	60.2	73.8	75.9	69.3	75.5	74.0	72.2
$0 \leq \Delta AIC_c \leq 2$	83.2	83.2	88.9	84.2	90	92.2	88.3	90	90.6	90.7
$2 < \Delta AIC_c \leq 10$	16.6	16.5	10.9	15.3	9.7	7.7	11.3	9.8	9.2	9.2
$\Delta AIC_c > 10$	0.2	0.3	0.2	0.5	0.3	0.1	0.4	0.2	0.2	0.1
	Scenario									
	231	**321**	**131**	**233**	**323**	**332**	**133**	**331**	**333**	
K	9	9	10	10	10	10	11	11	12	
$\Delta AIC_c = 0$	72.0	71.0	70.3	86.5	87.4	86.6	83.6	84.2	99.9	
$0 \leq \Delta AIC_c \leq 2$	90	90.8	89.5	93.9	95.3	94.8	94.8	95	100	
$2 < \Delta AIC_c \leq 10$	9.8	8.8	10.4	5.9	4.6	5	4.9	4.8	0	
$\Delta AIC_c > 10$	0.2	0.4	0.1	0.2	0.1	0.2	0.3	0.2	0	

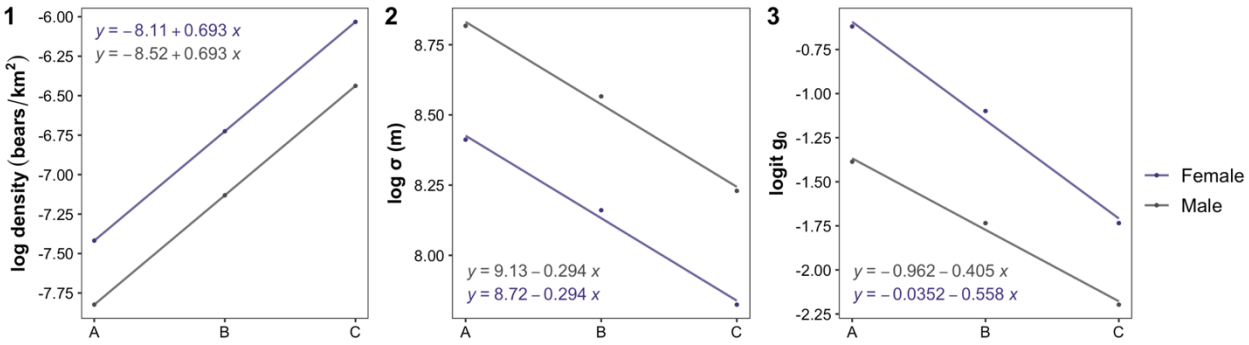

Figure 2.1. Interactive plot displaying differences in density (D; plot 1), spatial scale parameter (σ; plot 2), and detection probability (g_0; plot 3) among sexes and sampling areas (A, B, C) on the link scale for simulated female and male black bears. Parallel lines indicate an additive effect for D and σ and non-parallel lines indicate a slight interactive effect for g_0.

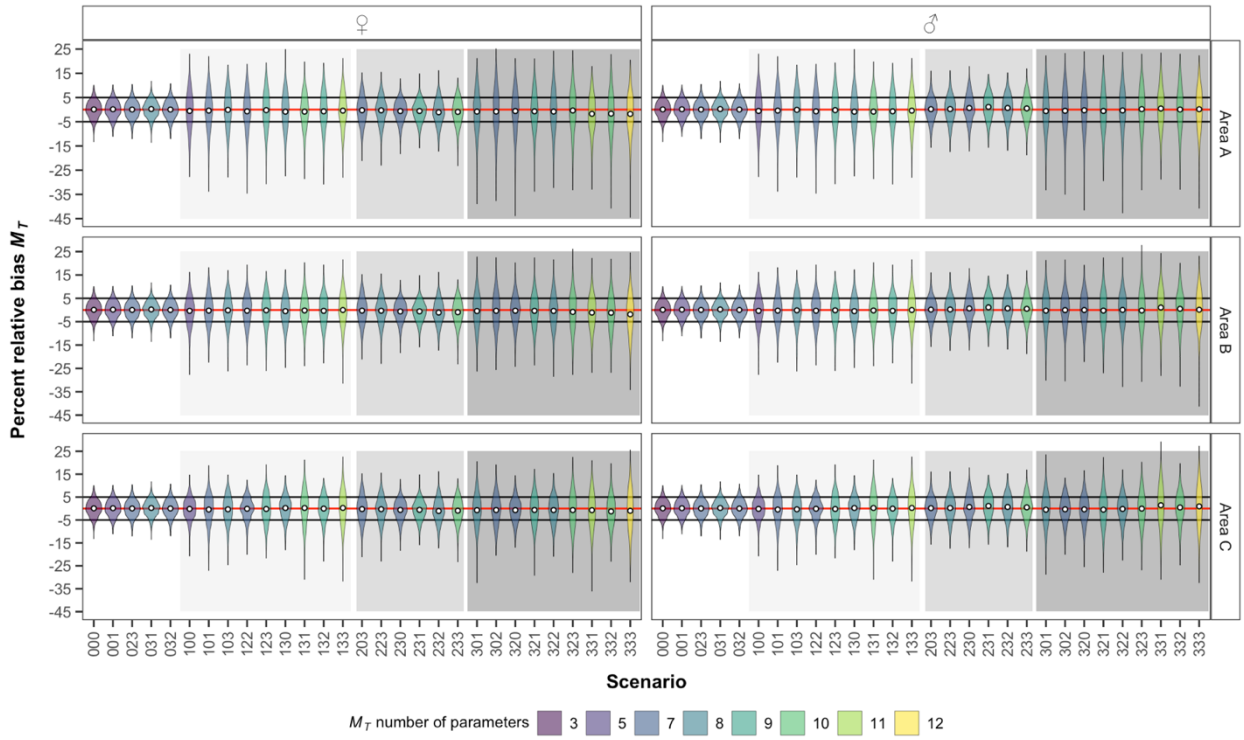

Figure 2.2. Percent relative bias (PRB) of female (♀) and male (♂) black bear density estimates for the true data generating model (M_T) across study areas (A, B, C), for 1000 simulations of each scenario. Scenarios are coded by variables corresponding to whether the parameters (D, g_0, σ) were constant across areas and sexes (0), or varied by area (1), sex (2), or both sex and area (3); see table 1 for more detailed summary of scenarios. White dots within the violins represent the mean percent bias and colours of violins represent the number of parameters in M_T.Thick black horizontal lines represent PRB within 5% and red horizontal lines no bias. Background colors correspond to the four levels of variation in density: constant density (white), density varies by area (light gray), sex (medium gray), and both area and sex (dark gray).

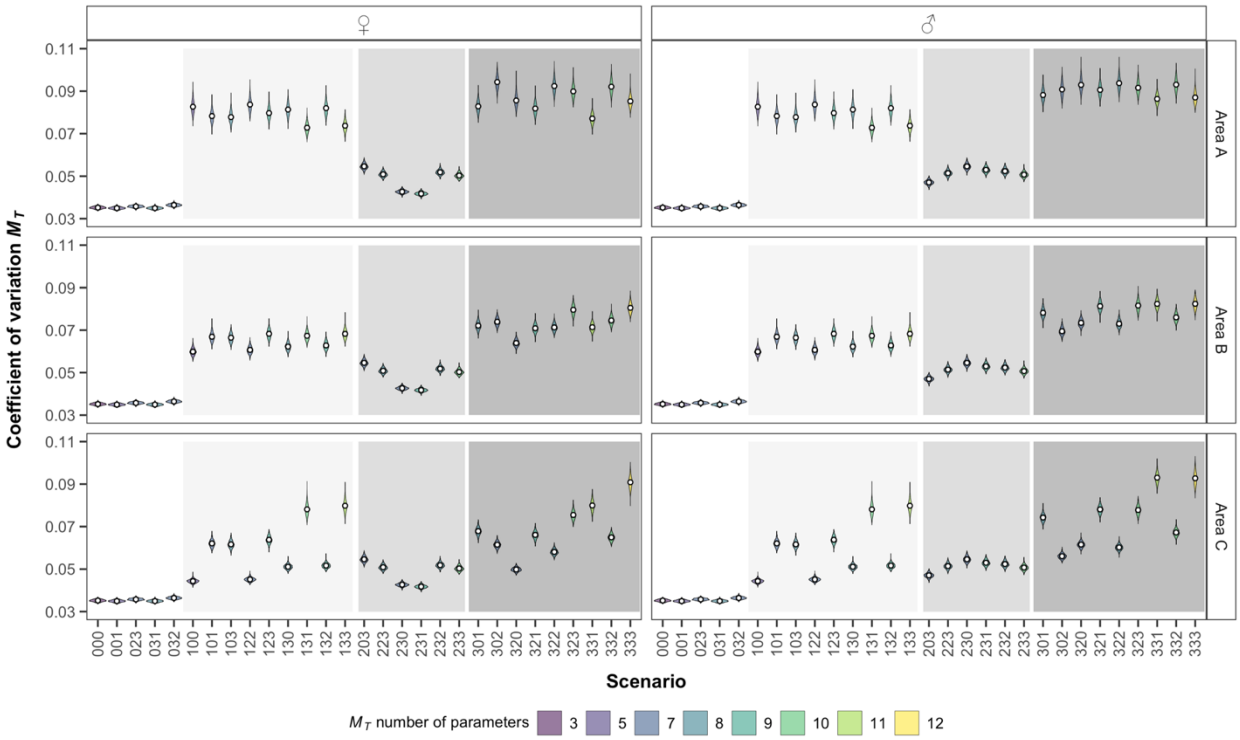

Figure 2.3. Boxplots displaying the coefficient of variation (CV) of female (♀) and male (♂) black bear density estimates for the true data generating model (M_T) across study areas (A, B, C), for 1000 simulations of each scenario. Scenarios are coded by variables corresponding to whether the parameters (D, g_0, σ) were constant across areas and sexes (0), or varied by area (1), sex (2), or both sex and area (3); see Table 1 for more detailed summary of scenarios. White dots within the violins represent the mean CV and colours of violins represent the number of parameters in M_T. Background colors correspond to the four levels of variation in density: constant density (white), density varies by area (light gray), sex (medium gray), and both area and sex (dark gray).

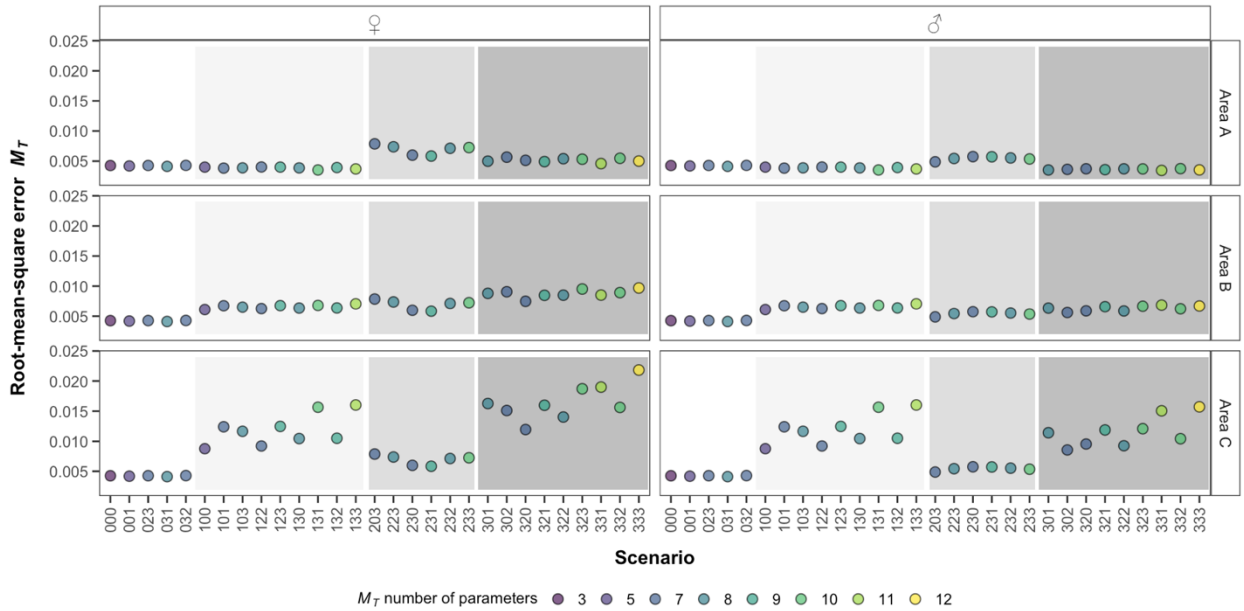

Figure 2.4. Root-mean-squared error (RMSE) of female (♀) and male (♂) black bear density estimates (bear/km^2) for the true data generating model (M_T) across study areas (A, B, C) from 1000 simulations of each scenario. Scenarios are coded by variables corresponding to whether the parameters (D, g_0, σ) were constant across areas and sexes (0), or varied by area (1), sex (2), or both sex and area (3); see Table 1 for more detailed summary of scenarios. Colors of the dots indicates the number of parameters in M_T for each scenario. Background colors correspond to the four levels of variation in density: constant density (white), density varies by area (light gray), sex (medium gray), and both area and sex (dark gray).

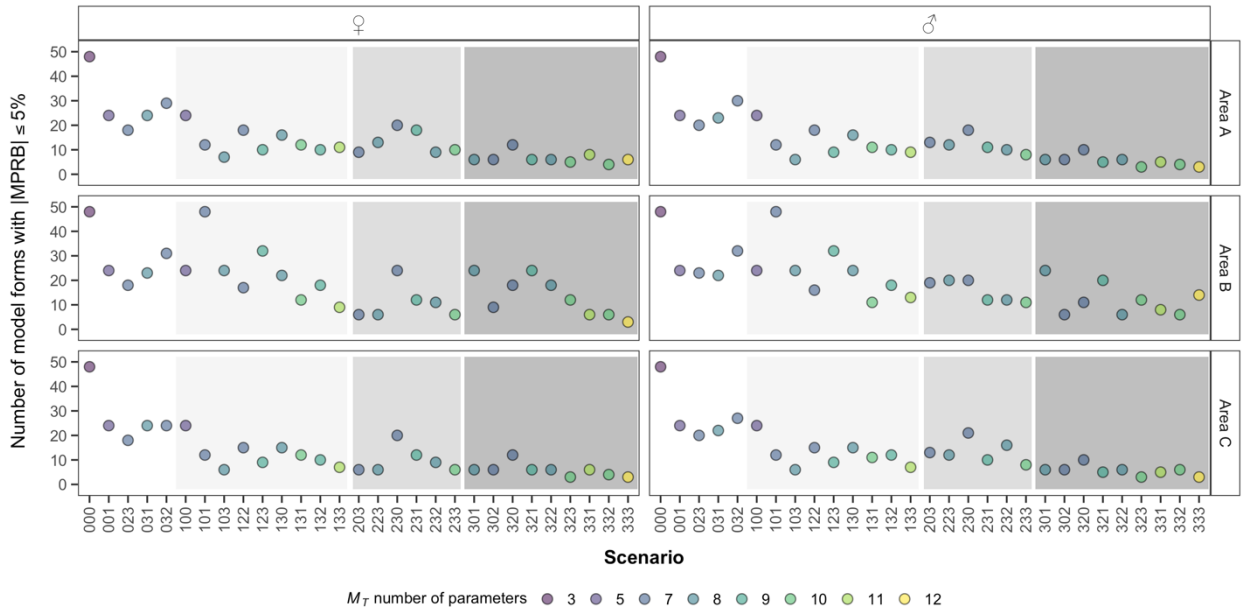

Figure 2.5. Number of candidate model forms where the absolute mean percent relative bias (|MPRB|), out of 1000 simulations, of female (♀) and male (♂) black bear density estimates was ≤ 5%, across study areas (A, B, C). The color of the circles denotes the number of parameters in the true data generating model (M_T) for each scenario. Scenarios are coded by variables corresponding to whether the parameters (D, g_0, σ) are constant (0) or vary by area (1), sex (2), or sex and area (3); see Table 1 for more detailed summary of scenarios. For each scenario, 48 candidate models forms were fit. Background colors correspond to the four levels of variation in density: constant density (white), density varies by area (light gray), sex (medium gray), and both area and sex (dark gray).

2.5 Discussion

Statistical methods for estimating population density and its variance accurately and precisely are fundamental for effective management and conservation of wildlife populations. Although the use of SECR models for estimating density has become increasingly widespread, their application may outpace rigorous testing of their performance using real-worlds datasets (Gerber and Parmenter 2015). This work addresses this concern, specifically in relation to realistic levels of sex-based and spatial heterogeneity. We demonstrate that when a good approximating model is included in the set of candidate models, SECR methods coupled with AIC_c model selection generally yielded accurate estimates with nominal CI coverage. However, we identify some situations in which these methods are prone to bias.

In our series of simulations the critical factor contributing to SECR models' effectiveness is an inverse pattern between the performance of SECR models and AIC_c model selection. For scenarios with low to moderate levels of complexity in M_T ($3 \leq K > 9$), AIC_c less successfully identified the approximate true data generating model (Table 2.3) and was prone to overfitting (Appendix A Section 5: Table A.5.1). However, selecting an unnecessarily complex model generally had minor effects on density estimates as there was generally low bias (Appendix A Section 5: Table A.5.1). This pattern could be explained by the additional modeled effects being so small such that the density estimates for these scenarios were largely unaffected. Conversely, where the underlying approximate true data generating model was complex ($K \geq 10$), top-ranked models that were misspecified produced density estimates with severe negative and positive bias for female and male black bears, respectively (Appendix A Section 5: Table A.5.1). However, for such scenarios, M_T was almost always selected as the top-ranked model (Table 2.3; Appendix

A Section 5: Table A.5.1) and therefore obtaining unbiase and precise estimates is likely, provided that a good approximating model is included in the candidate set.

While SECR model performance was influenced by variation in all model parameters, in our series of simulations, variation in density more strongly influenced model performance than variation in detection parameters. When M_T was not selected as the top-ranked model, misspecification of the density sub-model generally caused more bias than misspecification of the detection sub-model (Appendix A Section 5: Table A.5.1). The severe bias introduced from model misspecification for the more complex scenarios demonstrates that failure to account for heterogeneity in SECR models is of greater concern when pooling data from sub-populations that display high variation in density, and to a lesser extent, detection. This has important implications for monitoring because carnivore density is likely to vary spatially across gradients of habitat productivity and human influence that might be unknown to researchers. Thus, these findings demonstrate that if there is potential for variation in density between sexes or in space, this needs to be accounted for by including relevant covariates of density in candidate model sets. Elsewise, the estimates of density are likely to be bias.

Our findings that for more complex scenarios misspecified models yielded biased sex-specific densities is a shortcoming for managing harvested populations with high heterogeneity. As adult male black bears are more likely to be harvested than females (Obbard et al. 2017; Appendix D Section 6: Figure D.6.1), inflated estimates may lead to sub-optimal management decisions that place populations at risk (Obbard et al. 2010). Further, because females are critical for long-term population stability (Humm and Clark 2021), accurate estimates are critical for monitoring and predicting populations' response to shift in land-use and environmental

conditions. While our simulations focus on black bears, such consequences are pertinent to other large game populations, particularly species of conservation concern.

Moreover, even when M_T was selected as the top-ranked model, scenarios where density varied by area or area and sex were the most challenging to produce unbiased density estimates with high precision and, to a lesser extent, accuracy. Collectively, this work highlights that while SECR models coupled with AIC_c selection generally perform well, it is more challenging for highly heterogenous populations, particularly those with varying densities.

These findings further expand on simulation studies of bias caused by heterogeneity in SECR detection parameters. As demonstrated by Efford and Mowat (2014), for sex-based heterogeneity in detection parameters, scenarios where detection parameters varied in the same direction (reinforcing heterogeneity) displayed large bias; in contrast those where detection parameters varied in opposite direction (compensatory heterogeneity) displayed small or zero bias. Our simulations increased the level of complexity of the scenarios to represent wild carnivore populations by varying both density and detectability by sex and area and found a similar pattern: scenarios where both detection parameters varied by sex and area displayed relatively larger bias (Figure 2.2). As some of our scenarios had detection parameters vary in the same direction (Table 2.2), the larger bias for these scenarios could be partly explained by the simulation structure itself.

2.5.1 Limitations and future areas of research and development

Although our series of simulations provide insight into areas where SECR methods are robust as well as areas where caution is warrented, there is scope for refinement. While these simulations were more extensive than many existing SECR studies on carnivores, we did not account for general or site-specific learned responses to detectors (b and bk, respectively)

commonly included in SECR analyses of carnivores, specifically bears (examples include Howe et al. 2013, Lamb et al. 2018, Loosen et al. 2018, Azad et al. 2019, Humm and Clark 2021). Further, heterogeneity among individual detection may be attributed to a combination of intrinsic and extrinsic factors other than sex and area, as we focused on here, that may be difficult to observe or unknown to the researcher. In cases where unmodeled heterogeneity remains, mixture models may be used to reduce bias (Borchers and Efford 2008); however, such approaches are demanding of data which limits the practical application for many real-word datasets on elusive species. Failing to account for sources of heterogeneity by fitting an inappropriate model is likely to lead to biased density estimates of black bears (Howe et al. 2013). Thus, we anticipate that further sources of heterogeneity, if unaccounted for, would lead to more severe bias than we reported.

While we attempted to remove the issue of data sparsity, this was not entirely possible due to the trade-off between selecting parameter values that were biologically realistic for the study system and values that maintain a relatively consistent number of recaptures. As expected, for some scenarios, increased number of spatial re-captures slightly improved precision and reduced bias of density estimates, similar to previous SECR studies (Sollmann et al. 2012, Sun et al. 2014, Dupont et al. 2019).

Testing for violations of model assumptions remains an ongoing challenge for SECR studies. As recently recommended (Moqanaki et al. 2021), goodness-of-fit tests for SECR methods could help identify unmodeled sex and spatial variation in density or detectability and determine if there is a need to account for such variations in the model. In our simulations, misspecified SECR models for less complex scenarios generally performed well; however, this may not be the case for other studies or species, and such a test could help identify cases of concern. These tests

would be particularly useful for populations expected to display high levels of heterogeneity where model misspecification can lead to extremely biased estimates, as demonstrated here. While Bayesian p-values have been suggested as a goodness-of-fit test for Bayesian SECR models, specific tests for SECR models fit using likelihood have yet to be fully developed and remain an important knowledge gap to be addressed (Moqanaki et al. 2021).

2.6 Conclusion and recommendations

Despite SECR being one of the most powerful tools for enumerating wildlife, variation in density and detectability is often inevitable. Pooling data across time or space is a frequent approach to mitigate the challenges of data sparsity common to SECR studies for such rare and elusive species. However, researchers may inadvertently risk biased density estimates if they do not include complex models that account for variation in detection, and most importantly density, in the candidate model set. In these situations, reliable density estimates therefore depends on obtaining sufficient sample sizes so that researchers can include multiple covariates to model and detect such variability. However, using highly parameterized models is challenging for field studies with sparse data. In such cases, we encourage researchers to include covariates likely to be the most influential on heterogeneity in density and detection. Choosing meaningful covariates should be based on knowledge of the study system and the species biology and ecology. Specifically, for many wide-ranging and elusive species such as carnivores, sex and spatial heterogeneity are key factors to consider.

Nevertheless, unmodeled heterogeneity is inherent in SECR studies. Carnivores are likely to exhibit individual heterogeneity in detection probabilities that extend beyond what can be explained by sex and spatial effects (i.e., age and social status). While mixture distributions may be used to account for such heterogeneity (Borchers and Efford 2008), this approach is often

demanding of data; which limits the practical application for many real-word datasets. In many cases, unfortunately, expensive and time-consuming data collection efforts will lead to sparse datasets that are not useable for fitting complex models and the density estimates from models with few parameters are not only potentially biased, but may overstate precision. Therefore, we encourage researchers and wildlife managers to pay particular attention to the impact of unmodeled heterogeneity, both known and unknown, when conducting analyses and interpreting results, particularly in the context of conservation and management.

Our work reinforces the need to simulate populations with realistic levels of variation in density and detection parameters, particularly when simulations are intended to inform the design of SECR studies. Elsewise it risks survey design and subsequent analyses being based on insufficient knowledge of the study population that may lead to flawed inferences. Further, while pilot studies of small sampling areas may suggest that less intensive surveys are adequate for enumerating populations, the assumption that detection and density parameters remain constant must be taken into account, particularly as the spatial extent of the study area and, in turn, the variability of the sampled population increases. As our findings demonstrate, not accounting for possible violations of this assumption can result in pronounced bias, particularly when heterogeneity in density and detectability is high. Collectively, out analysis reinforces the importance of understanding the limitations and assumptions of statistical methods. Doing so can help reduce the potential for basing conservation, management, and policy decisions on flawed population estimates. Such an understanding will contribute to improving the robustness of field-based density estimates of carnivores.

Chapter 3: Factors shaping black bear densities across gradients in productivity and human disturbance using spatially explicit capture-recapture

Brynn A. McLellan[1], Joseph M. Northrup[1,2], Eric Howe[2]

[1]Environmental and Life Sciences Graduate Program, Trent University.

[2]Wildlife Research and Monitoring Section, Ontario Ministry of Natural Resources and Forestry

.

3.1 Abstract

Understanding the spatial ecology of large-bodied, terrestrial carnivores is a primary goal of ecology and fundamental to wildlife management and conservation. Population-level assessments conducted at sufficiently large spatial extents can capture meaningful patterns for wide-ranging species that exhibit considerable variation in density-habitat relationships. Here, we use three years of American black bear (*Ursus americanus*) capture-recapture data collected across 498, 022 km^2 of Ontario, Canada to assess factors driving fine-scale variation in local densities. We use spatially explicit capture-recapture models to estimate black bear density as a function of spatial covariates representing ecosystem productivity and human disturbances and determine differences among forest regions and sexes. We collected capture-recapture data from 65 study areas, and 3858 individuals (1645 female; 2212 male). Across Ontario, black bear densities were negatively associated with roads and human influences. In the more productive forests regions with higher intensity of human influence, black bear densities were positively associated with less productive coniferous forests and negatively associated with more productive deciduous forest and agriculture, suggesting bears may be prioritizing security when there is ample food supply. Opposite trends were observed in the less productive forest region where food is limited, as bears may be seeking out habitats with available food. Our research provides insight into factors influencing black bear space-use from one of the largest datasets collected on the species and at a large geographic extent with application to the species population and habitat management. Our conclusions underscore the importance of accounting for landscape heterogeneity when studying generalist and wide-ranging species.

3.2 Introduction

Global declines in large-bodied and wide-ranging species, in particular large mammalian carnivores (hereafter, carnivores), are widely linked to the rapidly expanding human footprint coupled with changing environmental conditions (Laliberte and Ripple 2004, Tilman et al. 2017). Carnivores are often revered for their economic, cultural, and aesthetic values and important role regulating terrestrial ecosystems (Beschta and Ripple 2009, Estes et al. 2011, Ripple et al. 2014). However, these species require large and interconnected habitats and their wide-ranging behaviors often bring them into conflict with humans (Treves and Karanth 2003). Consequently, as humans continue to transform natural landscapes, facilitating coexistence between humans and carnivores has become a pressing and controversial challenge for those tasked with conserving and managing carnivores (Lute et al. 2018, Lamb et al. 2020). Resolving these challenges necessitates reliable methods to estimate species abundance and distribution and an understating of population-level responses to habitat loss and land use and climate changes.

Estimating population density and understanding how and why density changes across space is a fundamental pursuit in ecology. This topic structures many conservation and management programs (Sutherland et al. 2013, Royle et al. 2014, Lamb et al. 2019). Patterns in population density, and the underlying processes (e.g., vital rates, movement, habitat selection and space use), can vary across space and time and are associated with landscape heterogeneity (Turner 1989, Scheiner and Willig 2008). Failing to account for the effect of landscape heterogeneity can result in misinterpretation of ecological processes or biased density estimates (Royle et al. 2013) and therefore accounting for this variability is critical to understanding factors limiting and regulating ecological communities (Hunter and Price 1992, Royle et al. 2013). However, for wide-ranging and habitat generalist species, identifying spatial drivers of

population density can be challenging because local results can be highly nuanced, limiting general conclusions. This issue can be addressed by conducting studies over geographical extents large enough to sufficiently capture meaningful variation in ecological processes that influence populations, but such studies are often limited by logistical and financial constraints.

The American black bear (*Ursus americanus*) typifies the characteristics that make it difficult to identify factors shaping population density of wildlife species. In North America, black bears are widely distributed across multi-use landscapes composed of natural habitats and clusters of cities, rural communities, agriculture, and roads. Moreover, the species exhibits dynamic relationships with humans that can differ across space and time, as well as across individuals and by sex (Baruch-Mordo et al. 2014, Johnson et al. 2015, Evans et al. 2017, Zeller et al. 2019). Because black bears are an omnivorous species that depends on accumulated fat storage during hibernation and for reproduction, their demographic rates and space-use patterns are often contingent on the availability, quality, and diversity of food (Costello et al. 2003, Mccall et al. 2017). As a result, depletion of natural food sources associated with habitat loss and fragmentation can influence their distribution and survival (Baruch-Mordo et al. 2014, Murphy et al. 2017, Laufenberg et al. 2018). Concurrently, black bears are vulnerable to human-caused mortality because of their slow reproductive rates and large body size (Kolenosky 1990). Further, the species have extensive home ranges and are habitat generalists, which allows them to occupy human-modified landscapes and exploit anthropogenic food sources that is often related to conflict behaviours (Ryan et al. 2007, Garshelis and Noyce 2008, Baruch-Mordo et al. 2014, Obbard et al. 2014, Lewis et al. 2015, Van Manen et al. 2020). Consequently, hunting, vehicle collisions and human-bear conflicts are dominant mortality sources for the species (Hebblewhite et al. 2003, Garshelis and Noyce 2008, Hostetler et al. 2009, Obbard et al. 2017,

Gantchoff et al. 2020). These two primary factors influencing black bear ecology and biology, human disturbances and food availability, vary considerably over black bears range (Potter and Obbard 2017, Rettler et al. 2021). As such, it is both challenging and critical to account for variability in these factors when assessing drivers of the species density.

The advent and increasing application of non-invasive sampling methods of wildlife, coupled with advances in statistical modeling techniques and computing power, have allowed for quantification of density-habitat relationships over larger, more heterogenous landscapes (Lewis et al. 2018, Lamb et al. 2019). Spatially explicit capture-recapture (SECR; Efford 2004, Borchers and Efford 2008; Royle et al. 2014) offers a powerful framework for addressing questions of animal abundance and distribution because this approach links individual and population-level processes to landscape-level spatial patterns. SECR models are built upon a detection model that regards animal detection probability as a function of distance from an individual's activity center paired with a density model that predicts the spatial distribution of animal activity centers as a spatial Poisson or binomial point process. In this approach, there is an uncorrelated distribution of activity centers across a region of interest, but spatial covariates can be used to model the distribution of activity centers as a function of spatial covariates using an inhomogeneous Poisson point process. Because SECR models provide spatially referenced estimates of abundance and density that can be leveraged for targeted monitoring and management, they have been readily adopted for use with elusive and low-density species such as black bears (e.g., Sollmann et al. 2012, Howe et al. 2013, Hooker et al. 2015, Humm et al. 2017, Murphy et al. 2017, Sun et al. 2017, Gardner et al. 2010, Obbard et al. 2010, Welfelt et al. 2019, Humm et al. 2021, Howe et al. 2022).

To evaluate factors shaping carnivore population densities we focus on black bears in Ontario, Canada. The species is widely distributed across a multi-use landscape with a latitudinal gradient in productivity where bears are exposed to a mosaic of anthropogenic mortality risks and ongoing land-use changes. Due to their popularity as a game animal, coupled with their tendency to come into conflict with humans and livestock (Poulin et al. 2003; Obbard et al. 2014; Northrup et al. *in press*), effective monitoring is necessary for sound black bear management and the population's persistence. Over the last two decades, the Ontario Ministry of Natural Resources and Forestry (MNRF) established genetic spatial capture-recapture surveys across most huntable wildlife management units (WMUs) in the province to estimate black bear densities (Obbard et al. 2010, Howe et al. 2013, Howe et al. 2022). These surveys constitute one of the largest multi-year datasets collected on the species.

Here, we investigate factors driving black bear density using three years of the MNRF genetic spatial capture-recapture datasets collected from 65 replicate study areas in Ontario, Canada. Using SECR models we test the effect of ecosystem productivity and human disturbances on variation in local black bear densities across study areas. The broad geographical scope of our study it provides a unique opportunity to capture fine-scale spatial heterogeneity in population drivers across large gradients in productivity and human influences.

3.3 Methods

3.3.1 Study Area

Our study was conducted within black bear range in the boreal and Great Lakes – St Lawrence (GLSL) forest regions (Rowe 1972) in Ontario, Canada across approximately 498, 022 km^2 (Figure 3.1). Southern Ontario is generally characterized by a humid continental climate, with cold winters and warm summers, while northern Ontario is characterized by a subarctic

climate with colder winters and cooler, shorter summers (Drever et al. 2010). The study area was a multi-use landscape with uses including recreation, forestry, agriculture, and mining. Most of the human population and development occurs in the southeast of the province, predominantly bordering Lake Erie and Lake Ontario, but there were medium-sized cities across much of the study area. Black bear hunting was permitted in designated WMUs during open seasons in the fall and spring (the latter being previously reinstated in some WMUs in 2014 and across Ontario in 2016, following the 1999 moratorium; Poulin et al. 2003, Newton and Obbard 2018, Northrup et al. *in press*).

Landcover varied across the study area due to the broad geographic extent and included wetlands, shorelines, grasslands, shrublands, human settlement and agriculture, and forests. Forests were the predominant landcover with coniferous and mixed forests dominating the boreal region; the primary coniferous tree species in the boreal forest included eastern white cedar (*Thuja occidentalis*), black and white spruce (*Picea mariana, Picea glauca*), balsam fir (*Abies balsamea*), jack pine (*Pinus banksiana*) and tamarack (*Larix laricina*) and the main deciduous species included poplar (*Populus*) and white birch (*Betula papyrifera*; Perera et al. 2000). Hardwood forests dominated the GLSL and included maple (*Acer* spp.), oak (*Quercus* spp.) and yellow birch (*Betula alleghaniensis*), mixed with some coniferous species (Perera et al. 2000). Although productivity is generally higher in the GLSL than the boreal, abundance of soft and hard mast that are important for black bears vary by year (Howe et al. 2012, Potter and Obbard 2017), with food failure events more common in the boreal forests (Poulin et al. 2003).

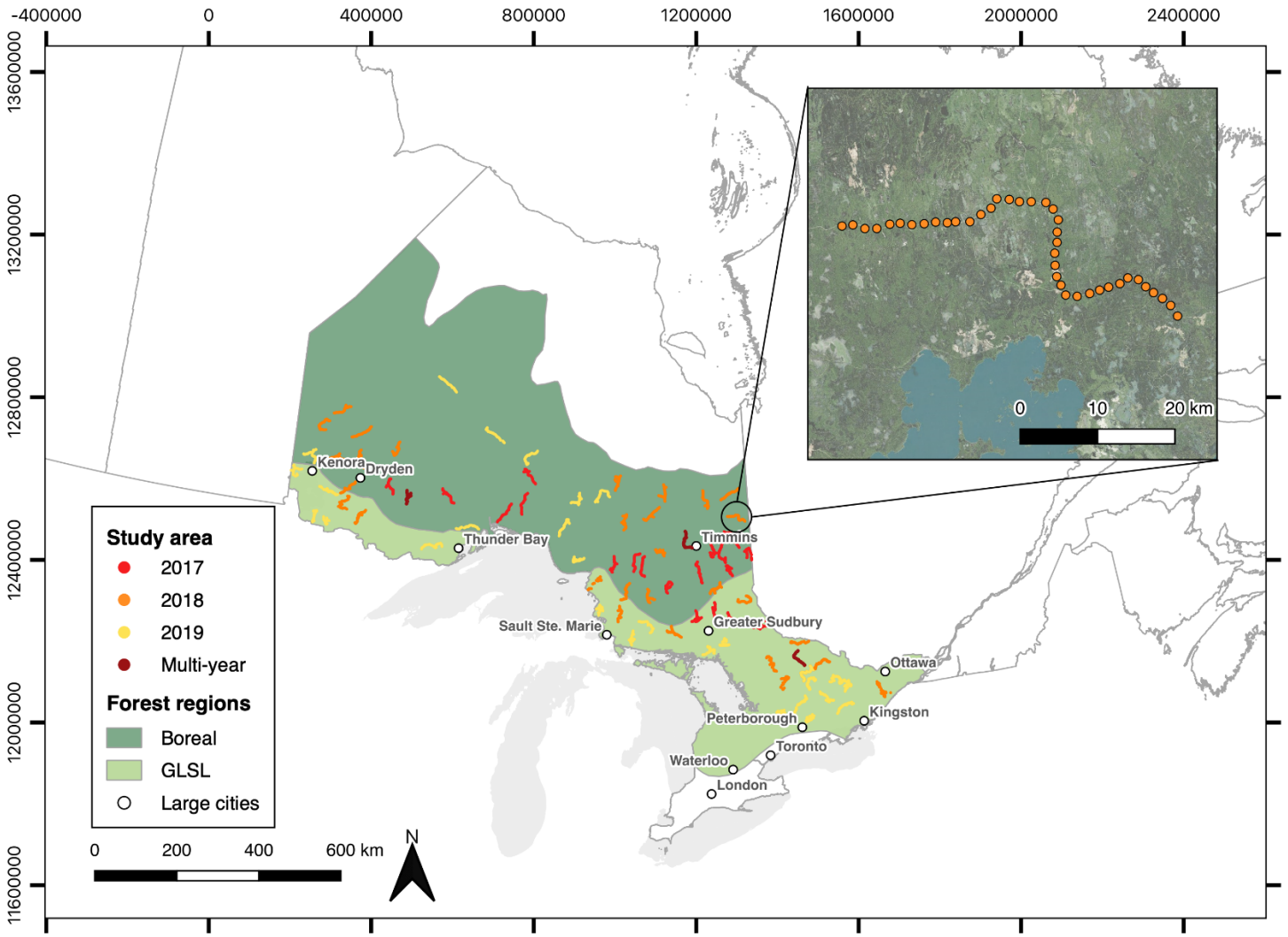

Figure 3.1. Location of arrays of baited barbed wire hair corrals across the Great Lakes – St Lawrence (GLSL) and boreal forest regions in Ontario, Canada where black bear hair samples were collected between 2017 – 2019. At this scale, arrays appear as thin lines. Orange circles in inlay figure represent an array of corrals.

3.3.2 Sampling design

Black bears were sampled across 78 study areas using curvilinear arrays of approximately 40 baited barbed-wire hair corrals (hereafter detectors; Woods et al. 1999) over five consecutive weekly sampling occasions in the spring and early summer of 2017 to 2019 (sampling occasions range from May 21st to June 30th). As black bears typically occupy stable home ranges and focus their movements within smaller areas during these times it is assumed resident populations were sampled (Obbard et al. 2010, Howe et al. 2013). Adjacent detectors were spaced approximately 1.5km apart (some detectors were spaced further apart to avoid human development or agriculture). While detectors were placed alongside roads and trails to allow for vehicle access, roads and trails with curves and branches were selected to best avoid having a bear's home ranges elongated in a consistent direction with respect to arrays. Detectors consisted of an approximately 5 x 5 meter fenced area created by stringing a single strand of barbed wire at a height of 50 cm around trees with partially opened tins of sardines in oil suspended from a board nailed 2.5 meters high on a central tree that was >2 m from the barbed-wire perimeter. Physical capture data from black bears in Ontario showed that the average 1-year old black bear was < 50 cm at the shoulder (MNRF *unpublished data*). Detectors were therefore assumed to exclude cubs and yearlings and samples represent bears >1 year of age. Each week, detectors were visited, hair samples were collected and stored in paper envelopes and detectors were rebaited. To assign an individual and sex to hair samples, we used methods described in Howe et al. (2022).

3.3.3 SECR analysis

SECR model framework — SECR is a hierarchical model composed of two components – a state model and detection model – that are fit to spatial detection histories of animals. The detection model describes the probability of detecting an animal at each detector as a function of distance

from an animal's latent activity center, where an activity center is the centroid or average of the space that an animal occupies during the period in which detectors are active. Parameters g_0 and σ jointly define the detection model: g_0 is the baseline detection probability of a trap placed at an animal's activity center; σ describes the spatial scale over which detection probability declines with increasing Euclidean distance between the detector and an animal's activity center. The state model describes the distribution of unobserved locations of activity centers within the state space. The state space is a discretized plane that includes all detectors buffered by an area large enough to include all animals at risk of being detected by any detectors, where areas of non-habitat can be removed. This portion of the model can be formulated as a homogeneous Poisson point process where activity centers are distributed randomly according to the intensity parameter across the state space, or an inhomogeneous point process can be used in which the intensity parameter is modeled as a function of spatially referenced covariates and a vector of regression coefficients β. In this analysis, we took the latter approach, examining the influence of a suite of spatially reference covariates on local density within each array of detectors to explain variation in density across a study area.

All analyses were implemented through R 4.0.4 using the 'secr' package version 4.3.3 (Efford 2020a) and ArcMap version 10.7.1; the following functions are in reference to the 'secr' package. A high-performance computing cluster provided by Compute Canada (computecanada.ca; RRG: hyf-453-ab) was used to simultaneously fit many models because the computationally time of SECR models was prohibitively slow with a stand-alone personal computer.

Habitat data — We used six variables to assess the influence of habitat productivity and human disturbances on black bear density. See Appendix C Section 1 for descriptions of original

datasets and data sources. All covariates were summarized with a 4480 m and 8290 m radius moving window (63 km^2 and 216 km^2 area circle, respectively), selected based on 95% circular space use radius derived from female and male σ estimates ($\sigma\sqrt{5.99}$; Royle et al. 2014) from an initial analysis of the MNRF data and SECR studies in Ontario (Obbard et al. 2010, Howe et al. 2013, Howe et al. 2022). A moving window analysis calculates the average of the set of pixels within a specified radius of a focal pixel, with the result representing the mean attribute value of the covariate within the circular landscape (Apps et al. 2004). Therefore, these values represent the broader scale at which wide-ranging bears may respond to habitat conditions based on the area they use during the study period. Processed resolution of layers were set at 500 m to reduce computation time, excluding human settlement, which was quantified at 10m because decreasing the resolution resulted in spatial rasters with little variation.

Landcover classes were obtained at 30 m resolution from the North American land change monitoring system based on 2015 Landsat satellite imagery (NALCMS 2020). Land cover classes were selected and grouped into four categories that were potentially important to black bears (agriculture, deciduous forests, coniferous forests, mixed forests) based on previous black bear SECR studies (Sun et al. 2014, Humm et al. 2017, Welfelt et al. 2019). We developed separate layers for each category. To do so, raster cells were coded with the focal cover layer (e.g., mixed forest) as 1 and all other cover types as 0 and the mean value of each cell was calculated using a circular moving window. The produced layers therefore represent the percentage of the landcover class within the circular moving window.

Anthropogenic covariates included density of roads and human settlement. Roads current to 2021 were obtained from the Statistics Canada National Road Network (Statistics Canada 2022). Roads classified as freeway, highway, collector, arterial, local, ramps and resource and

recreation were combined into a layer and female and male road length was calculated using a radius of 4480m and 8290m, respectively, to obtain the density of roads (km/km^2) surrounding each pixel. As a proxy for anthropogenic presence, a human settlement raster layer was created using data from the global human settlement built-up grid (GHS-BUILD-S2 R202A). This global dataset represents the build-up area (i.e., constructed structures in the forms of buildings within a pixel) expressed in terms of a probability density grid at 10 meters spatial resolution. The data were derived from a Sentinel-2 global image composite for 2018 using Convolutional Neutral Networks (Corbane et al. 2020).

We considered the normalized difference vegetation index (NDVI) as a potential covariate representing coarse vegetative productivity. NDVI is widely used in animal ecology as an index of vegetative productivity (Pettorelli et al. 2011) and is a continuous representation of vegetation as opposed to the discretized landcover classes. However, in Ontario, important green vegetation for black bears during the spring and early summer (e.g. clover, common dandelion, hawkweed; Romain et al. 2013) are typically associated with regenerating clear-cuts and disturbed areas such as roads and gravel borrow pits that typically exhibit lower NDVI values. Thus, we considered NDVI as unlikely to represent important black bear foods during our study period and was additionally likely to be confounded by other processes and patterns, such as forest cover and types (see Appendix C for further discussion of NDVI and SECR model results that including NDVI as a density covariate).

State space — The state space consists of a discretize plane of a mesh of points where latent activity centers can occur, over which density is estimated. We defined the state space for each study area as a 500m resolution raster that extended 20 km around all detectors. This buffer falls within the 3 - 4σ_{max} recommendation to ensure that any animal with an activity center on the

edge or outside of the state space has negligible probability of capture (Royle 2014, Efford 2019). Although excessive for most females, using an area of integration too small can positively bias density estimates, whereas using a too large an area does not as density estimates asymptote with larger buffer widths (Royle et al. 2014). During our analysis, if a larger buffer was suggested using the function 'suggest.buffer', this value was used. We intentionally selected a fine grid point spacing because we were interested in bears' response to fine-scale habitat heterogeneity. Vector data representing Canadas's surface waters as of 2019 were collected from Natural Resources Canada CanVec Series Hydrographic Features (Natural Resources Canada 2019) and permanent waterbodies were excluded as non-bear habitat from each state space mask. Pixel values from the spatial rasters were assigned to each pixel of the state space mask to use as a covariate for the density model. Covariates were standardized by subtracting the mean and dividing by the standard deviation to facilitate model convergence and ensure resulting coefficients were directly comparable (Grueber et al. 2011).

3.3.4 Two stage SECR models

Data were analyzed using two different approaches. First, we fit sex-specific SECR models to datasets from each independent study area (hereafter, study area approach). This approach minimizes spatial heterogeneity in the detection parameters and provides results meaningful to each individual study area but is more subject to influence from small sample sizes. Secondly, we pooled datasets from study areas in the same forest region to create four sex-specific multi-session SECR datasets (hereafter, pooled approach): GLSL male; GLSL female; boreal male; boreal female. For the latter approach, we treated study areas as sessions when fitting SECR models and simultaneously estimated parameters using the combined datasets. The pooled approach provides more power to detect and model sources of variation in density and detection,

although potentially smoothing over differences among study areas. Taken together, these two approaches allow for robust inference to the spatial factors influencing density. For the pooled approach, we built separate models for each forest region due to differences in bear movements and home ranges size between the forest regions (Howe et al. 2013). Further, factors shaping density markedly vary across the two forest regions; the GLSL is more densely populated with generally higher natural productivity and the boreal is characterized by lower human influences and productivity. To reduce challenges of modeling spatial effects due to data sparsity, for both analyses we excluded study-area and sex-specific datasets with less than 20 recaptures (recommended minimum number of recaptures for SECR models; Efford et al. 2004, Sun et al. 2014). Despite this, the study area data were fit to relatively sparse, if not insufficient, datasets coupled with little variation in the covariate values that resulted in numerous models failing to converge or yielding inflated estimates of variance. Consequently, we only focus on the pooled approach in the following sections. Although pooling of datasets may risk masking spatial heterogeneity that could lead to spurious or weak and inclusive results (Lesmerises and St-Laurent 2017), it does protect against small sample variance. Our overall conclusions of black bears' responses to habitat features were generally consistent between the study area and pooled analyses (full methods and results for the study area analyses are provided in Appendix C Section 3). Therefore, we feel this decision did not unduly impact our overall inferences.

As fitting SECR models can be time and computationally intensive, we fit models in a two-stage approach following other bear (*Ursus* spp.) SECR studies (Morehouse et al. 2016, Evans et al. 2017, Sun et al. 2017, Lamb et al. 2018, McLellan et al. 2019). In the first stage, we fit four models where density was assumed constant (i.e., a homogenous Poisson point process was assumed for the state model). We fit a null model and combination of models where g_0 varied as

a function of a trap-specific response (*bk*) and σ by sampling occasion (*t*). Differences in g_0 and σ among sex and forest types were accounted for as models were fit to sex-and-forest region specific datasets. We intentionally kept our detection models simple because preliminary runs of more parameterized detection models often failed to converge. Despite this, the simpler detection models still provide a reasonable representation of bear behaviour. Akaike's Information Criterion corrected for small sample size (AIC_c) was used to evaluate the relative support for each of the competing detection models (Hurvitch and Tsai 1989, Burnham and Anderson, 2002).

In the second stage, the most parsimonious detection model was used in the subsequent runs of the full SECR models with density covariates (i.e., with an inhomogeneous Poisson point process). Instead of evaluating the full set of density models including all additive combinations of covariates, we constructed a set of *a priori* univariate and multivariate models including covariates based on previous studies and black bear biology and including only two forest cover types in the same model. Covariates on the density model included percent forest types (coniferous, deciduous, mixed), percent agriculture land cover, human settlement density and road density. Further, as correlation between variables can lead to unstable models with decreased precision that may produce erroneous estimates, pairs of covariates were tested for Pearson's correlation coefficient $|r| \geq 0.7$ (Dormann et al. 2013; Appendix C Section 5: Table C.5.2). We experienced challenges with convergance of some of the models in this second stage using the defult Newton-Raphson optimizor. Thus, to confirm that models had converged, all models were re-fit sequentially four times, using two optimizors (the defult Newton-Raphson and more robust Nelder-Mead) with the starting values set as the estimates from the previous fits. Models were considered to be converged when log likelihoods and β parameter coefficient

estimates stabilized to consistent values. For both the detection and density models, β estimates and their SE and confidence intervals were visually inspected for unreasonably large estimates that could indicate failure to converge and overparameterization or non-identifiability (O'Brien and Kinnaird, 2011). Effects were evaluated on the coefficient slope (i.e., β estimate) and were considered significant if the 95% confidence intervals did not overlap 0 (Welfelt et al. 2019).

3.4 Results

3.4.1 Summary of hair collection and capture statistics

Between 2017 and 2019, we identified 3857 individuals (1645 female; 2212 male) from 12731 detections (5484 female; 7247 male). The number of individuals, detections, and recaptures in each study area ranged from 8 to 111 (4 - 52 female; 3 - 59 male), 9 to 485 (5-165 female; 4 - 344 male) and 1 to 407 (0 - 134 female; 0 - 293 male), respectively. See Appendix B for capture statistics summary. Out of the 164 datasets from 78 study areas, we retained datasets from the last year of sampling for three study areas sampled across multiple years. A further 32 datasets from 20 study areas were omitted due to insufficient recaptures (16 female datasets and 16 male datasets) and two datasets from one study area due to data quality; see Appendix B for datasets. As a result, models in both analyses were fit to 122 datasets from 65 study areas.

3.4.2 SECR detection models and habitat effects on density

Female GLSL and boreal models included 20 and 41 study areas, respectively. Male GLSL and boreal models included 19 and 42 study areas, respectively. For detection models fit in the first stage of our modeling approach, the top ranked ($\Delta AIC_c = 0$) male GLSL and boreal and female boreal models included a behavioural response (*bk*) on g_0 and sampling occasion (*t*) effect on σ. The top ranked-model for female GLSL included a trap-specific behavioural response (*bk*) on g_0 and constant σ. See Appendix C Section 5 for AIC_c detection model results.

Models in the second stage successfully converged, indicated by consistent log-likelihood and β estimates, after the second fit of the Nelder-Mead optimzor for the boreal models and the first fit of the Newton-Raphson optimizor for the GLSL models. The direction and magnitude of β parameter estimates were similar between the univariate and multivariate models (Appendix C Section 4); thus for simplicity we only discuss the univariate models when making inferences in the following sections.

In the GLSL, for both males and females, deciduous forests were negatively associated with density and coniferous forests positively associated, with both effects being significant (Table 3.1). Human density was negatively related to male density and mixed forests negatively related to female density with both effects being significant. The remaining covariates in the GLSL models were negatively associated with density; however, the 95% confidence intervals included zero that indicated non-significant effects (Table 3.1). For both sexes in the boreal forest, roads and mixed forests were negatively associated with bear density (Table 3.1). Males in the boreal also had a significant negative and positive effect of humans and deciduous forests, respectively (Table 3.1); females displayed the same pattern, but effects were non-significant, and females had a significant positive effect on crops. There was also a non-significant negative association between coniferous forests and density for both sexes. The importance of the covariates, as indicated by the magnitude of the β coefficients, and their uncertainty varied by forest region and between males and females (Table 3.1).

Table 3.1. β parameter estimates, standard errors (SE) and 95% confidence intervals (lower [LCL] and upper [UCL] confidence limits) of univariate SECR density models fit to female and male black bear capture-recapture datasets in the Great Lakes – St Lawrence (GLSL) and boreal forest regions, Ontario, Canada, 2017–2019. Bold text indicates models with significant β parameter estimates (95% confidence intervals do not include 0). β estimates were standardized to allow for covariate comparison within study area by sex.

Predictor	Female GLSL				Female Boreal			
	β estimate†	**SE**	**LCL**	**UCL**	**β estimate†**	**SE**	**LCL**	**UCL**
Human	-0.158	0.131	-0.415	0.100	-0.105	0.194	-0.485	0.276
Road	-0.063	0.051	-0.162	0.036	**-0.403**	**0.073**	**-0.546**	**-0.261**
Coniferous forest	**0.214**	**0.051**	**0.114**	**0.315**	-0.051	0.040	-0.130	0.028
Deciduous forest	**-0.124**	**0.050**	**-0.223**	**-0.025**	0.070	0.036	-0.002	0.141
Mixed forest	**-0.090**	**0.045**	**-0.178**	**-0.003**	**-0.097**	**0.035**	**-0.166**	**-0.028**
Crop	-0.077	0.050	-0.175	0.021	**0.238**	**0.073**	**0.096**	**0.381**
Predictor	**Male GLSL**				**Male Boreal**			
	β estimate†	**SE**	**LCL**	**UCL**	**β estimate†**	**SE**	**LCL**	**UCL**
Human	**-0.245**	**0.103**	**-0.448**	**-0.043**	**-0.287**	**0.125**	**-0.532**	**-0.043**
Road	-0.068	0.052	-0.170	0.034	**-0.152**	**0.046**	**-0.241**	**-0.062**
Coniferous forest	**0.263**	**0.046**	**0.173**	**0.353**	-0.043	0.030	-0.101	0.016
Deciduous forest	**-0.189**	**0.047**	**-0.282**	**-0.096**	**0.106**	**0.028**	**0.051**	**0.161**
Mixed forest	-0.034	0.042	-0.117	0.049	**-0.103**	**0.027**	**-0.156**	**-0.049**
Crop	-0.092	0.051	-0.193	0.009	0.034	0.063	-0.089	0.157

† Baseline density on the log scale is reference category; all covariates standardized (mean = 0, standard deviation = 1) such that the β parameter estimate indicates the change in the standard deviation of the baseline density (bears/hectare) on the log scale for one unit change in the standard deviation of the covariates value.

3.5 Discussion

Understanding how wildlife species are impacted by human modification of landscapes and changing environmental conditions is essential for conservation and management of large-bodied and wide-ranging species, such as the American black bear. Here we leveraged a large-scale genetic spatial-capture recapture dataset of black bears and SECR models to uniquely capture the relationship between fine-scale habitat heterogeneity and the species densities across an expansive spatial extent. Our findings indicate a negative impact of roads and human settlement on the distribution of black bears, with both male and female bears at higher density in areas with lower road density in the boreal forest and male bears being found in areas with lower human impacts across the province. Moreover, black bear association with agriculture and forest types varied by forest region and followed patterns reflecting what habitat types and resources were likely to be most limiting to the species during the spring and early summer.

Numerous studies have examined the influence of human disturbances on bear populations that have in part been motivated by the ongoing expansion of human activities into wildlife habitats. We found that the influence of roads mirrored many other large carnivore SECR studies where roads were associated with reduced bear densities (Humm et al. 2017, Lamb et al. 2018). These results also support other studies, conducted using radio collaring techniques, that show fine-scale avoidance of roads by bears (Kasworm and Manly 1990, Waller and Servheen 2005). Such trends may arise through a combination of mortality from vehicle collisions, avoidance linked to auditory and visual effects of vehicle traffic, barriers to movement, and increased human access leading to heightened hunting and human-bear conflicts (Hostetler et al. 2009, Northrup et al. 2012, McFadden-Hiller et al. 2016). Clearly, our results show that, at least in the boreal forest, roads are a strong driver of fine-scale distribution of black bears. Interestingly, the

effect of roads was not significant in the GLSL. The GLSL is substantially more populated, with higher road density on average. Road density across the state space of all study areas in the GLSL and boreal were 0.42 and 0.20 km/km^2, respectively. The non-significant effect of roads in the GLSL could possibly reflect the pervasive nature of roads in this region, acclimatization of black bears living in more developed areas (Zeller et al. 2019) or bears frequenting roads where spring-green up occurs in the early spring (Mosnier et al. 2008, Tigner et al. 2014). Alternatively, the difference in road response across forest regions could be related to bear hunter behavior in the spring. Because there are fewer roads in the boreal forest, harvest activity may become concentrated along the few roads there are, leading to depressed local densities. However, this inference is speculative and warrants further research.

Although there is consensus that bear density is typically higher in areas with less humans, studies report mixed results in human-dominated landscapes. Human settlement has been correlated with higher densities (Beckmann and Berger 2003, Fusaro et al. 2017), lower densities (Humm et al. 2017, Welfelt et al. 2019, Lamb et al. 2020) and linked to changes in natural food availability (Laufenberg et al. 2018) and housing density (Evans et al. 2017). Further, human settlements are often a source of food for bears. We found a negative association between human settlement and black bear densities; however, the effect was significant only for males. The difference between sexes could be in part due to male black bears in Ontario being harvested more than females; males are more likely to come into conflict with people (Kolenosky 1986; Obbard et al. 2017). We did not sample in areas with high human development (i.e., urban and exurban developments) and therefore we have little information on bear responses to high human activity and cannot make inference to more heavily developed areas. While it is optimistic that sampling with baited-barbed wire hair corrals near more heavily developed areas could occur

safely, the use of fine-scale telemetry data could help address this knowledge gap. Such information could enhance our understanding of black bear responses to the compounding effects of roads and human development to target land use management and bear safety outreach programs.

Black bears' association with agricultural land cover varied by forest region; density was positively associated with crops in the boreal and negatively, but not significantly, associated in the GLSL. This aligns with previous research demonstrating that black bears' selection for agricultural areas varies spatially and by individual, season and time of day (McLaughlin et al. 1994, Johnson et al. 2015, Zeller et al. 2019). Our results suggest behavioural trade-offs possibly related to gradients in productivity and human disturbances across the broad forest regions. In the less productive boreal forests where food is more limiting, black bears may seek out apiaries and cultivated crops as a supplemental food source (Ditmer et al. 2016), especially when agricultural areas are on the periphery of bear habitat and contain higher concentrations of foods than surrounding areas. Comparatively, in the GLSL where natural hard and soft mast is more abundant (Potter and Obbard 2017), bears may avoid coming into conflict with humans in agricultural areas (McFadden-Hiller et al. 2016). Furthermore, it is important to note that we assumed our crop covariate includes, to some extent, foods consumed by black bears during our study period; we did not specify the type of crop nor account for if crops were ripe so this assumption may not hold across all study areas and could explain the lack of a significant effects observed in the GLSL.

The contrasting patterns between black bears' association with forest cover types in the GLSL and boreal are consistent with black bear behaviour and gradients of productivity and human disturbances across the province. In the GLSL, black bear density was positively

associated with coniferous forests. While the GLSL has higher productivity, the region is more populated and has higher human disturbances and thus cover habitat may be the primary factor limiting bears. Further, because we sampled during the breeding season, cover may be of high importance to breeding females and all males except for the most dominate, breeding males. Our observed trend contrasts with findings from the lower peninsula in Michigan, USA. In this study male and female black bear habitat selection was positively associated with aspen forests and for females with northern hardwood and mixed hardwood (Carter et al. 2010). We did, however, find a positive association with deciduous forests in the boreal, although not significant for females; nerveless that pattern aligns with reports of black bear avoiding mature coniferous forest at their home-range scale in southern Quebec, Canada (Brodeur et al. 2008). Our findings further align with reports of black bears feeding on willow and aspen leaves in the spring when protein content is high (Poulin et al. 2003, Romain et al. 2013). This finding supports our prediction that density is correlated with forests stands containing greater abundance, diverse vegetative food sources in the less productive boreal forest. The lack of significant association to coniferous forests in the boreal for both sexes could be explained by the study areas being composed of predominately coniferous forests such that bears have little other land covers to select from or that when deciduous forest stands are available, bears seek them out for available foods. Collectively, these patterns in the GLSL and boreal reflect black bear behavioural responses to different habitat types and resources are likely to be most limiting to the species. In the boreal, food is limited and bears thus might be seeking out available food in deciduous forests. Comparatively, in the GLSL deciduous and mixed forests are more common, and food is less limited, and thus bears might be prioritizing the security of coniferous forests where there is still ample food supply.

In line with these patterns in the deciduous and coniferous forests, we expected black bears to seek out mixed forest in less productive boreal forest regions. Interestingly, we found a negative effect of mixed forest on black bears across both the boreal and GLSL regions that does not align with trends of the other forest cover types. This spatial covariate may capture another factor or processes we did not consider, especially provided the consistent effect across the study regions.

3.5.1 Methodological considerations, study limitations and future research

Our results provided further insight into the impact of human disturbances and environmental conditions on a widely distributed and generalist carnivore, yet there are limitations to the inferences that can be drawn from this study. A prevalent challenge of both analyses was selecting an appropriate model structure for the datasets, highlighting a long-standing challenge in statistical ecology (Brewer et al. 2016). It was possible that correlation among spatial predictors (although $|r| < 0.7$; Dormann et al. 2013) influenced our multivariate model results (Graham et al. 2003). Moreover, data sparsity paired with minimal variation in some covariates limited the complexity of models we could run without risking overparameterization, issues with convergence or models failing to estimate parameters (Schmidt et al. 2022). To that end, our models likely omitted important predictors of density, and their interactions, and thus were unable to fully capture the complexity of carnivore habitat-relationships linked to fine-scale factors. Further, assessment of model convergence was challenging and imperfect, especially provided the inflated SE and CI for some of the more parameterized models that suggests nonconvergence or collinearity (Gruber et al. 2011, Dorman et al. 2013). Considering the complexities involved with fitting multivariate models, we therefore based our main results on univariate models from the pooled analysis. Nonetheless, we note that a limited number of multivariate models showed similar effects as the univariate models (Appendix C Section 4) and

trends from the landscape and pooled analyses were similar; therefore, we feel that excluding landscape analysis and multivariate models had minor impacts on our overall inferences.

It is possible our study was biased towards sampling bears with roads in their home ranges because we placed our detectors alongside roads and trails. While raised as a possible source of bias (Sadeghpour and Ginnett 2011), the influence of detectors' proximity to roads has yet to be fully investigated for black bear and warrants further research for the species and other elusive carnivores living in multi-use landscapes. However, because we found a consistent negative relationship between roads density and bear density it suggests that if we sampled bears more tolerant to roads, that the true response to these features is even stronger than what we documented. Additionally, to simplify the number of parameters in our models we grouped all types of roads into one covariate. Investigating the influence of specific road types or vehicle traffic would improve our understanding and prediction of bears responses to specific road features that could be leveraged for more targeted land-use and recreation planning. However, it is unlikely that SECR data are sufficiently fine-scale to show relationships with these sorts of data and thus other finer-scale data, such as telemetry data, would be needed.

3.6 Conclusions

Effective management of carnivores in human-modified landscapes will increasingly depend on monitoring population trends and understanding and predicting population responses to changing land-use and environmental conditions. Similar to many carnivore studies, we demonstrate a negative impact of human disturbances on black bear densities. These results support the long history of research showing roads in particular, often related to timber harvest and other industrial activities, can displace bears, whether due to direct mortality or behavioral effects. The effect of agriculture and forest types on black bear populations varied by forest

region and followed patterns reflecting differences in habitat types and trade-offs between food resources and avoidance of human activities, suggesting nuance in the manner in which bears cope with human impacts to the environment. Collectively, our findings highlight the marked spatial variation in environmental and anthropogenic drivers of density across a species' range and demonstrate how populations in different landscapes may experience impacts from drivers of density in different ways. This variation, in turn, suggests complexities in the way bears will likely respond to climate and as land-use change. Studies have predicted shifts in the distribution of bear vegetative food resources and habitat quality, as well as interactions with humans under a range of climate changes (Su et al. 2018, Penteriani et al. 2019, Ashrafzadeh et al. 2022). Thus, as climate change alters broad forest characteristics and land-use change continues to fragment and alter habitats, our results suggest that bears will respond in nuanced ways depending on how these factors alter the processes most limiting on the species locally. As such, continued monitoring of populations is key to understanding how and whether black bears can cope with large scale global change.

This complexity and scale-dependent nature of black bear habitat-relationships reinforces the importance of conducting studies for wide-ranging and generalist species across large spatial extents to fully capture heterogeneity in mechanisms shaping density. Our findings further contribute to the growing body of literature investigating changes in carnivore density in relation to landscape-level shifts in habitat conditions and human disturbances. Such knowledge is essential for managing and conserving carnivores in increasingly human-modified landscapes.

Chapter 4: Factors shaping black bear densities at large spatial extents: linking large scale monitoring and spatially explicit capture-recapture

Brynn A. McLellan[1], Eric Howe[2], Joseph M. Northrup[1,2]

[1]Environmental and Life Sciences Graduate Program, Trent University.

[2]Wildlife Research and Monitoring Section, Ontario Ministry of Natural Resources and Forestry

.

4.1 Abstract

Understanding the spatial ecology of large carnivores in increasingly human modified landscapes is critical for conservation and management. Complementary to this need are robust monitoring and statistical techniques to understand factors shaping population densities across the species' large ranges. Here we analyze three years of a genetic capture-recapture dataset of 3857 individual black bears over 498, 022 km^2 of Ontario, Canada. Using spatially explicit capture-recapture models (SECR), we examine the influence of forested land cover and human influences, representing bottom-up and top-down processes, in shaping population densities across the province and forest regions. We propose a two-step modeling approach that allows for modeling the effect of spatial covariates on density when it is computationally restrictive to use data-intensive SECR models common to such large scale analyses. Black bears' association with human influences and forested land cover varied across spatial scales reflecting differences in gradients of habitat quality and human disturbances and bear ecology. At the provincial scale, black bear density was largely driven by forested land cover, where higher densities were associated with more productive deciduous forests. Associations of black bear density within forest regions reflected trade-offs between intensity of human disturbances and productivity gradients. More bears were harvested in areas of higher bear density, expect for lower quality habitats where male densities were potentially supressed by harvest. These findings highlight the scale-and-context dependent nature of black bear density-habitat relationships and underscores the importance of conducting studies for wide-ranging and generalist species across large extents to capture heterogeneity in factors driving population processes. Such information is important for management of wildlife species in habitats undergoing landscape-level shifts in land-cover and human disturbances that can drive variability in bottom-up and top-down processes.

4.2 Introduction

Human-induced changes to terrestrial ecosystems are intensifying, with widespread impacts on large-bodied mammalian carnivores (hereafter, carnivores) that have contributed to population declines and range contractions in recent decades (Ceballos et al. 2002, Laliberte and Ripple 2004, Márquez et al. 2022). Due to the importance of carnivores in structuring terrestrial ecosystems and providing socio-economic benefits (Ripple et al. 2004), quantifying the impacts of changing land-use and climatic conditions on their abundance and distribution are increasingly important for informing wildlife management and conservation.

Understanding what factors regulate and limit population density, specifically bottom-up food resources and top-down mortality, is the focus of many carnivore monitoring and management programs. However, understanding the relative importance of these processes remains a long-standing subject of considerable debate among ecologists (Hunter and Price 1992, Sinclair and Krebs 2002). Studying the relationship between bottom-up and top down dualities and population density is not always straight forward (Rettler et al. 2021); both processes can simultaneously influence population processes, where the magnitude of their effects can differ spatially and temporally and shift with changes in habitat quality and human disturbances (Fretwell and Lucas 1969, Turner 1989). For wide-ranging species that occur over large areas, characterization of bottom-up and top-down factors across large spatial extents are often required to fully capture heterogeneity in these factors. However, while these population-level assessments are typically sought after in ecology, they remain rare due to the substantial logistical and analytical challenges they present (Jones 2011, Bischof et al. 2020).

Complementary to the need for a better understanding of the drivers of carnivore distribution and abundance are robust monitoring and statistical techniques to estimate population density, a

state variable of interest in many wildlife monitoring, management and conservation programs (Sutherland et al. 2013, Morin et al. 2022). Yet, those tasked with wildlife management and conservation face the long-standing challenge of identifying how to obtain robust estimates of density over large areas (Lamb et al. 2019, Bischof et al. 2020). These challenges are amplified for elusive and wide-ranging carnivores that often exist at low and heterogenous densities and detectability. The ability to estimate wildlife abundance and distribution over large spatial extents has improved with the advent and application of non-invasive sampling coupled with advances in statistical techniques and computing power (Lamb et al. 2019). Spatially explicit capture-recapture (SECR) models are a common approach for modeling wildlife distribution in space, as well as investigating the drivers of this distribution, when animals are uniquely identifiable (Efford 2004, Royle et al. 2014). SECR models pair two spatially explicit sub-models: a detection model, where the detection probability is modeled as a function of a detector's location relative to the estimated center of an animal's space use (i.e., its activity centre), and a density model that uses a spatial Poisson or binomial point process to predict the distribution of animal activity centres within a discretized plane of interests over which density is estimated. The density model can be formulated such that activity centers are distributed randomly, or spatial covariates can be used to model the distribution of activity centers as a function of ecological factors of interest. Covariates can also be attributed to the detection model and typically include individual, detector or temporal factors (Royle et al. 2014).

With over a decade of development, SECR models have become increasingly customizable and flexible to answer a range of research questions including those related to demography, resource selection, space use, and movement and dispersal (see reviews by Royle et al. 2018, Tourani 2021). However, while SECR models offer an intriguing opportunity for assessing

factors influencing population density over large scales, alongside these advancements and more sophisticated analyses come numerous computational and logistical challenges (Stevenson et al. 2021, Howe et al. 2022, Schmidt et al. 2022). When larger landscapes are sampled, heterogeneity in detectability and inhomogeneous density are more likely (Jones 2011). Failing to account for important sources of heterogeneity in the model structure can introduce bias in parameter estimates (Sollmann et al. 2011, Moqanaki et al. 2021, Stevenson et al. 2021, Howe et al. 2022; Chapter 2 of this thesis). To that end, application of SECR models to large scale analyses, such as those fit to large capture-recapture datasets collected across broad areas, are more prone to biased estimates unless models sufficiently capture detection heterogeneity (Howe et al. 2022, Marrotte et al. 2022). Despite the rapid growth in computer processing and ease of parallel processing, SECR models quickly become computationally intensive (Milleret et al. 2019, Morin et al. 2022). In these cases, one alternative is to fit separate models to subsets of data; however, this approach is not always practical as it can lower the detection and recapture information such that it is impossible to estimate parameters. This can lead to issues with precision, and is difficult to account for potential sources of heterogeneity due to the restricted number of parameters that can be included relative to sample size (Stetz et al. 2014, Schmidt et al. 2022). Moreover, models fit to sub-sets of data are subject to influence from small sample sizes such that predictions may not be reliably extended to unsampled areas. Collectively, these issues highlight the ongoing challenge of identifying the optimal trade-off between the size of the datasets, model complexity to account for population heterogeneity, and tractability (i.e., computational resources and run times of models).

American black bears (*Ursus americanus*) are a widely distributed and abundant ursid in North America (Scheick and McCown 2014). Their population dynamics are largely driven by

interrelated bottom-up food availability and top-down mortality that can vary across landscape conditions and time, as well as by sex and individual, among other factors (Baruch-Mordo et al. 2014, Johnson et al. 2015, Evans et al. 2017, Kristensen et al. 2019, Zeller et al. 2019). As with many carnivores, human are often the predominant top-down force influencing black bear survival, directly through hunting or vehicle collisions or indirectly through human-wildlife conflict (Hebblewhite et al. 2003, Gantchoff et al. 2020). Moreover, as humans continue to transform natural landscapes, modification of habitat can increase or decrease important food resources while exposing populations to a mosaic of human mortality risks associated with anthropogenic food sources and overlap between human activities and bear habitat (Treves and Karanth 2003, Laufenberg et al. 2018). As a result, black bears are often the subject of management programs across their range; population information is both challenging to obtain, yet critical for their management and conservation (Hristienko and McDonald 2007, Obbard et al. 2014, Humm and Clark 2021). To that end, black bears present an important case study for assessing the relative influence of top-down and bottom-up forces on carnivore populations.

In this study, we examine the influence of anthropogenic and environmental factors on black bear populations in Ontario, Canada. Over the last two decades, the Ontario Ministry of Natural Resources and Forestry (MNRF) has estimated black bear densities and abundance across the province using genetic spatial capture-recapture surveys in most huntable wildlife management units (WMUs; Obbard et al. 2010, Howe et al. 2013, Howe et al. 2022, Marrotte et al. 2022). These surveys span a gradient in natural productivity and a mosaic of human influences, providing a unique opportunity to capture the effect of spatial heterogeneity on factors structuring black bear densities across the population's range. These spatially expansive

studies are particularly important for generalist and wide-ranging species, such as black bears, that can take advantage of an array of habitat conditions.

Using three years of black bear genetic spatial-capture recapture data collected in the boreal and Great Lakes – St Lawrence Forest regions of Ontario (Rowe 1972), we test the influence of forest type, harvest, human influence, and roads, representing bottom-up and top-down process, on variation in black bear densities across the province and within forest regions. Further, this work was in part motivated by the need to explore alternative modeling approaches to computationally and data-intensive SECR models common to large capture-recapture datasets. Thus, we used our expansive dataset to assess the trade-offs of different modeling approaches. Our study not only provides information from one of the largest genetic black bear datasets but provides insight to the opportunities and difficulties of using large capture-recapture datasets within a SECR framework for large-scale monitoring and management.

4.3 Methods

4.3.1 Study area

Our study spanned the boreal and Great Lakes – St Lawrence Forest regions (GLSL; Rowe 1972) in Ontario, Canada, encompassing a 498, 022 km^2 region of continuous black bear habitat (Figure 4.1). The region comprised mostly forests, but also included shorelines, grasslands, wetlands, human settlement, and agriculture. Mixed woods and deciduous stands dominated the GLSL and common tree species included sugar maple (*Acer saccharum),* red oak (*Quercus rubra),* yellow birch (*Betula alleghaniensis*), beech (*Fagus grandifolia),* hemlock (*Tsuga canadensis),* white pine (*Pinus strobus),* trembling aspen (*Populus tremuloides*), and balsam fir (*Abies balsamea*). Coniferous and mixed wood forests dominated the boreal region; common coniferous tree species included jack pine (*Pinus banksiana),* black and white spruce (*Picea*

mariana, Picea glauca), balsam fir (*Abies balsamea*) and in wetter sites tamarack (*Larix laricina*) and less commonly, eastern white cedar (*Thuja occidentalis;* Perera et al. 2000). Further, white birch (*Betula papyrifera*) and trembling aspen were common hard wood species. A gradient in climate exists across the region: southern Ontario is generally characterized by a humid continental climate, with cold winters and warm summers and northern Ontario by a subarctic climate with colder winters and cooler, shorter summers (Drever et al. 2010). Compared to the GLSL, boreal forests experience more extreme seasonal variation in climate, with a shortened growing season and generally lower productivity.

The study area was a multi-use landscape that includes recreation, forestry, agriculture, and mining. Medium sized cities are dispersed through the study area, with most of the human population and development in the southeast of the province. Harvest of black bears was permitted in designated WMUs during open seasons in the fall and spring, with the latter being previously reinstated in some WMUs in 2014 and across Ontario in 2016 following the 1999 moratorium (Poulin et al. 2003, Lemelin 2008, Northrup et al. *in press*). Females with cubs of the year are protected from harvest during the spring, but not the fall hunting season.

4.3.2 Sampling design

Black bears were sampled across 78 study areas over five consecutive weekly sampling occasions in the spring and summer from 2017 to 2019 (sampling occasions range from May 21st to June 30th). We assumed resident populations were sampled because black bears typically focus their movements within smaller areas and occupy smaller home ranges during this period, after which they undertake extensive forays in search of seasonally available foods (Howe et al. 2013). Study areas consisted of curvilinear arrays of roughly 40 barbed-wire hair corrals baited with partially opened tins of sardines in oil (hereafter detectors; Woods et al. 1999). Adjacent

detectors were spaced approximately 1.5 km apart and were placed alongside roads and trails to allow for vehicle access; roads with curves and branches were selected to avoid having bears home ranges elongated in same direction as an array. Detectors consisted of an approximate 5 x 5-meter fenced area of a single strand of barbed wire at a height of 50 cm around trees. This height corresponds with physical capture data indicating an average 1-year old black bear in Ontario is < 50 cm at the shoulder (MNRF *unpublished data*). Samples are assumed to represent bears >1 year of age. Detectors were visited and checked for hair samples at roughly 1-week intervals and rebaited. Using methods detailed in Howe et al. (2022), individual and sex were assigned to hair samples.

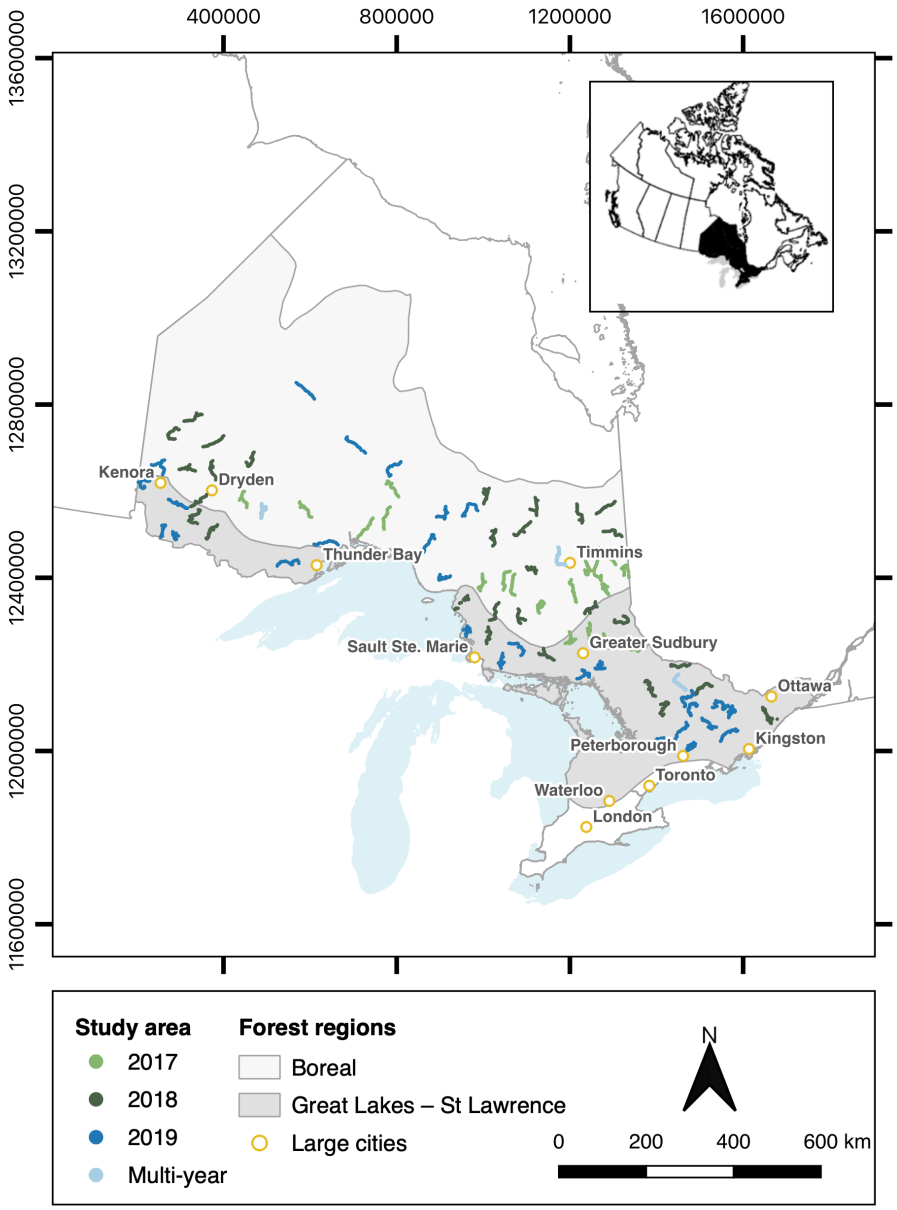

Figure 4.1. Location of arrays of baited barbed wire hair corrals across the Great Lakes – St Lawrence and boreal forest regions in Ontario, Canada where black bear hair samples were collected between 2017 – 2019. At this scale, arrays appear as thin colored lines.

4.3.3 SECR analysis

4.3.3.1 Habitat and harvest data

As we were interested in broad-scale patterns influencing black bear density, for each covariate we quantified a single value for each study area. We selected habitat covariates documented to be biologically important for black bears and for which there was sufficient variation across the study region to allow for model convergence and meaningful inference. All covariates were quantified within a buffer surrounding each array of detectors. We delineated the buffer size based on the biology of our species and used raw movement data from the MNRF capture-recapture datasets (i.e., the mean maximum straight-line distance between detections of an individual). To explore the distance over which human and environmental factors may affect the distribution of black bears' we tested three buffer sizes corresponding to the median, 62.5% and 75% quantiles of the observed range length for each sex (Appendix D Section 2 for further details). Because all covariates were highly positively correlated across buffer widths (range r = 0.95 – 1*;* mean r = 0.99*;* Appendix D Section 2: Table D.2.2), we used the 75% quantile buffer width of 4430m and 8740m for females and males, respectively. Out of our tested buffers, these values were most similar to spring 95% utilization distribution estimates of female black bears in boreal forests of Ontario (see Appendix D Section 2 for further details). Using this buffer approach resulted in sex and study-area specific values for each covariate.

We were interested in two broad spatial classes to represent top-down and bottom-up processes, respectively: (1) human disturbances; and (2) forest regions. See Appendix D Section 1 for description of covariates and original data sources. Covariates representing human disturbances included roads, a human influence index (HII) and black bear harvest. The HII dataset is a satellite-derived aggregated ranking of nine global data layers covering human

footprint, produced by the Wildlife Conservation Society and the Columbia University Center for International Earth Science Information Network (WCS and CIESIN 2005). Roads current to 2021 were obtained from the Statistics Canada National Road Network (Statistics Canada 2022) and classified as freeway, highway, collector, arterial, local, and resource and recreation and combined into a layer to calculate the density of roads (km of roads/km^2) for each buffer (i.e., total length of roads within the buffer divided by area). To represent harvest, we divided the average annual number of bears harvested in each WMU by the area of the WMU and averaged this value over the previous seven years, or the approximate species' generation time (Onorato et al. 2004)

Natural productivity varies across forest regions in Ontario. Because we were interested in capturing broad-scale habitat patterns, we used landcover classes from the North American land change monitoring system based on 2015 Landsat satellite imagery as a coarse proxy for productivity (NALCMS 2020). Selected land cover classes were grouped into deciduous and coniferous forests. For each class we developed separate raster layers by coding the focal cover layer as 1 and all other cover types as 0. We then calculated the mean value of each cell within the buffer such that the produced layers represented the average percentage of the landcover class (either deciduous or coniferous) within the buffer.

We assessed pairwise correlations between all covariates and ensured no pairs were correlated at $|r| > 0.6$ (Dormann et al. 2013). Covariates were standardized by subtracting the mean and dividing by the standard deviation to ensure resulting coefficients were directly comparable. Spatial analyses were implemented through R 4.0.4 and ArcMap version 10.7.1.

4.3.3.2 SECR Model

We estimated black bear densities as a function of spatially referenced covariates using likelihood-based SECR models in the R package 'secr' version 4.3.3 (Efford 2020a; Efford et al. 2004, Borchers and Efford 2008). SECR models comprise a spatial model of detection and a spatial state model of the population that are jointly fit to capture-recapture histories of detected individuals. The state model describes the unobserved distribution of activity centers across a landscape, where each animal is represented by an activity center that is the centroid or average of the space that an individual occupies during sampling. Location of activity centers are distributed over a two-dimensional plane, referred to as a state space, large enough that animals outside the state space are not detected and typically delineated by adding a buffered area around the detectors. Activity centers may be distributed randomly across the state space as a realization of the spatial Poisson or binomial point process, or an inhomogeneous point process can be used in which activity centers are distributed as a function of spatially referenced covariates. Here we took the latter approach, allowing activity centers to be distributed across the state space as a function of the additive effects of road density, human influence index, harvest density and percent coniferous and deciduous forests. We defined a discrete state space for each study area as a 1km resolution raster that extended 20 km around all traps, excluding permanent waterbodies as non-bear habitat. This buffer represents the extreme edge of detection for individuals in our study areas and falls within the 3 - 4σ_{max} buffer recommendation (Royle 2014, Efford 2019). We verified that using a 1km grid point spacing had negligible effects on density estimates and used the function 'suggest.buffer' to verify that 20km was an appropriate buffer width; if a larger buffer was suggested, this value was used. The detection model requires two parameters: g_0 that describes the probability of detection for an animal with a detector placed at its center of activity,

and σ that describes the spatial scale over which detection probability declines with increasing Euclidean distance between the detector and activity center. We allowed g_0 to vary as a function of a trap-specific response (*bk)* and study area, and σ by sampling occasion (t), linear time trend over occasions (T), study area, and forest region.

To account for differences in movement between males and female bears, sex-specific datasets from study areas were analyzed simultaneously using multi-session models where study areas were modeled as sessions. This approach allowed for data to be pooled across study areas to examine the overall effect of the covariates on population density. Data were analyzed using two approaches: first, all datasets were combined to create two sex-specific SECR models (hereafter, pooled approach), then datasets from study areas in the same forest region were pooled to create four sex-specific SECR models (hereafter, forest region approach). Because data sparsity can introduce challenges with convergence of highly parametrized models, we excluded sex and study-area specific datasets with less than 20 recaptures following the recommended minimum number of re-captures for these types of models (Efford et al. 2004, Schmidt et al. 2013, Sun et al. 2014). Additionally, for study areas sampled across multiple years we retained datasets only from the first year of sampling.

We defined a candidate set of models that included the additive effect of all density covariates and combinations of detection covariates, excluding the forest region covariate for the forest region approach and repetitive covariates for the pooled approach (i.e., forest region and study area; for complete list of models see Appendix D Section 5: Table D.5.1). Akaike Information Criterion corrected for small sample size (AIC_c) was used to select the most parsimonious model for the pooled approach. Because we were interested in comparing model estimates between the pooled and forest region models, we used the most parsimonious model

structure identified in the pooled model approach for the forest region models to maintain consistency. Models were fit maximizing the full likelihood for proximity detectors and using a half-normal detection function. As computation time of SECR models was prohibitively slow with a stand-alone personal computer, a high-performance computing cluster provided by Compute Canada was used to simultaneously fit many models (computecanada.ca; RRG: hyf-453-ab).

We inspected coefficient estimates (β) and their standard errors (SE) for unreasonably large values that may indicate converge issues (Gimenez et al. 2004, O'Brien and Kinnaird 2011). Due to uncertainty with convergence of some models, all models were re-fit sequentially up to ten times, using the more robust Nelder-Mead optimizer, with the starting values set as the estimates from the previous fits. Models were considered converged when the log likelihood values stabilized and β estimates were similar. We evaluated effects based on the β values and considered effects to be significant if the 95% confidence intervals did not overlap zero.

4.3.4 Two step modeling approach

The above approach was computationally intensive and, in many cases did not allow for the maximum complexity in detection models to be fit across study areas. As such, we explored two different two-stage approaches to assessing the influence of our spatial covariates on density. First, density estimates were derived using single-session SECR models fit to each study area and sex separately. We used a simple state model where density was estimated using a homogeneous Poisson point process. We allowed the detection model parameters g_0 to vary as a function of a trap-specific response (*bk)* and σ by a linear time trend over occasions (*T*). Models were fit maximizing the conditional likelihood for proximity detectors and density was derived as a parameter using the Horvitz-Thompson-like estimator (see Borchers and Efford 2008). We

compared the fit of models using AIC_c and retained the top ranked model to estimate density. See Appendix D Section 4 for further details. Following density estimation, we fit sex-specific generalized linear models (GLM) in R with a gamma error distribution and log-link function. Female and male estimates of black bear density at each study area were used as the response variable, with the same spatial covariates as the SECR models, above, as the explanatory variables. We fit 6 models: 1 each to the pooled datasets for each sex and 1 model for each sex and forest region (either boreal or GLSL) combination.

The GLM approach does not account for uncertainty in the density estimates, despite the fact that such uncertainty exists. In our second two-stage approach, we then used Monte Carlo (MC) sampling to assess the influence of density estimates on the β coefficient estimates. The mean and standard error of the SECR derived density estimates for each sex and study area were used to generate lognormal distributions. We then sampled a random variable from these distributions as the response variable in the GLM model. We generated 1000 Monte Carlo samples from each distribution and refit the GLM to each dataset. The resulting distribution of coefficient estimates represents uncertainty in the mean effect of each covariate due to uncertainty in density estimates. We derived 95% percent confidence intervals from the resulting distributions of coefficients for each spatial covariate.

4.4 Results

4.4.1 Capture summary

Over the course of three years, we identified 3857 individuals (1645 female; 2212 male) from 12731 detections (5484 female; 7247 male) where the number of individuals, detections, and recaptures in each study varied (see Appendix B for capture statistics summary). Out of the 164 datasets from 78 study areas, we removed 32 datasets from 20 study areas due to insufficient

recaptures (16 datasets female and 16 male) and two datasets from one study area due to insufficent data quality. For study areas sampled across multiple years we only retained datasets from the first year of sampling. This resulted in models being fit to 122 datasets from 65 study areas, with more datasets from the boreal. Female GLSL and boreal models included 20 and 41 study areas, respectively. Male GLSL and boreal models included 19 and 42 study areas, respectively.

4.4.2 SECR models

For the pooled datasets, models where g_0 varied by t failed to converge and models where g_0 or σ varied by study area did not converge within the 28-day limit of the advanced resource computing system cluster. Model forms with these covariates were therefore omitted. The direction of effect and magnitude of the β estimates were generally similar across candidate-models forms, with slight differences (Appendix D Section 5: Figure D.5.1). For both sexes the top ranked model included a behavioural response (bk) on g_0 and additive effect of a linear time trend (T) and forest region on σ. See Appendix D Section 5 for AIC_c model selection criteria. As noted above, this model structure was subsequently used for fitting of the forest region models. Forest region models converged, as indicated by stabilization of the log likelihood values and β estimates.

4.4.3 Model comparison

The direction of effect and magnitude of the β parameter point estimates for each covariate were generally similar across the SECR and two-step modeling approaches for both the pooled and forest region models, with some exceptions of the confidence interval coverage and significances (Figure 4.2, Figure 4.3). For both modeling approaches, SECR models generally

provided the smallest magnitude of β estimates with smaller confidence intervals compared to the GLM and MC models (Figure 4.2, Figure 4.3).

4.4.4 Bottom-up and top-down effects on density

Pooled models displayed a negative effect of coniferous forests and positive effect of roads, harvest and deciduous forests on male and female densities, with the exception of male SECR models that had a negative effect of deciduous forests (Figure 4.2). Human influence was positivity associated with female density and negatively associated with male density (Figure 4.2). Most covariates and model forms displayed non-significant effects as indicated by confidence intervals including zero (Figure 4.2). Notable exceptions included a significant positive effect of deciduous forest on female density for both two-stage approaches, and significant positive effects of harvest on female density in the MC approach and SECR approach, with only a small overlap of the 95% confidence interval with 0 for the GLM approach.

For the forest region models, roads and coniferous forests displayed similar patterns to the pooled models; coniferous forests and roads were negatively and positively associated with female and male densities across both forest regions, respectively, although these effects were non-significant (Figure 4.3). For the remining covariates there were differences among the boreal and GLSL forest regions that varied by sex (Figure 4.3). Deciduous forests displayed a significant positive association with female density in the boreal and a weak non-significant positive association in the GLSL. Deciduous forests were also significantly and positively associated with male density in the boreal, but in contrast were negatively associated in the GLSL where the effect was significant for the MC model. Harvest was positively associated with female density across both forest regions but was significant for the MC model in the GLSL only. For males, harvest displayed a negative association with density in the boreal that was non-

significant and a positive association with density in the GLSL that was significant. For both sexes, human influence was negatively associated with density in the boreal and positively associated with density in the GLSL; these effects were non-significant.

For both the pooled and forest region models, the magnitude of the β estimates varied by sex, forest region, and modeling method (Figure 4.2, Figure 4.3). In general, harvest and forest types displayed the largest magnitude of the β estimates.

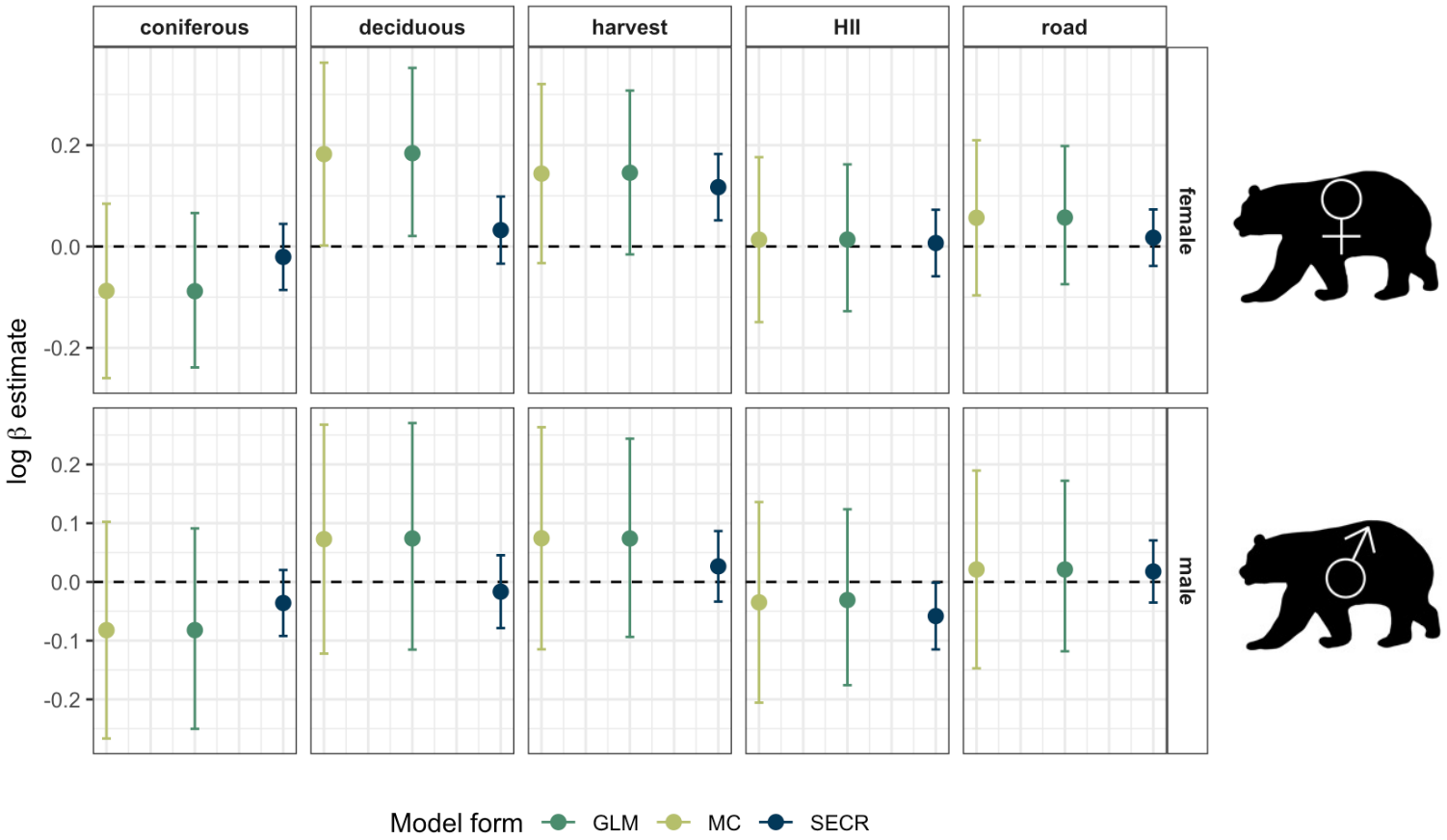

Figure 4. 2. Log-scale effect size (β parameter estimates) of pooled female (♀) and male (♂) models (generalized linear models [GLM]; Monte Carlo models [MC]; spatially explicit capture-recapture models [SECR]) with density covariates including percent forest types (coniferous, deciduous), human influence index (HII), road density (road) and harvest density (harvest). β estimates standardized to allow for covariate comparison within sex. The effect size indicates the change in the baseline density (bears/hectare) on the log scale for one unit change in the covariate value. Vertical lines indicate 95% confidence limits and dashed black horizontal lines no effect of the covariate on density.

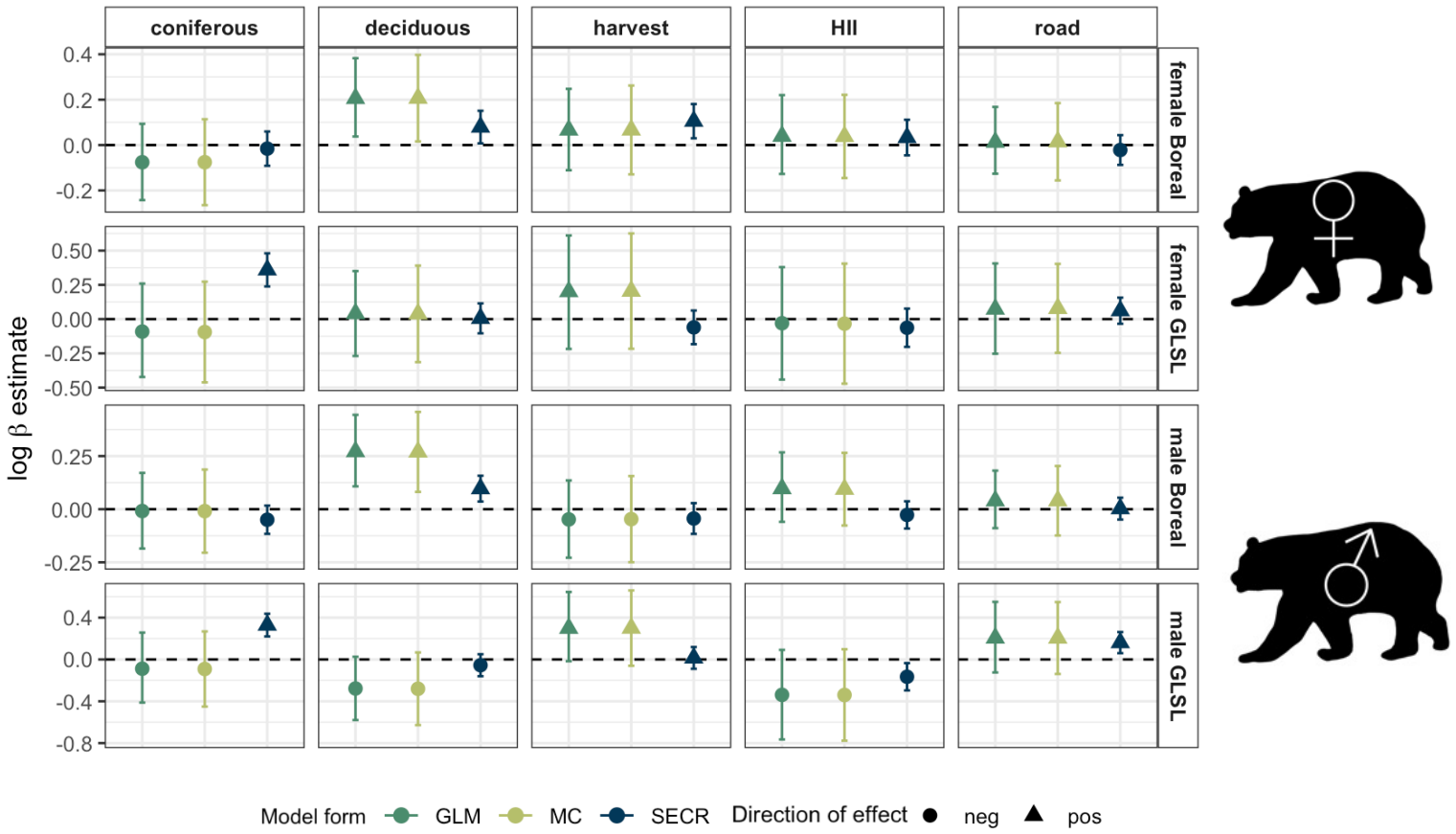

Figure 4. 3. Log-scale effect size (β parameter estimates and upper and lower 95% confidence limits) of Great Lakes – St Lawrence (GLSL) and boreal forest female and male generalized linear models (GLM), Monte Carlo models (MC), and spatially explicit capture-recapture (SECR) models. Density covariates included percent forest types (coniferous, deciduous), human influence index (HII), road density (road) and harvest density (harvest). β estimates standardized to allow for covariate comparison within a forest region and sex. The effect size indicates the change in the baseline density (bears/hectare) on the log scale for one unit change in the covariates value.

4.5 Discussion

The continued loss of biodiversity due to the expanding human footprint remains one of the most pressing challenges facing conservationists today. Addressing this problem requires robust monitoring methods to assess populations' responses to changing landscapes and environmental conditions (Jones 2011, Bischof et al. 2020). Using an extensive dataset spanning a gradient of land cover and climate, we found that black bear relationships with human influences and forest land cover varied across the province of Ontario and within forest regions, reflecting gradients of habitat quality, intensity of human disturbances and bear ecology. Forested land cover explained most patterns of black bear density at the provincial scale, where higher densities were associated with more productive forest types (i.e., deciduous forests). When gradients of natural productivity and differences in human disturbances between forest regions were accounted for, association of bear population density with human influences and forested land cover varied within forest regions, reflecting trade-offs between food resources and avoidance of human activities and mortality risks. These results provide key understanding for broad scale drivers of black bear density in Ontario and offer insight to the relative influence of top-down and bottom-up forces in driving variation in carnivore density. Specifically, our findings highlight how anthropogenic and environmental factors can act as both bottom-up or top-down processes that varies with spatial extent, ecological conditions and intensity of human disturbances.

We used three different modeling approaches to assess the influence of anthropogenic and environmental factors on black bear density. These approaches reflected trade-offs between computation time and accounting for uncertainty in estimates of density. Even with high-performance computing systems, our large datasets restricted us from running SECR models that accounted for study area level variation in detection and density parameters due to computational

requirements that exceeded the computing cluster's time limit. However, we were able to better account for study-area variation in detection and density in the two-step modeling approach. Nonetheless, the MC models displayed similar confidence intervals as the GLM models (Figure 4. 2; Figure 4. 3), suggesting that uncertainty in density estimates did not largely influence our β estimates. To that end, we base our inferences in the following sections on the β estimates derived from the GLM methods. Estimates from the MC and GLM models were generally consistent (Figure 4. 2, Figure 4. 3) and therefore, we feel this decision did not unduly impact our overall inferences. Further, because both the MC and GLM models allow for maximal flexibility in detection across study areas, we assume that differences in the direction of coefficient effects between the two-step modeling approaches and the SECR approach are most likely due to our inability to account for study area level variation in detection in the SECR models.

4.5.1 Factors driving black bear density

Forested land cover was the most consistent, strongest, and most certain driver of black bear density across the province and within forest regions. At the provincial scale (i.e., the pooled approach), black bear density was positively associated with deciduous forests and negatively with coniferous forests with the effect of deciduous forest on female density being significant. The GLSL forest, which has a much higher proportion of deciduous trees, is more productive than the boreal; bears to be more abundant in this region (Howe et al. 2013, Howe et al. 2022). Thus, at this scale, the pooled results are likely reflecting these broad patterns where GLSL study areas had consistently higher proportions of deciduous forest and more bears.

Similar patterns were observed in the boreal forest when data were analyzed alone such that black bear density was positively associated with deciduous forests and negatively with

coniferous forests. Herbaceous vegetation constitutes the bulk of spring and early summer diets for bears in Ontario (Romain et al. 2013) and hardwood forest stands contain higher abundance and diversity of these foods during the spring and early summer seasons when other resources are limited. Thus, the strong and positive significant effect of deciduous forests on female and male bears in the boreal is likely due to food being a limiting factor in these habitats reflecting the generally lower abundance and diversity of food resources in coniferous forests (Obbard et al. 2017, Potter and Obbard 2017). These results are consistent with finer-scale studies demonstrating black bears avoiding mature coniferous forests in the boreal (Brodeur et al. 2008) and negative association of black bear densities with less productive evergreen forests (Humm et al. 2021).

Comparatively, in the GLSL forest region male density was negatively associated with both coniferous and deciduous forest types. Although both effects had confidence intervals overlapping zero, the deciduous forest was close to being significant. Females showed no strong patterns with equivocal results relative to forest type. In the GLSL region, there is higher intensity of human disturbances, but food resources are more widely available. Consequently, the finding for females is not entirely surprising as they have ample natural foods. However, the negative, though relatively uncertain relationship between deciduous forest and male density warrants consideration. Differences between sexes could be a function of males being more conflict-prone in part due to their wider ranging movement bringing them into contact with human activities and anthropogenic food sources (Rogers et al. 1976). This pattern may be more pronounced in the southern study areas of the GLSL that are composed primary of deciduous forests but are also more populated and have higher fragmentation and developed habitats such that males' larger home ranges overlap with human activities. Similarly, in northern Wisconsin

black bears select for coniferous forests over deciduous forests (Sadeghpour and Ginnett 2011). However, as suggested in the study, this pattern may be an artefact of the time of sampling such that if sampling were to occur in the fall bears would likely be associated with deciduous forests due to availability of important hard mast species. We predict a similar trend in Ontario in the late summer and fall, particularly in the GLSL when hard mast beech and oak trees are important energy sources during hyperphagia (Poulin et al. 2003).

Most of our covariates associated with human disturbance or direct mortality of bears showed uncertain results. However, there were some general patterns that provide insight to how bear populations respond to human influence. We observed higher male black bear densities in areas with greater human influences, as measured by the human influence index, in the boreal, and observed higher male densities in areas with less human influences in the GLSL. Although these effects were uncertain, the confidence intervals only slightly overlapped 0 in both cases. These effects match well with our expectations of how bears respond to humans based on the differences in the intensity of human disturbances in the two forest regions. The GLSL is more densely populated and highly fragmented than the boreal. Thus, bear populations may be depressed in habitats at the urban-wildlife interface because these areas can be associated with heightened human-bear conflicts linked to human activities and anthropogenic food sources (Evans et al. 2014, Hagani et al. 2021). The equivocal results for females could be reflective of the fact that male bears are more likely to come into conflict with people and that males represent nearly 2/3rd of the harvest in Ontario (Appendix D Section 6: Figure D.6.1). Comparatively, in less productive boreal regions, characterized by lower human disturbances and more continuous dense forests, bears may be using habitats near humans for supplemental food or because these more open and disturbed areas contain early spring and summer vegetation.

However, because we were unable to sample close to human settlements, our populations likely represent bears with generally low human activities in their ranges, particularly in the boreal. The most developed areas sampled in the boreal are relatively less developed than most of the areas sampled in the GLSL, so in the boreal, bears may be responding to the only moderate levels of human influence. This pattern is consistent with studies linking higher black bear densities with human settlements (Beckmann and Berger 2003, Fusaro et al. 2017) and changes in natural food availability (Laufenberg et al. 2018). In comparison, when datasets were pooled, human influences had a weak effect on shaping provincial-scale patterns in bear density, likely due to the contrasting forest region patterns. As previously noted, the negative effect for males in the pooled analysis may be due to their conflict prone behaviours (Rogers et al. 1976) and is further supported by the negative effect of human influence on males in the highly populated GLSL.

All pooled models revealed a positive relationship between harvest density and black bear densities, such that WMUs with higher bear densities tended to have more bears harvested per unit area. This effect was nearly significant for females, though more uncertain for males. This finding contrasts with previous studies displaying a negative influence of harvest on female bear densities (Loosen et al. 2018). Such differences could be due to the broad scale of our analysis paired with how we measured harvest. While black bear density was a static estimate for each study area, harvest density was measured at a much broader WMU extent and averaged over a bear generation time (i.e., seven years) prior to sampling. Accordingly, our measure of harvest was unlikely to capture the finer temporal and spatial influence of harvest on density. Thus, we presume that the positive relationship between harvest and density actually reflects that, at this broad scale, more bears are harvested in areas that simply have more bears.

The forest region-specific analyses support our above assertion that more bears are harvested in areas that have more bears. The GLSL, which is more populated and has higher densities of roads, displayed the stronger positive relationship between bear density and harvest. We suggest that these results indicate that black bears are primarily harvested in areas where there are sufficient habitats to support higher densities in the GLSL. In comparison, in the boreal, harvest may not be an artefact of bear density because habitat quality is generally lower and reduced road access may restrict hunters' access to bear habitats, such that harvest may not be concentrated to higher quality habitats with more bears. We did, however, find a negative effect of harvest on males and positive effect on females in the boreal, although, the effects were again not significant. This finding may be due to differences between sexes and productivity and human disturbances across forest regions. Males are typically subject to higher harvest (Obbard et al. 2017, Gantchoff et al. 2020), with females accounting for approximately one-third of total harvest from 2010-2019 in Ontario (Appendix D Section 6: Figure D.6.1). However, the above is largely speculative and therefore further assessment of harvest on black bear densities at finer temporal and spatial scales is warranted to clarify these uncertainties. Nonetheless, these findings suggest that the effect of harvest on bear populations may in part be mediated by habitat quality and further underscores the importance of forested landcover in shaping black bear densities in our study system.

Interestingly, we found a non-significant, positive effect of roads on female and male densities for all models. These findings contrast with studies generally demonstrating negative association of bears with roads (Humm et al. 2017, Lamb et al. 2018) often linked to top-down mortality including hunting access, vehicle collisions and human-bear conflict from increased human access into bear habitats (Hostetler et al. 2009, Wynn-Grant et al. 2018). Our findings do,

however, align with studies reporting association of higher black bear densities with roads in some areas (Humm et al. 2017) and bears favouring habitats closer to roads in the spring in boreal forests (Mosnier et al. 2008). Further there are numerous reports of bears foraging alongside roads where early vegetative plant growth occurs during the spring green-up due to disturbance and the edge effect when other food resources are limited (Mosnier et al. 2008, Romin et al. 2013, Tigner et al. 2014). Presumably, the consistent positive and non-significant effect of roads at both the provincial and forest region extents suggests that, at our scale of analyses and time of sampling, roads on their own are not depressing bear density at this scale. Despite the generally equivocal results relative to roads, males in the GLSL showed a more certain (as indicated by the larger β parameter), though still non-significant response. A potential biological explanation for this effect could be black bears in the GLSL being acclimated to living in more developed areas where there are higher density of roads (Zeller et al. 2019). Lastly, these observed patterns may also be a result of including the human influence index covariate in the multivariate model that may have accounted for some of the effect of roads; however, the two variables were not strongly correlated at both the forest region and pooled scales (Appendix D Section 3: Table D.3.1).

4.5.2 Alternatives to computationally demanding SECR models

Despite increasing recognition that large capture-recapture datasets and more complex SECR models can be computationally challenging (Morin et al. 2022), techniques to improve model tractability remain surprisingly rare (exceptions include Milleret et al. 2019). Here, we demonstrate how our proposed two-step approach can expand the utility of SECR models when modeling spatial effects on density across large extents is computationally restrictive. Overall, we found that the direction of effect and magnitude of the β estimates were generally similar

across the three modeling approaches and the confidence interval coverage of the three modeling methods overlapped for all covariates (Figure 4. 2). Density and detection parameters were nested within the hierarchical SECR model, but not in the two-step approach when the GLM or MC sampling was used to estimate effects on density covariates. The excessive run times associated with fitting SECR models to large datasets, even with access to high-performance computing systems, restricted us from fitting models that account for study area variation in detection and density. In such cases, the two-step modeling approach proposed here could be used to assess the influence of spatial covariates on density while better accounting for these sources of heterogeneity. Our results, showing in many cases opposite direction of effects for some covariates between SECR and the other two-stage approaches would suggest that the two-stage approaches are preferable in these cases. While we recognize that further work examining the robustness of this approach for other species and sizes of capture-recapture datasets is needed, this approach may provide a feasible option for practitioners without access to high-performance computing or could be used to test the effect of spatial covariates on density before running demanding SECR models. Nonetheless, we suggest that researchers take into careful consideration the study population, study design, sample size and model assumptions and select density estimation methods based on these factors.

4.6 Conclusion

Understanding how bottom-up and top-down processes shape broad-scale patterns in wildlife populations remains an enduring challenge that requires monitoring across large extents and robust statistical frameworks for handling large spatial analyses. Here, we use one of the largest spatial capture-recapture datasets on black bears collected across an expansive extent to quantify mechanisms shaping patterns in population density. To address the challenges of highly

parameterized and computationally restrictive SECR models common to large datasets, we propose a two-step modeling process that improves model tractability while producing comparable results and accounting for more aspects of spatial heterogeneity in detection and density. Our results demonstrate that factors shaping broad spatial patterns in black bear densities are dynamic and vary by spatial extent, ecological conditions and intensity of human disturbances. Bottom-up forces, as measured by forest types, were the main drivers of bear density at the broad scale. While top-down forces from human disturbances and harvest influenced bear densities, these effects were more nuanced and likely acted at finer scales than our coarse analyses could account for. This is important, because most management actions related to black bears focus on top-down mortality factors, which is, indeed, easier to manage than bottom-up forces. Thus, managers should continue to consider that broad productivity patterns may be dominant in large jurisdictions and manage accordingly. Collectively, our findings demonstrate the scale-dependent and context-specific way in which black bears respond to human impacts to the environment and indicates how management should consider the effect of land-use and climatic changes that drive variability in productivity and human-caused mortality. Specifically, our results show that broad changes in forest composition in Ontario could have major implications for black bear populations. Thus, sustained monitoring of black bear densities across scales and over large heterogenous landscapes to capture broad and fine scale changes in bottom-up and top-down factors is critical for management of the species in dynamic and multi-use landscapes.

Chapter 5: Conclusion and Synthesis

Combining advanced statistical models with information-rich genetic and geospatial data has allowed ecologists to identify mechanisms driving patterns in population size and distribution at increasingly finer resolution and over larger extents (Long et al. 2008, Lewis et al. 2018, Lamb et al. 2019). However, with this ever-increasing ability to address more complex processes using more advanced models comes many technical challenges and the need for critical evaluation of model assumptions in relation to the ecology and behaviour of the species and study system. Framed within the context of the American black bear in Ontario, this thesis highlights the opportunities and challenges of working with elusive and wide-ranging species across multiple scales and over large extents.

5.1 Summary of key findings

In this thesis I leveraged three years of black bear spatial capture-recapture data to assess broad and fine scale drivers of black bear density and distribution in Ontario. I first assessed the robustness of SECR models to spatial and sex-based variation in detection and density (Chapter 2) and provide suggestions to reduce the risks of obtaining biased density estimates. This chapter also provided context for the modeling structures in the subsequent chapters of this thesis and, more broadly, for large carnivore monitoring and management. Next, I identified fine-grained environmental and anthropogenic drivers of black bear distribution within study areas (Chapter 3). However, assessments at this finer scale are prone to sampling bias, such that local study area results may be nuanced, limiting general conclusions that are more likely to emerge at broad scales because the effects of local heterogeneity are smoothed out, making ecological patterns appear more consistent (Wiens 1989). I then assessed population-level patterns of black bear density as a function of coarse-grained landscape-level environmental and anthropogenic

features (Chapter 4). Taken together, this multi-scale approach allows for robust inference to the mechanisms structuring fine and broad scale patterns in black bear densities and offers insight to the relative influence of top-down and bottom-up forces in driving these patterns.

Collectively, this thesis demonstrates that Ontario black bear densities are shaped by both environmental and anthropogenic factors, where the relative influence of these factors varies with the spatial extent of the analysis. Bottom-up forces were more dominate at the broad extent, with environmental variables, specifically forest cover representing differences in productivity, the most consistent and strong driver of density across the province (Chapter 4). Anthropogenic variables, measured with fine grained covariates, were consistently important only within study areas at a finer extents such that black bears distributed themselves according to avoidance of people (Chapter 3). When differences in forest regions were accounted for (Chapter 3 and 4), forest type and human influences acted as both bottom-up and top-down forces that were consistent with ecological influences on black bear foods and intensity of human influences on black bear avoidance of riskier, developed areas. Comparison of patterns in black bear density-habitat relationships at both the fine (Chapters 3) and broad (Chapter 4) scales are summarized in Table 5.1 and described in further detail in the subsequent paragraphs. These patterns support the multiple hypotheses outlined in Chapter 1 (Table 1.1, Figure 1.1).

Table 5.1. Direction of effect for β parameter estimates of environmental and anthropogenic variables in the fine (Chapters 3) and broad (Chapter 4) scale analyses. Results summarized by the spatial extent of analysis where black bear capture-recapture data were aggregated by: within a study area (study area); within a forest region (Boreal; Great Lakes – St Lawrence [GLSL]); across all study areas (Province). Gray outlined boxes indicate difference in effect between female and male black bears.

Sex	Variable	Fine scale analysis (Chapter 3) †			Broad scale analysis (Chapter 4) †		
		Study area ‡	Boreal *	GLSL *	Boreal *	GLSL *	Province **
Female	Human influence ***	—	—	—	+	—	+
	Road	—	—	—	+	+	+
	Harvest				+	+	+
	Coniferous forest	—	—	+	—	—	—
	Deciduous forest	+	+	—	+	+	+
	Mixed forest	—	—	—			
	Crop		+	—			
	NDVI	—	—	—			
Male		**Study area ‡**	**Boreal ***	**GLSL ***	**Boreal ***	**GLSL ***	**Province ****
	Human influence ***	—	—	—	+	—	—
	Road	—	—	—	+	+	+
	Harvest				—	+	+
	Coniferous forest	—	—	+	—	—	—
	Deciduous forest	+	+	—	+	—	+
	Mixed forest	+	—	—			
	Crop		+	—			
	NDVI	—	—	—			

† inference from univariate SECR models (Chapter 3) and multivariate generalized linear models in the two-stage approach (Chapter 4)

‡ values indicate the median of β estimates across all study areas for each variable (Chapter 3, Appendix C Section 3: Figure C.3.2)

* referred to as the pooled analysis (Chapter 3) and forest region analysis (Chapter 4)

** referred to as the pooled analysis (Chapter 4)

*** different data sources used in Chapter 3 (human build-up grid) and Chapter 4 (human influence index)

A key finding of this thesis was that forested land cover was the most consistent driver of black bear density across scales. This effect was most pronounced at the broad scale (Chapter 4), where higher densities of black bears were found in more productive deciduous forests than coniferous forest which follows patterns consistent with previous studies (Brodeur et al. 2008, Zeller et al. 2019). However, when assessed at the finer scale (Chapter 3), more nuanced patterns emerged. In the GLSL region, characterised by wide-spread human development and fragmentation, higher densities of bears were found in coniferous forests that may provide cover and security and in areas with less agricultural land cover. Conversely, in the boreal, with less intensive human influences and higher proportion of less productive coniferous forests, bear densities were higher in deciduous forests and areas with more agricultural landcover. The latter two land covers are generally associated with greater diversity and abundance of natural and anthropogenic food sources for bears (Romain et al. 2013, Ditmer et al. 2016). Collectively, these findings suggest that black bear use of landscapes at a finer scale is driven by the trade-offs between the benefits of food resources and avoidance of risky human-developed areas (Johnson et al. 2015, Zeller et al. 2019). Further, although datasets in this thesis were grouped based on broad forest regions, there are differences in both productivity and intensity of human influence between the east and west GLSL regions that have been documented to influence black bear densities (Howe et al. 2013). Analyses of the GLSL data split by east and west may provide further insight into the more complex and nuanced behaviour of the species, however, there are likely to be challenges associated with data sparsity for such analyses (see section 5.2 for further discussion on this topic).

While top-down forces, as measured primarily through harvest and anthropogenic disturbance, had an influence on spatial patterns of black bear densities across all scales, these

effects were less certain. At the finer scale, black bears consistently distributed themselves according to avoidance of roads and human settlement (Chapter 3) that coincides with documentation of fine-scale avoidance of roads by bears and reduced bear densities near human development (Kasworm and Manly 1990, Waller and Servheen 2005, Northrup et al. 2012, Humm et al. 2017, Lamb et al. 2018, Proctor et al. 2019).

While black bears clearly avoid human disturbances at the fine scale, this effect of roads and, to a lesser extent human influences, were not detected with the coarse resolution variables used in Chapter 4 (Table 5.1). The weak but consistent positive effect of roads on broad-scale patterns of density (Chapter 4) could be a consequence of the multivariate models such that the inclusion of the human influence index reduced the strength of the road variable in these models. However, there were some general patterns for human development that possibly reflected forest region differences in the intensity of human disturbances and bear biology. Human influence was negatively associated with male black bear densities across the province and for both sexes in the GLSL region, however, these effects were not significant. In contrast, human influence was positively associated with female density across the province and for both sexes in the boreal, although effects were also not significant. Bear populations may be depressed in habitats at the urban-wildlife interface, such as the GLSL, because these areas are typically associated with heightened human-bear conflicts linked to human activities and anthropogenic food sources (Hristienko and Mcdonald 2007, Evans et al. 2014, Hagani et al. 2021). Males are more conflict prone (Rogers et al. 1976) and subject to higher harvest rates (Kolenosky 1986, Obbard et al. 2017, Gantchoff et al. 2022); this may further explain the differences between sexes. Overall, the less certain results for top-down factors in this thesis may be reflective of sampling in moderately to slightly developed areas that could limit the power to observe a strong effect of

human influences; this effect is likely pronounced in the boreal and pooled models because the boreal study areas are less developed and comprised 69% and 67% of the total study areas for the males and female datasets, respectively. Moreover, higher densities of black bears have been found to exist in intermediate housing densities (Johnson et al. 2015) and exurban areas compared to rural or urban (Evans et al. 2017), suggesting a threshold in which bears cannot exit in developed areas. The strong avoidance of black bears to human activities at the fine scale (Chapter 3) provides a mechanism for this process.

Similar to human disturbances, I observed uncertain results for the effect of hunting at the provincial scale (Chapter 4). More bears were harvested in areas with higher bear densities, a result that mirrors previous studies in Ontario (Wightman et al. 2022). Interestingly, when differences in forest region were accounted for, there was slight evidence of suppression of male densities by harvest in the boreal, but not females in either forest region. These finding align with males being more heavily harvested in Ontario than females (Kolenosky 1986, Obbard et al. 2017; Appendix D Section 6: Figure D.6.1) and may suggest that at broad scales, bottom-up processes offset the effects of harvest in higher quality bear habitat. However, these assertions are largely speculative and further studies at finer temporal and spatial scales are warranted.

5.2 Confronting uncertainty in ecological models: opportunities, limitations, and directions for future research

As with many analytical frameworks, alongside the rapid development of SECR methods have come increased computational demands and difficulties completing analyses and interpreting results (Levin 1997, Green et al. 2005, Grueber et al. 2011, Morin et al. 2022). Table 5.2 (Chapter 5) summarizes common challenges identified throughout this thesis of applying SECR models to large scale analyses and suggests potential solutions and associated drawbacks.

Indeed, a common difficulty in this thesis was identifying the optimal trade-off amoung the size of the datasets, complexity of the model structure to account for population heterogeneity, and tractability (i.e., computational time and resources). As clearly demonstrated in Chapter 2 and repeatedly illustrated in literature (Tobler and Powell 2013, Moqanaki et al. 2021, Stevenson et al. 2021, Marrotte et al. 2022), bias can be induced when violations of SECR model assumptions are substantial. This is a concern for large-scale surveys because variability in detection and density are likely to increase with study area size (Jones 2011, Howe et al. 2022). Therefore, the black bear populations in this thesis likely exhibit heterogeneity that extends beyond what I accounted for in the models provided the relatively sparse datasets; this was most clearly reflected in the study area analysis (Chapter 3) where univariate density models were used to prevent overfitting. In contrast, when datasets were pooled (Chapter 4), it permitted more highly parameterized models due to larger datasets. However, as previously documented (Millerete et al. 2019), when I scaled SECR models to larger extents they quickly became computationally intensive and were prohibitively slow despite access to a Federal computing cluster. In response to this challenge, I explored alternatives to improve the tractability of the data-intensive and computationally burdening SECR models and proposed a two-stage approach in Chapter 4 that produced generally comparable estimates while also accounting for more aspects of heterogeneity in detectability and density. While further assessment of the robustness of this approach are warranted and I caution the use of this method to replace SECR models that sufficiently account for important sources of variation in model parameters, this avenue of research could be of interest of practitioners with limited computing resources or a method to assess spatial drivers of density on datasets prior to running computationally burdening SECR models.

A further difficulty in my work was selecting the appropriate scale of observation on animal space use, a longstanding challenge in ecology that has received increasing attention (Apps et al. 2001, Apps et al. 2004, Ciarniello et al. 2007). I used two methods to quantify the grain of spatial covariates in this thesis: a moving window approximating the 95% space use radius derived from σ estimates (Chapter 3) and a buffer based on the movement distances from the raw capture-recapture data (Chapter 4). I did not use data-driven modeling (i.e., comparing different models across grain or extent sizes) to avoid overfitting due to the large number of models this would entail. Nonetheless, optimization of the grain size warrants further consideration for SECR studies using these datasets (see Marrotte et al. 2022). This underscores the wide range of methods to quantify geo-spatial data and the implications for interpretation of results.

Animals respond to environments at finer scales than SECR data and models allow (Theng et al. 2022). The broad covariates in this thesis could have been collected at inappropriate scales that do not match how bears perceive their environment or other important factors may have be omitted from models (Stetz et al. 2019, Howe et al. 2022). These challenges, however, are ubiquitous to the use of models and geospatial data in ecology. Despite these concerns, I found consistent patterns of black bear density association with forest types, and to a lesser extent human influences, across two spatial extents that strengthens the conclusion that black bear density in the study systems are shaped by habitat conditions.

Collectively, the results of this thesis demonstrate that SECR models can provide unbiased inferences of density-habitat relationships across scales, but only if specific conditions are met and models account for important sources of heterogeneity in detection and density. SECR studies conducted across large heterogenous landscapes are more prone to bias, requiring careful consideration of the study population, study design and sample size in relation to model

assumptions. However, if these issues area addressed, large scale programs such as the one outlined here, offer substantial opportunity for understanding how large carnivore populations are shaped.

5.3 Future outlook and management implications

Below I highlight management suggestions for black bears in Ontario that rely on findings of this thesis, but in many cases these suggestions apply more broadly to generalist carnivores living in human-modified landscapes.

Findings of my thesis demonstrate how species should be broadly managed according to landscape productivity and intensity of human influences. Management activities focused on creating early successional forests would be beneficial for providing important bear foods found in disturbed areas and regenerating forest stands associated with forestry, agriculture, and fire (Mosnier et al. 2008, Romin et al. 2013, Rettler et al. 2021), particularly in the less productive boreal regions. However, these actions must be balanced with impacts to other species and retention of mature forests patches and corridors that act as escape cover for black bears (Howe et al. 2005). Moreover, human-bear conflict and black bear mortality has been linked with overlap between humans and bears at the wildlife-urban interface (Evans et al. 2014, Johnson et al. 2015, Wynn-Grant et al. 2018, Hagani et al. 2021). Given that forestry and agriculture bring with them increases in humans and roads, using these activities to promote habitat improvements for bears is a double-edge sword and there is likely a threshold of forestry and agricultural activities above which bear populations will be negatively impacted. Thus, allowing more natural disturbance regimes to dominate, particularly in the boreal forest, is most likely to promote bear habitat improvements while reducing the risk posed by roads and people. In contrast to the boreal, in more urbanized landscapes and more productive areas, such as the GLSL, maintaining

large continuously forested areas with a diversity of forest stands to provide black bear foods and cover should be of priority (Garshelis and Noyce 2008). Given the predicted increase in frequency of droughts and late spring frosts with climate change (Karl et al. 2009) and the associated reduction in mast production for black bears, it may escalate their use of developed areas during poor food years (Johnson et al. 2005, Howe et al. 2013). Given that measuring food availability is time-intensive and costly for wide-ranging black bears (Rettler et al. 2021), predicting food shortages using climate variables and land-use composition could help managers identify areas vulnerable to human-bear conflict that warrants further research (Howe et al. 2013).

This thesis alludes to the complex relationships between food resources and mortality risks associated with roads. While we found that bears distributed themselves away from roads at a finer scale (Chapter 3), this effect was not observed at larger extents and coarser resolutions (Chapter 4). Further studies examining the types and intensity of motorized and non-motorized use could help identify spatial and temporal patterns that may elevate, due to vegetation near roads in the spring, or decrease habitat effectiveness and mortality risks for black bears to allow for targeted land-use and recreational access management (Lamb et al. 2018, Ladle et al. 2018, Proctor et al. 2019).

Ontario has changes its black bear hunting policies that have been subject to highly publicized and politically charged debates (Poulin et al. 2003, Newton and Obbard 2018). While this thesis suggests that the effects of harvest may be mediated by habitat quality, these inferences were largely speculative and require further research to resolve these uncertainties. Incorporating data on the age distribution of harvested populations from premolar teeth submitted by hunters to the MNRF could allow for more robust assessment of whether harvest

rates are sustainable under current and predicted landscape conditions and to identify areas of concern at finer spatial and temporal scales more suited for harvest management (Newton and Obbard 2018).

Overall, the collective findings of this thesis highlight the necessity for robust population monitoring across scales and over large extents to capture the complexity in which generalist and wide-ranging carnivores respond to changing land-use and climate conditions. While large scale monitoring projects can provide regional and provincial population context for wildlife management, they should be nested within finer-scale data that is more appropriate for localized decision making (Apps et al. 2016). Integration of different data sources into modeling frameworks that account for species survival, reproduction and behaviour and movement patterns could provide a more comprehensive understanding of how animals respond to both demographic and landscape factors. Such methods illustrate a shift towards increasingly quantitative and integrated research to better understand the effect of environmental change on carnivores with wide-ranging benefits to human well-being and global biodiversity conservation.

Table 5.2. Summary of SECR modeling challenges addressed in this thesis and possible solutions, including drawbacks to consider with each solution (matched by lower case letters). Last column includes a non-exhaustive list of examples from SECR studies.

Challenge	Solutions	Possible drawbacks	SECR references
Data sparsity			
Low number of detections and recaptures inflates variance, precludes model convergence, or negatively biases σ estimates and overestimates density[4]	a. pool datasets across space or time [1,2] b. combine with other data sources (telemetry, different detection methods, harvest, live trapping)[3,4,5,6] c. reassess the number of model parameters relative to the datasets size	a. trade-off between overfitting and risk of bias if important sources of heterogeneity are not accounted for[7] a/b. higher computational demands with increased spatial domain[8] b. introduces more sources of heterogeneity	[1] Howe et al. 2013 [2] Schmidt et al. 2022 [3] Morehouse and Boyce 2016 [4] Ruprecht et al. 2021 [5] Sutherland et al. 2019 [6] Welfelt et al. 2019 [7] Moqanaki et al. 2021 [8] Milleret et al. 2019
Trade-off between overfitting and risk of bias if detection or density model misspecified because limited number of covariates can be included relative to sample size [7,9,10,11]	a. simulate populations with expected levels of heterogeneity to examine violation of model assumptions	a. extensive computational time for complex simulations (particularly Bayesian implementation)[12,13]	[7] Moqanaki et al. 2021 [9] Tobler and Powell 2013 [10] Stevenson et al. 2021 [11] Sollmann et al. 2011 [12] Morin et al. 2022 [13] Theng et al. 2022
Large recapture distances produce tails on the detection distribution, biasing estimates or making model convergence difficult; more pronounced at smaller sample sizes.	a. evaluate maximum distance moved by individuals and consider truncation[2]; assess sensitivity of density to removal of outliers[14]	a. reduces samples size	[2] Schmidt et al. 2022 [14] Kendall et al. 2019

Table 5.2 (continued).

Challenge	Solutions	Possible drawbacks	SECR references
Model complexity to account for population heterogeneity			
Account for variable density and detectability across individuals, sexes, and space and time	a. include covariates on the detection and density model b. run separate models split by main source(s) of variation c. if sample sizes allow, include mixture-models[5,15]	a. potential overfitting; uncertainty with model selection; superius effects with greater covariates and collinearity; reduces model tractability b. data sparsity challenges b. smaller groups prone to sampling bias c. requires large amounts of data; difficult to interpret biologically	[5] Borchers and Efford 2008 [15] Obbard et al. 2010
Model tractability			
More parameterized models required to account for heterogeneity in large capture-recapture datasets to minimize bias, yet such models are often computationally intensive[11]	a. parallel processing and advanced research computing systems may reduce run times and allows for fitting of many models simultaneously[13,16] b. reduce number of parameters[17] c. divide datasets based on groups and run separate models d. optimize masks resolution and buffer	a. models may still have excessive run times b. introduce bias from model misspecification c. data sparsity challenges c. small groups prone to sampling bias	[11] Millerette et al. 2018 [13] Theng et al. 2022 [16] Howe et al. 2013 [17] Stez et al. 2014
Increased run times due to inclusion of density covariates	a. use univariate density models[18], check similar trends to multivariate models b. simplify models; remove density covariates of least importance to species biology and ecology and/or study objectives c. refine buffer width and mask point spacing	a. ignores possible interactive or additive effects among covariates b. study system/population may be poorly understood to guide what covariates to remove [22]	[18] Loosen et al. 2018 [19] Howe et al. 2022

Table 5.2 (continued).

Challenge	Solutions	Possible drawbacks	SECR references
Model implementation			
Uncertainty selecting the scale to quantify density covariates	a. select buffer or moving window size based on animal biology (if possible, from telemetry, elsewise consider movement data from capture-recapture data)[20] b. derive 95% home range size from sigma c. data driven model selection process	b. estimates likely inaccurate[13]	[20] Lamb et al. 2018 [21] Murphy et al. 2013 [13] Theng et al. 2022
Models fail to converge or parameters and/or their variance calculation failed[17]	a. try different optimization methods b. re-fit models, using starting values from previous fits c. simplify models[17] d. for multi-session models, split into separate models based on groups	c. introduce bias from model misspecification[7,9] d. data sparsity challenges d. small groups prone to sampling bias	[7] Moqanaki et al. 2021 [9] Tobler and Powell 2013 [17] Stez et al. 2014
Uncertainty with model convergence	a. goodness-of-fit tests b. re-run models using the starting values from previous fits; check for stabilization of loglikelihood values and β estimates c. try different optimization methods	a. limited options and methods remain underdeveloped, particularly for more complex models[12,19,22]	[12] Morin et al. 2022 [19] Howe et al. 2022 [22] Tourani et al. 2021
Sampling bias[19]	a. expand sampling to larger extent and pool datasets from across species range	a. introduce bias from model misspecification; higher computational demands with increased spatial domain[8] a. smooths over heterogeneity, limiting inferences to local conditions that may be context specific	[8] Milleret et al. 2019 [19] Howe et al. 2022 [23] Marrotte et al. 2022

References

Apps, C. D., B. N. McLellan, T. A. Kinley, and J. P. Flaa. 2001. Scale–dependent habitat selection by mountain caribou, Columbia Mountains, British Columbia. The Journal of Wildlife Management 65:65–77.

Apps, C. D., B. N. McLellan, J. G. Woods, and M. F. Proctor. 2004. Estimating Grizzly bear distribution and abundance relative to habitat and human influence. The Journal of Wildlife Management 68:138–152.

Apps, C. D., B. N. McLellan, M. F. Proctor, G. B. Stenhouse, and C. Servheen. 2016. Predicting spatial variation in grizzly bear abundance to inform conservation. The Journal of Wildlife Management 80:396–413.

Ashrafzadeh, M. R., R. Khosravi, A. Mohammadi, A. A. Naghipour, H. Khosnamvand, M. Haidarian, and V. Penteriani. 2022. Modeling climate change impacts on the distribution of an endangered brown bear population in its critical habitat in Iran. Science of the Total Environment 155753.

Azad, S., K. Mcfadden, J. D. Clark, T. Wactor, and D. S. Jachowski. 2019. Applying spatially explicit capture–recapture models to estimate black bear density in South Carolina. Wildlife Society Bulletin 43:500–507.

Baruch-Mordo, S., K. R. Wilson, D. L. Lewis, J. Broderick, J. S. Mao, and S. W. Breck. 2014. Stochasticity in natural forage production affects use of urban areas by black bears: implications to management of human-bear conflicts. PLoS ONE 9:e85122.

Beckmann, J. P., and J. Berger. 2003. Rapid ecological and behavioral changes in carnivores: the response of black bears (*Ursus americanus*) to altered food. The Zoological Society of London 261:207–212.

Beschta, R. L., and W. J. Ripple. 2009. Large predators and tropic cascades in terrestrial ecosystems of the western United States. Biological Conservation 142:240–2414.

Bischof, R., C. Milleret, P. Dupont, J. Chipperfield, M. Tourani., A. Ordiz., P. de Valpine., D. Turek, A. J. Royle., O. Gimenez, Ø. Flagstad, M. Åkesson, L. Svensson, H. Brøseth, and J. Kindberg. 2020. Estimating and forecasting spatial population dynamics of apex predators using transnational genetic monitoring. Proceedings of the National Academy of Sciences 117:20531–30538.

Blanc, L., E. Marboutin, S. Gatti, and O. Gimenez. 2013. Abundance of rare and elusive species: empirical investigation of closed versus spatially explicit capture–recapture models with lynx as a case study. The Journal of Wildlife Management 77:372–378.

Borchers, D. L., and M. G. Efford. 2008. Spatially explicit maximum likelihood methods for capture-recapture studies. Biometrics 64:377–385.

Boulanger, J., S. E. Nielsen, and G. B. Stenhouse. 2018. Using spatial mark-recapture for conservation monitoring of grizzly bear populations in Alberta. Scientific Reports 8:5204.

Brewer, M. J., A. Butler, and S. L. Cooksley. 2016. The relative performance of AIC, AIC_c and BIC in the presence of unobserved heterogeneity. Methods in Ecology and Evolution 7:679–692.

Brodeur, V., J. P. Ouellet, R. Courtois, and D. Fortin. 2008. Habitat selection by black bears in an intensively logged boreal forest. Canadian Journal of Zoology 86:1307–1316.

Brown, J. H. 1984. On the relationship between abundance and distribution of species. The American Naturalist 124:255–279.

Burnham K., and D. Anderson. 2002. Model selection and multimodel inference: a practical information–theoretic approach. Second edition. Springer, New York, New York, USA.
Burton, A. C., E. Neilson, D. Moreira, A. Ladle, R. Steenweg, J. T. Fisher, B. Erin, and S. Boutin. 2015. Wildlife camera trapping: a review and recommendations for linking surveys to ecological processes. Journal of Applied Ecology 52:675–685.
Cardillo, M., A. Purvis, W. Sechrest, J. L. Gittleman, J. Bielby, and G. M. Mace. 2004. Human population density and extinction risk in the world's carnivores. PLoS Biology 2:0909–0914.
Carter, N. H., D. G. Brown, D. R. Etter, and L. G. Visser. 2010. American black bear habitat selection in northern Lower Peninsula, Michigan, USA, using discrete–choice modeling. Ursus 1:57–71.
Ceballos, G., and P. R. Ehrlich. 2002. Mammal population losses and the extinction crisis. Science 296:904–907.
Ciarniello, L. M., M. S. Boyce, D. R. Seip, and D. C. Heard. 2007. Grizzly bear habitat selection is scale dependent. Ecological Applications 17:1424–1440.
Clark, J. D. 2017. Comparing clustered sampling designs for spatially explicit estimation of population density. Population Ecology 61:93–101.
Corbane, C., F. Sabo, P. Politis, and V. Syrris. 2020. GHS-BUILT-S2 R2020A - GHS built-up grid, derived from Sentinel-2 global image composite for reference year 2018 using Convolutional Neural Networks (GHS-S2Net). European Commission, Joint Research Center doi: 10.2905/016D1A34-B184-42DC-B586-E10B915DD863
Costello, C. M., D. E. Jones, R. M. Inman, K. H. Inman, B. C. Thompson, and H. B. Quigley. 2003. Relationship of variable mast production to American black bear reproductive parameters in New Mexico. Ursus 14:1–16.
Ditmer, M. A., D. L. Garshelis, K. V. Noyce, A. W. Haveles, and J. R. Fieberg. 2016. Are American black bears in an agricultural landscape being sustained by crops? Journal of Mammalogy 97:54–67.
Drever, C. R., J. Snider, and M. C. Drever. 2010. Rare forest types in northeastern Ontario: a classification and analysis of representation in protected areas. Canadian Journal of Forest Research 40:423–435.
Dröge, E., S. Creel, M. S. Becker, A. J. Loveridge, L. L Sousa, and D. W. Macdonald. 2020. Assessing the performance of index calibration survey methods to monitor populations of wide-ranging low-density carnivores. Ecology and Evolution 10:3276–3292.
Dupont, P., C. Milleret, O. Gimenez, and R. Bischof. 2019. Population closure and the bias-precision trade-off in spatial capture–recapture. Methods in Ecology and Evolution 10:661–672
Dupont, G., J. A. Royle, M. A. Nawaz, and C. Sutherland. 2021. Optimal sampling design for spatial capture–recapture. Ecology 102:1–9.
Duquette, J. F., J. L. Belant, C. M. Wilton, N. Fowler, B. W. Waller, D. E. Beyer, N. J. Svoboda, S. L. Simek, and J. Beringer. 2017. Black bear (*Ursus americanus*) functional resource selection relative to intraspecific competition and human risk. Canadian Journal of Zoology 95:203–212.
Efford, M. 2004. Density estimation in live-trapping studies. Oikos 106:598–610.
Efford, M. G. 2019. Non-circular home ranges and the estimation of population density. Ecology 100:e02580.

Efford, M. G. 2020a. secr: spatially explicit capture–recapture models. R package version 4.3.3. <https://CRAN.R-project.org/package=secr>.
Efford, M. G. 2020b. secrdesign: sampling design for spatially explicit capture–recapture. R package version 2.5.11. <https://CRAN.R-project.org/package=secrdesign>.
Efford, M. G., and J. Boulanger. 2019. Fast evaluation of study designs for spatially explicit capture–recapture. Methods in Ecology and Evolution 10:1529–1535.
Efford, M. G., and G. Mowat. 2014. Compensatory heterogeneity in spatially explicit capture–recapture data. Ecology 95:1341–1348.
Enders, M. S., and S. B. Vander Wall. 2012. Black bears *Ursus americanus* are effective seed dispersers, with a little help from their friends. Oikos 121:589–596.
Estes, J. A., J. Terborgh., J. S. Brashares, M. E. Powers, J. Berger, W. J. Bond, S. R. Carpenter, T. E. Essington, R. D. Holt, J. B. C. Jackson, R. J. Marquis, L. Oksanen, T. Oksanen, R. T. Paine, E. K. Pikitch, W. J. Ripple, S. A. Sandin, M. Scheffer, T. W. Schoener, J. B. Shurin, R. E. Sinclair, M. E. Soulé, R. Virtanen, D. A. Wardel. 2011. Tropical downgrading of planet earth. Science 33:301–306.
Evans, M. J., J. E. Hawley, P. W. Rego, and T. A. G. Rittenhouse. 2014. Exurban land use facilitates human-black bear conflicts. Journal of Wildlife Management 78:1477–1485.
Evans, M. J., T. A. G. Rittenhouse, J. E. Hawley, and P. W. Rego. 2017. Black bear recolonization patterns in a human-dominated landscape vary based on housing: new insights from spatially explicit density models. Landscape and Urban Planning 162:13–24.
Fretwell, S. D., and H. L. Lucas. 1969. On territorial behavior and other factors influencing habitat distribution in birds. Acta biotheoretica 19:45–52.
Fuller, A. K., C. Sutherland, J. A. Royle, and M. P. Hare. 2016. Estimating population density and connectivity of American mink using spatial capture–recapture. Ecological Applications 26:1125–1135.
Fusaro, J. L., M. M. Conner, M. R. Conover, T. J. Taylor, M. W. Kenyon, J. R. Sherman, and H. B. Ernest. 2017. Comparing urban and wildland bear densities with a DNA-based capture-mark-recapture approach. Human–Wildlife Interactions 11:50–63.
Gantchoff, M. G., J. E. Hill, K. F. Kellner, N. L. Fowler, T. R. Petroelje, L. Conlee, L., D. E. Beyer Jr., and J. L. Belant. 2020. Mortality of a large wide–ranging mammal largely caused by anthropogenic activities. Scientific Reports 10:8498.
Gardener, B. J. A. Royle, M. T. Wegan, R. E. Rainbolt, P. D. Curtis. 2010. Estimating black bear density using DNA from hair snares. The Journal of Wildlife Management 74:318–325.
Garshelis, D. L. and K. V. Noyce. 2008. Seeing the world through the nose of a bear–diversity of foods fosters behavioral and demographic stability. Pages 139–163 *in* T. E. Fulbright and D. G. Hewitt, editor. Wildlife science: linking ecological theory and management applications. CRC Press, Taylor and Francis Group, Boca Raton, Florida, USA.
Gerber, B. D., and R. R. Parmenter. 2015. Spatial capture-recapture model performance with known small-mammal densities. Ecological Applications 25:695–705.
Graham, M. H. Confronting multicollinearity in ecological multiple regression. Ecology 84:2809–2815.
Green, J. L., A. Hastings, P. Arzberger, F. J. Ayala, K. L. Cottingham, K. Cuddington, F. Davis, J. A. Dunne, M. Fortin, L. Gerger, and M. Neubert. 2005. Complexity in ecology and conservation: mathematical, statistical, and computational challenges. BioScience 55:501–510.

Grueber, C. E., S. Nakagawa, R. J. Laws, and I. G. Jamieson. 2011. Multimodel inference in ecology and evolution: challenges and solutions. Journal of Evolutionary Biology 24:699–711.
Hagani, J. S., S. M. Kross, M. Clark, R. Wynn-Grant, and M. Blair. 2021. Mapping and modeling human-black bear interactions in the Catskills region of New York using resource selection probability functions. PLoS ONE 16:e0257716.
Hallowell, A. I. Bear ceremonialism in the northern hemisphere. American Anthropologist 28:1–174.
Hebblewhite, M., M. Percy, and R. Serrouya. 2003. Black bear (*Ursus americanus*) survival and demography in the Bow Valley of Banff National Park, Alberta. Biological Conservation 112:415–425.
Herrero S. 1972. Aspects of evolution and adaptation in American black bears (*Ursus americanus Pal- las*) and brown and grizzly bears (*U. arctos Linne.*) of North America. International Conference on Bear Research and Management 2:221–231.
Hobbs, N. T. 2003. Challenges and opportunities in integrating ecological knowledge across scales. Forest Ecology and Management 81:223–238.
Hooker, M. J., J. S. Laufenberg, A. K. Ashley, J. T. Sylvest, and M. J. Chamberlain. 2015. Abundance and density estimation of the American black bear population in central Georgia. Ursus 26:107–115.
Hostetler, J. A., J. W. McCown, E. P., Garrison, A. M. Neils, M. A. Barrett, M. E. Sunquist, S. L. Simek, M. K. Oil. 2009. Demographic consequences of anthropogenic influences: Florida black bears in north-central Florida. Biological Conservation 142:2456–2463.
Howe, E. J., M. E. Obbard, and C. J. Kyle. 2013. Combining data from 43 standardized surveys to estimate densities of female American black bears by spatially explicit capture–recapture. Population Ecology 55:595–607
Howe, E. J., M. E. Obbard, and J. A. Schaefer. 2005. Extirpation risk of an isolated black bear population under different management scenarios. The Journal of Wildlife Management 71:603–612.
Howe, E. J., D. Potter, K. B. Beauclerc, K. E. Jackson, and J. M. Northrup. 2022. Estimating animal abundance at multiple scales by spatially explicit capture–recapture. Ecological Applications e2638.
Hristienko, H. and J. E. Mcdonald. 2007. Going into the 21st Century: a perspective on trends and controversies in the management of the American black bear. Ursus 18:72–88.
Humm, J., and J. D. Clark. 2021. Estimates of abundance and harvest rates of female black bears across a large spatial extent. The Journal of Wildlife Management 85:1321–1331.
Humm, J. M., J. W. McCown, B. K. Scheick, and J. D. Clark. 2017. Spatially explicit population estimates for black bears based on cluster sampling. Journal of Wildlife Management 81:1187–1201.
Hunter, M. D., and P. W. Price. 1992. Playing chutes and ladders: heterogeneity and the relative roles of bottom–up and top–down forces in natural communities. Ecology 73:724–732.
Hurvitch, C. M., and C-L. Tsai. 1989. Regression and time series model selection in small samples. Biometrika 76:297–307.
Johnson, H. E., S. W. Breck, S. Baruch-Mordo, D. L. Lewis, C. W. Lackey, K. R. Wilson, J. Broderick, J. S. Mao, and J. P. Beckmann. 2015. Shifting perceptions of risk and reward: dynamic selection for human development by black bears in the western United States. Biological Conservation 187:164–172.

Jones, J. P. G. 2011. Monitoring species abundance and distribution at the landscape scale. Journal of Applied Ecology 48:9–13.
Jones, M. D., and M. R. Pelton. 2003. Female American black bear use of managed forest and agricultural lands in coastal North Carolina. Ursus 14:188–197.
Jonker, S. A., J. A. Parkhurst, R. Field, and T. K. Fuller. Black bear depredation on agricultural commodities in Massachusetts. Wildlife Society Bulletin 26:318–324.
Karanth, K. U., and R. Chellam. 2009. Carnivore conservation at the crossroads. Oryx 43:1–2.
Karl, T. R., J. M. Meliool, and T. C., Hassol, editors. 2009. Peterson. Global Climate Change Impacts in the United States. Cambridge University Press, New York.
Kasworm, W. F., and T. L. Manley. 1990. Road and trail influences on grizzly bears and black bears in Northwest Montana. International Conference Bear Research and Management 8:79–84.
Kendall, K. C., T. A. Graves, J. A. Royle, A. C. Macleod, K. S. McKelvey, J. Boulanger, and J. S. Waller. 2019. Using bear rub data and spatial capture–recapture models to estimates trend in a brown bear population. Scientific Reports 9:16804.
Kolenosky, G. 1990. Reproductive biology of black bears in East-Central Ontario. International Conference on Bear Research and Management 8:385–392.
Kolenosky, G. B. 1986. The effects of hunting on an Ontario black bear population. International Conference Bear Research and Management 6:45–55.
Kristensen, T., M., Means, L. S., Eggert, K. G., Smith, and D. White. 2019. Demographics of American black bear populations following changes in harvest policy. Ursus 29:147–162.
Ladle, A., T. Avgar, M. Wheatley, G. B. Stenhouse, S. N. Nielsen, and M. S. Boyce. 2019. Grizzly bear response to spatio–temporal variability in human recreational activity. Journal of Applied Ecology 56:375–386.
Laliberte, A. S., and W. J. Ripple. 2004. Range contractions of North American carnivores and ungulates. BioScience 54:123–138.
Lamb, C. T., A. T. Ford, B. N. McLellan, M. F. Proctor, G. Mowat, L. Ciarniello, and S. Boutin. 2020. The ecology of human–carnivore coexistence. Proceedings of the National Academy of Sciences 117:17876–17883.
Lamb, C. T., A. T. Ford, M. F. Proctor, J. A. Royle, G. Mowat, and S. Boutin. 2019. Genetic tagging in the Anthropocene: scaling ecology from alleles to ecosystems. Ecological Applications 29:e01876.
Lamb, C. T., G. Mowat, A. Reid, L. Smit, M. Proctor, B. N. McLellan, S. E. Nielsen, and S. Boutin. 2018. Effects of habitat quality and access management on the density of a recovering grizzly bear population. Journal of Applied Ecology 55:1406–1417.
Laufenberg, J. S., H. E. Johnson, P. F. Doherty, and S. W. Breck. 2018. Compounding effects of human development and a natural food shortage on a black bear population along a human development–wildlife interface. Biological Conservation 224:188–198.
Lesmerises, R., and M. H. St-Laurent. 2017. Not accounting for interindividual variability can mask habitat selection patterns: a case study on black bears. Oecologia 185:415–425.
Levin, S. A. 1992. The problem of pattern and scale in ecology: the Robert H. MacArthur award lecture. Ecology 73:1943–1967.
Lewis, D. L., S. Baruch-Mordo, K. R. Wildon, S. W. Breck, J. S. Mao, and J. Broderick. 2015. Foraging ecology of black bears in urban environments: guidance for human–bear conflict mitigation. Ecosphere 6:141.

Lewis, K. P., E. Vander Wal, and D. A. Fifield. 2018. Wildlife biology, big data, and reproducible research. Wildlife Society Bulletin 42:172–179.
Long, R. A., P. MacKay, W. J. Zielinski, and J. C. Ray, editors. 2008. Noninvasive survey methods for carnivores. Island Press, Washington, District of Columbia, USA.
Loosen, A. E., A. T. Morehouse, and M. S. Boyce. 2018. Land tenure shapes black bear density and abundance on a multi-use landscape. Ecology and Evolution 9:73–89.
Lozano, J. A. Olszańska, Z. Morales-Reyes, A. A. Castro, A. F. Malo, M. Moleón, J. A. Sánchez-Zapata, A. Cortés-Avizandah, H. von Wehrdena, I., Dorresteijni, R. Kanskyj, J. Fischera, and B. Martín-Lópeza. 2019. Human-carnivore relations: a systematic review. Biological Conservation 237:480–492.
Lute, M. L., N. H. Carter, J. V. López-Bao, and J. D. C. Linnell. 2018. Conservation professionals agree on challenges to coexisting with large carnivores but not on solutions. Biological Conservation 218:233–232.
MacKenzie, D. I., J. D. Nichols, N. Sutton, K. Kawanishi, and L. L. Bailey. 2005. Improving inferences in population studies of rare species that are detected imperfectly. Ecology 86:1101–1113.
Marrotte, R. R., E. J. Howe, K. B. Beauclerc, D. Potter, and J. M. Northrup. 2022. Explaining detection heterogeneity with finite mixture and non-Euclidean movement in spatially explicit capture-recapture models. PeerJ 10:e13490.
Mccall, B. S., M. S. Mitchell, M. K. Schwartz, S. A. Cushman, P. Zager, P., and W. F. Kasworm. 2017. Combined use of mark–recapture and genetic analyses reveals response of a black bear population to changes in food productivity. The Journal of Wildlife Management, 77:1572–1582.
McFadden-Hiller, J. E., D. E. Beyer, and J. L. Belant. 2016. Spatial distribution of black bear incident reports in Michigan. PLoS ONE 11:e0154474.
McLaughlin, C. R., G. J., Jr. Matula, and R. J. O'Connor. 1994. Synchronous reproduction by Maine black bears. International Conference on Bear Research and Management 9:471–479.
McLellan, B. N. 1989. Dynamics of a grizzly bear population during a period of industrial resource extraction. II. Mortality rates and cause of death. Canadian Journal of Zoology, 67:1861–1864.
McLellan, M. L., B. N. McLellan, R. Sollmann, C. T. Lamb, C. D. Apps, and H. U. Wittmer. 2019. Divergent population trends following the cessation of legal grizzly bear hunting in southwestern British Columbia, Canada. Biological Conservation 233:247–254.
Milleret, C., P. Dupont, C. Bonenfant, H. Brøseth, Ø. Flagstad, C. Sutherland, and R. Bischof. 2019. A local evaluation of the individual state-space to scale up Bayesian spatial capture–recapture. Ecology and Evolution 9:352–363.
Moqanaki, E. M., C. Milleret, M. Tourani, P. Dupont, and R. Bischof. 2021. Consequences of ignoring variable and spatially-autocorrelated detection probability in spatial capture-recapture. Landscape Ecology 36:2879–2895.
Morehouse, A. T., and M. S Boyce. 2016. Grizzly bears without borders: spatially explicit capture–recapture in southwestern Alberta. The Journal of Wildlife Management 80:1152–1166.
Morin, D. J., J. Boulanger, R. Bischof, D. C. Lee, D. Ngoprasert, A. K., Fuller, B. McLellan, R. Steinmetz, S. Sharma, D. Garshelis, A. Gopalaswamy, M. A Nawaz, and U. Karanth. 2022.

Comparison of methods for estimating density and population trends for low–density Asian Bears. Global Ecology and Conservation 35:e02058.
Mosnier, A., J. Ouellet, and R. Courtois. 2008. Black bear adaptation to low productivity in the boreal forest. Écoscience 15:485–497.
Murphy, S. M., B. C. Augustine, W. A. Ulrey, J. M. Guthrie, B. K. Scheick, J. W. McCown, and J. J. Cox. 2017. Consequences of severe habitat fragmentation on density, genetics, and spatial capture-recapture analysis of a small bear population. PLoS ONE 12:1–21.
Natural Resources Canada. 2019. Lakes, River and Glaciers in Canada- CanVec Series – Hydrographic Features. <https://open.canada.ca/data/en/dataset/9d96e8c9-22fe-4ad2-b5e8-94a6991b744b>. Accessed June 5 2022.
Nawaz, M. A., B. U. Khan, A. Mahmood, M. Younas, J. U. Din, and C. Sutherland. 2021. An empirical demonstration of the effect of study design on density estimations. Scientific Reports 11:13104.
Newbold, T., L. N. Hudson, S. L. L. Hill, S. Contu, I. Lysenko, R. A. Senior, L. Börger, D. J. Bennett, A. Choimes, B. Collen, J. Day, A. De Palma, S. Díaz, S. Echeverria-Londoño, M.J. Edgar, A. Feldman, M. Garon, M. L. K. Harrison, T. Alhusseini, D. J. Ingram, Y. Itescu, J. Kattge, V. Kemp, L. Kirkpatrick, M. Kleyer, D. L. P. Correia, C. D. Martin, S. Meiri, M. Novosolov, Y. Pan, H. R. P. Phillips, D. W. Purves, A. Robinson, J. Simpson, S. L. Tuck, E. Weiher, H. J. White, R. M. Ewers, G. M. Mace, J. P. W. Scharlemann, and A. Purvis. 2015. Global effects of land use on local terrestrial biodiversity. Nature 520:45–50.
Newton, E. J., and M. E. Obbard. 2018. Can population reconstruction be used to estimate black bear abundance in Ontario? Ontario Ministry of Natural Resources and Forestry, Science and Research Branch, Peterborough, ON. Science and Research Information Report IR-12.
Nielsen, S. E., T. A., Larsen, G. B., Stenhouse, and S. C. P. Coogan. 2017. Complementary food resources of carnivory and frugivory affect local abundance of an omnivorous carnivore. Oikos 126: 369–380.
Northrup, J. M., E. Howe, J. Inglis, E. Newton, M. Obbard, B. Pond, and D. Potter. In press. Experimental test of the efficacy of hunting for controlling human–wildlife conflict. Journal of Wildlife Management and Wildlife Monographs.
Northrup, J. M., J. Pitt, T. B. Muhly, G. B. Stenhouse, M. Musiani, and M. S. Boyce. 2012. Vehicle traffic shapes grizzly bear behavior on a multiple–use landscape. Journal of Applied Ecology 49:1159–1167.
Nyhus, P. J. 2016. Human–wildlife conflict and coexistence. Annual Review of Environment and Resources 41:143–71.
Obbard, M. E., and E. J. Howe. 2008. Demography of black bears in hunted and unhunted areas of the boreal forest of Ontario. The Journal of Wildlife Management 72:869–880.
Obbard, M. E., E. J. Howe, and C. J. Kyle. 2010. Empirical comparison of density estimators for large carnivores. Journal of Applied Ecology 47:76–84.
Obbard, M. E., E. J. Howe, L. L. Wall, B. Allison, R. Black, P. Davis, L. Dix-Gibson, M. Grant, and M. N. Hall. 2014. Relationships among food availability, harvest, and human–bear conflict at landscape scales in Ontario, Canada. Ursus 25:98–110.
Obbard, M., E. J., Newton, D. Potter, A. Orton, B. R. Patterson, and B. D. Steinberg. 2017. Big enough for bears? American black bears at heightened risk of mortality during seasonal forays outside Algonquin Provincial Park, Ontario. Ursus 28:182–194.

O'Brien, T. G., and M. F. Kinnaird 2011. Density estimation of sympatric carnivores using spatially explicit capture-recapture methods and standard trapping grid. Ecological Applications 21:2908–2916.
Onorato, D. P, E. C. Hellgren, R. A. van den Bussche, D. L. Doan-Crider. 2004. Phylogeographic patterns within a metapopulation of black bears (*Ursus americanus*) in the American Southwest. Journal of Mammalogy 85:140–147. Ontario Ministry of Natural Resources [OMNRF]. 2009. Backgrounder on black bears in Ontario. Wildlife Section, Fish and Wildlife Branch, Ontario. Ministry of Natural Resources, Peterborough, ON, Canada.
Otis, D. L., K. P. Burnham, G. C. White, and D. R. Anderson. 1987. Statistical inference from capture data on closed animal populations. Wildlife Monographs 62:3–135.
Penteriani, V., A. Zarzo-Arias, A. Novo-Fernández, G. Bombieri, and C. A. López-Sánchez. 2019. Responses of an endangered brown bear population to climate change based on predictable food resource and shelter alterations. Global Change Biology 25:1133–1151.
Perera, A.H., D. L., Euler, and I. D. Thompson, editors. 2000. Ecology of a managed terrestrial landscape: patterns and processes of forest landscapes in Ontario. Ontario Ministry of Natural Resources, Toronto, Ontario, and UBC Press, Vancouver, British Columbia.
Pettorelli, N., S. Ryan, T. Mueller, N. Bunnefeld, B. Jedrzejewska, M. Lima, M., and K. L. Kausrud. 2011. The normalized difference vegetation index (NDVI): unforeseen successes in animal ecology. Climate Research 46:15–27.
Potter, D., and M. Obbard. 2017. Ontario wildlife food survey, 2016. Ontario Ministry of Natural Resources and Forestry, Science and Research Branch, Peterborough, Ontario. Science and Research Technical Report TR-18.
Poulin, R., J. Knight, M. Obbard, and G. Witherspoon. 2003. Nuisance bear review committee. Committee report and recommendations. Ontario Ministry of Natural Resources, Peterborough, ON, Canada.
Proctor, M., B. McLellan, J. Boulanger, C. Apps, G. Stenhouse, D. Paetkau, and G. Mowat. 2010. Ecological investigations of grizzly bears in Canada using DNA from hair, 1995–2005: a review of methods and progress. Ursus 21:169–188.
Proctor, M. F., B. N. McLellan, G. B. Stenhouse, G. Mowat, C. T. Lamb, C. T., and M. S. Boyce. 2019. Effects of roads and motorized human access on grizzly bear populations in British Columbia and Alberta, Canada. Ursus 30:16–39.
Rettler, S. J., A. N. Tri, V. St-Louis, J. D. Forester, D. L. Garshelis. 2021. Three decades of declining natural foods alters bottom-up pressures on American black bears. Forest Ecology and Management 493:119267.
Ripple, W. J., J. A. Estes, R. L. Beschta, C. C. Wilmers, E. G. Ritchie, M. Hebblewhite, J. Berger, B. Elmhagen, M. Letnic, M. P. Nelson, O. J. Schmitz, D. W. Smith, A. D. Wallach, A. J. Wirsing. 2014. Status and ecological effects of the world's largest carnivores. Science 343:1241484.
Rogers, L. L., D. W. Kuehn, A. W. Erickson, E. M. Harger, L. J. Verme, and J. J. Ozoga. 1976. Characteristics and management of black bears that feed in garbage dumps, campgrounds or residential areas. Third International Conference on Bears 169–175.
Romain, D. A., M. E. Obbard, and J. L. Atkinson. 2013. Temporal variation in food habits of the American Black Bear (*Ursus americanus*) in the boreal forest of northern Ontario. Canadian Field–Naturalist 127:118–130.
Rowe, J. S. 1972. Forest regions of Canada. Canadian Forestry Service Publication No. 1300. Environment Canada, Ottawa.

Royle, J. A., R. B., Chandler, R. Sollmann, and Gardner, B. 2014. Spatial capture–recapture. Academic Press, Waltham, Massachusetts, USA.
Royle, A. R. B. Chandler, C. C. Sun, A. K. Fuller. 2013. Integrating resource selection information with spatial capture–recapture. Methods in Ecology and Evolution 4:520–530.
Royle, J. A., A. K. Fuller, and C. Sutherland. 2018. Unifying population and landscape ecology with spatial capture–recapture. Ecography 41:444–456.
Royle, J. A., and Young K. V. A hierarchical model for spatial capture–recapture data. Ecology 89:2281–2289.
Ruphrecht, J. S., C. E. Eriksson, T. D. Forrester, D. A. Clark, M. J. Wisdom, M. M. Rowland, B. K. Johnson, and T. Levi. 2021. Evaluating and integrating spatial capture–recapture models with data of variable individual identifiability. Ecological Applications 31:e02405.
Ryan, C. W., J. C. Pack, W. K. Igo, and A. Billings. Influence of mast production on black bear non–hunting mortalities in West Virginia. Ursus 18:46–53.
Sadeghpour, M. H., and T. F Ginnett. 2011. Habitat selection by female American black bears in northern Wisconsin. Ursus 22:159–166.
Scheick, B. K., and W. McCown. 2014. Geographic distribution of American black bears in North America. Ursus 25:24–34.
Schneider, D. C. 2001. The rise of the concept of scale in ecology. BioScience 51:545–553.
Scheiner, S. M., and M. R. Willig. 2008. A general theory of ecology. Theoretical Ecology 1:21–28.
Schneider, D. C. 2001. The rise of the concept of scale in ecology. BioScience 51:545–553.
Schmidt, G. M., T. A. Graves, J. C. Pederson, and S. L. Caroll. 2022. Precision and bias of spatial–recapture estimates: a multi–site, multi–year Utah black bear case study. Ecological Applications doi:10.1002/eap.2618.
Schoen, J. W. 1990. Bear habitat management: a review and future perspective. International Association for Bear Research and Management 8:143–154.
Sinclair, A. R. E., and C. J. Krebs. 2002. Complex numerical responses to top–down and bottom–up processes in vertebrate populations. Philosophical Transactions of the Royal Society 357:1221–1231.
Sollmann, R., M. M. Furtado, B. Gardner, H. Hofer, A. T. A. Jácomo, N. M. Tôrres, and L. Silveira. 2011. Improving density estimates for elusive carnivores: accounting for sex–specific detection and movements using spatial capture–recapture models for jaguars in central Brazil. Biological conservation 144:1017–1024.
Sollmann, R., B. Gardner, and J. L. Belant. 2012. How does spatial study design influence density estimates from spatial capture–recapture models? PLoS ONE 7:e34575.
Statistics Canada. 2021. Corrected representation of the NDVI using historical AVHRR satellite images (1km resolution) from 1987 to 2021. < https://open.canada.ca/data/en/dataset/44ced2fa-afcc-47bd-b46e-8596a25e446e>. Accessed June 2022.
Statistics Canada. 2022. National Road Network. < https://open.canada.ca/data/en/dataset/3d282116-e556-400c-9306-ca1a3cada77f>. Accessed June 2022.
Stetz, J. B., K. C. Kendall, and A. C. Macleod. 2014. Black bear density in glacier national park, Montana. Wildlife Society Bulletin 38:60–70.
Stevenson, B. C., R. M. Fewster, and K. Sharma. 2021. Spatial correlation structures for detections of individuals in spatial–recapture models. Biometric methodology 1–11.

Su, J., and A. Aryal, I. M. Hegab, U. B. Shrestha, S. C. P. Coogan, S. Sathyakumar, M. Dalannast, Z. Dou, Y. Suo, X. Dabu, H. Fu, L. Wu, and W. Ji. 2018. Decreasing brown bear (*Ursus arctos*) habitat due to climate change in Central Asia and Asian Highlands. Ecology and Evolution 8:11887–11899.

Sun, C. C., A. K. Fuller, M. P. Hare, and J. E. Hurst. 2017. Evaluating populations expansion of black bears using spatial capture–recapture. The Journal of Wildlife Management 81:814–823.

Sun, C. C., A. K. Fuller, and J. A. Royle. 2014. Trap configuration and spacing influences parameter estimates in spatial capture–recapture models. PLoS ONE 9:e88025.

Sutherland, W. J., R. P. Freckleton, H. C. J. Godfray, S. R. Beissinger, T. Benton, D. D. Cameron, Y. Carmel., D. A. Coomes, T. Coulson, M. C. Emmerson, R. S. Hails, G. C. Hays, D. J. Hodgson, M. J. Hutchingsm D. Johnson, J. P. G. Jones, M. J. Keeling, H. Kokko, W. E. Kunin, Z. Lambin, O. T. Lewis, Y. Malhi, N. Mieszkowska, E. J. Milner-Gulland, K. Norris, A. B. Phillimoresm D. W. Purves, J. M. Reid, D. C. Reuman, K. Thompson, J. M. J. Travis, L. A. Turnbull, D. A. Wardle, and T. Wiegand. 2013. Identification of 100 fundamental ecological questions. Journal of Ecology 101:58–67.

Theng, M. C. Milleret, C. Bracis, P. Cassey, and S. Delean. 2022. Confronting spatial capture–recapture models with realistic animal movement simulations. Ecology doi: 10.1002/ecy.3676.

The North America Land Change Monitoring System [NALCMS]. 2020. 2015 Land cover of north America at 30 meters. < http://www.cec.org/north-american-environmental-atlas/land-cover-30m-2015-landsat-and-rapideye/>. Accessed June 5 2022.

Tigner, J., E. M. Bayne, and S. Boutin. 2014. Black bear use of seismic lines in Northern Canada. Journal of Wildlife Management 78:282–292.

Tilman, D., M. Clark, D. R. Williams, K. Kimmel, S. Polasky, and C. C. Packer. 2017. Future threats to biodiversity and pathways to their prevention. Nature 546:73–81.

Tobler, M. W., and G.V.N. Powell. 2013. Estimating jaguar densities with camera traps: problems with current designs and recommendations for future studies. Biological Conservation 159:109–118.

Tourani, M. 2021. A review of spatial capture–recapture: ecological insights, limitations, and prospects. Ecology and Evolution 12:e8468.

Towes, M., F. Juanes, and C. A. Burton. 2017. Mammal responses to human footprint vary with spatial extent but not with spatial grain. Ecosphere 8:e01735.

Travis, J. M. J., J. D. J. Murrell, and C. Dytham. 1999. The evolution of density–dependent dispersal. Proceedings of the Royal Society of London. Series B: Biological Sciences 266:1837-1842.

Treves, A., and K. U. Karanth. 2003. Human–carnivore conflict and perspectives on carnivore management worldwide. Conservation Biology 17:1491–1499.

Turchin, P. 1989. Does population ecology have general laws? Oikos 94:17–26.

Turner, M. G. 1989. Landscape ecology: the effect of pattern on process. Annual Review of Ecology and Systematics 20:171–197.

Turner, M. G. 2005. Landscape ecology: what is the state of the science? Annual Review of Ecology, Evolution, and Systematics 36:319–344.

van Manen, J. T., C. W. Lackey, J. P. Beckmann, L. I. Muller, and Z. Li. 2020. Assimilated diet patterns of American black bears in the Sierra Nevada and western Great Basin, Nevada, USA. Ursus 30e3:40–50.

Waller, J. S., and C. Servheen. 2005. Effects of Transportation Infrastructure on Grizzly Bears in Northwestern Montana. Journal of Wildlife Management 69: 985–1000.
Welfelt, L. S., R. A. Beausoleil, and R. B. Wielgus. 2019. Factors associated with black bear density and implications for management. The Journal of Wildlife Management 83:1527–1539.
Wheatley, M., and C. Johnson. 2009. Factors limiting our understanding of ecological scale. Ecological Complexity 6:150–159.
Wiens, J. A. 1989. Spatial Scaling in Ecology. Functional Ecology 3:385–397.
Wightman, N., E. Howe, A. Satura, and J. Northrup. 2022. Factors affecting age at primiparity in black bears. Journal of Wildlife Management e22297.
Wildlife Conservation Society [WCS] and Center for International Earth Science Information Network [CIESIN] Columbia University. 2005. Last of the Wild Project, Version 2, 2005 (LWP-2): Global Human Influence Index (HII) Dataset (Geographic). < https://doi.org/10.7927/H4BP00QC>. Accessed 28 February 2022 >. Accessed June 2022.
Wilton, C. M., E. E. Puckett, J. Beringer, B. Gardner, L. S. Eggert, and J. L. Belant. 2014. Trap array configuration influences estimates and precision of black bear density and abundance. PLoS ONE 9:e111257.
Woods, J. G., D. Paetkau, D. Lewis, B. N. McLellan, M. Proctor, and C. Strobeck, C. 1999. Genetic tagging of free–ranging black and brown bears. Wildlife Society Bulletin 27:616–627.
Wu, J. 2004. Effect of changing scale on landscape pattern analysis: scaling relations. Landscape Ecology 19:125–138.
Wu, J., M. Luck, D. E. Jelinski, and P. T. Tueller. 2000. Multiscale analysis of landscape heterogeneity: scale variance and pattern metrics. Geographic Information Sciences 6:6–19.
Wynn-Grant, R., J. R. Ginsberg, C. W. Lackey, E. J. Sterling, and J. P. Beckmann. 2018. Risky business: modeling mortality risk near the urban–wildland interface for a large carnivore. Global Ecology and Conservation 16:e00443.
Zeller, K. A., D. W. Wattles, L. Conlee, and S Destefano. 2019. Black bears alter movements in response to anthropogenic features with time of day and season. Movement Ecology 7:1–14.

Appendix A: Chapter 2

A.1 Chapter 2 list of candidate model forms

Table A.1.1. Candidate model forms with combination of covariates on the parameters density (D), spatial scale parameter (σ) and detection probability (g_0).

Model number †	Parameter			Model number †	Parameter		
	D	g_0	σ		D	g_0	σ
1	1	1	1	27	area	sex	area
2	area	1	1	28	sex	sex	area
3	sex	1	1	29	area+sex	sex	area
4	area+sex	1	1	30*	area×sex	sex	area
5*	area×sex	1	1	31	1	area+sex	area
6	1	sex	1	32	area	area+sex	area
7	area	sex	1	33	sex	area+sex	area
8	sex	sex	1	34	area+sex	area+sex	area
9	area +sex	sex	1	35*	area×sex	area+sex	area
10*	Area×sex	sex	1	36*	1	area×sex	area
11	1	area+sex	1	37*	area	area×sex	area
12	area	area+sex	1	38*	sex	area×sex	area
13	sex	area+sex	1	39*	area+sex	area×sex	area
14	area+sex	area+sex	1	40*	area×sex	area×sex	area
15*	area×sex	area+sex	1	41	1	1	sex
16*	1	area×sex	1	42	area	1	sex
17*	area	area×sex	1	43	sex	1	sex
18*	sex	area×sex	1	44	area+sex	1	sex
19*	area+sex	area×sex	1	45*	area×sex	1	sex
20*	area×sex	area×sex	1	46	1	sex	sex
21	1	1	area	47	area	sex	sex
22	area	1	area	48	sex	sex	sex
23	sex	1	area	49	area+sex	sex	sex
24	area+sex	1	area	50*	area×sex	sex	sex
25*	area×sex	1	area	51	1	area+sex	sex
26	1	sex	area	52	area	area+sex	sex

† Models indicated with asterisk (*) not presented in results or discussion. See section 4 of appendix for clarification.

Table A.1.1 (continued).

Model number †	Parameter			Model number †	Parameter		
	D	**g_0**	***σ***		**D**	**g_0**	***σ***
53	sex	area+sex	sex	80*	area×sex	area×sex	area+sex
54	area+sex	area+sex	sex	81*	1	1	area×sex
55*	area×sex	area+sex	sex	82*	area	1	area×sex
56*	1	area×sex	sex	83*	sex	1	area×sex
57*	area	area×sex	sex	84*	area+sex	1	area×sex
58*	sex	area×sex	sex	85*	area×sex	1	area×sex
59*	area+sex	area×sex	sex	86*	1	area	area×sex
60*	area×sex	area×sex	sex	87*	area	area	area×sex
61	1	1	area+sex	88*	sex	area	area×sex
62	area	1	area+sex	89*	area+sex	area	area×sex
63	sex	1	area+sex	90*	area×sex	area	area×sex
64	area+sex	1	area+sex	91*	1	sex	area×sex
65*	area×sex	1	area+sex	92*	area	sex	area×sex
66	1	sex	area+sex	93*	sex	sex	area×sex
67	area	sex	area+sex	94*	area+sex	sex	area×sex
68	sex	sex	area+sex	95*	area×sex	sex	area×sex
69	area+sex	sex	area+sex	96*	1	area+sex	area×sex
70*	area×sex	sex	area+sex	97*	area	area+sex	area×sex
71	1	area+sex	area+sex	98*	sex	area+sex	area×sex
72	area	area+sex	area+sex	99*	area+sex	area+sex	area×sex
73	sex	area+sex	area+sex	100*	area×sex	area+sex	area×sex
74	area+sex	area+sex	area+sex	101*	1	area×sex	area×sex
75*	area×sex	area+sex	area+sex	102*	area	area×sex	area×sex
76*	1	area×sex	area+sex	103*	sex	area× sex	area×sex
77*	area	area×sex	area+sex	104*	area+sex	area×sex	area×sex
78*	sex	area×sex	area+sex	105*	area×sex	area×sex	area×sex
79*	area+sex	area×sex	area+sex				

† Models indicated with asterisk (*) not presented in results or discussion. See section 4 of appendix for clarification.

A. 2 Chapter 2 summary of simulated populations

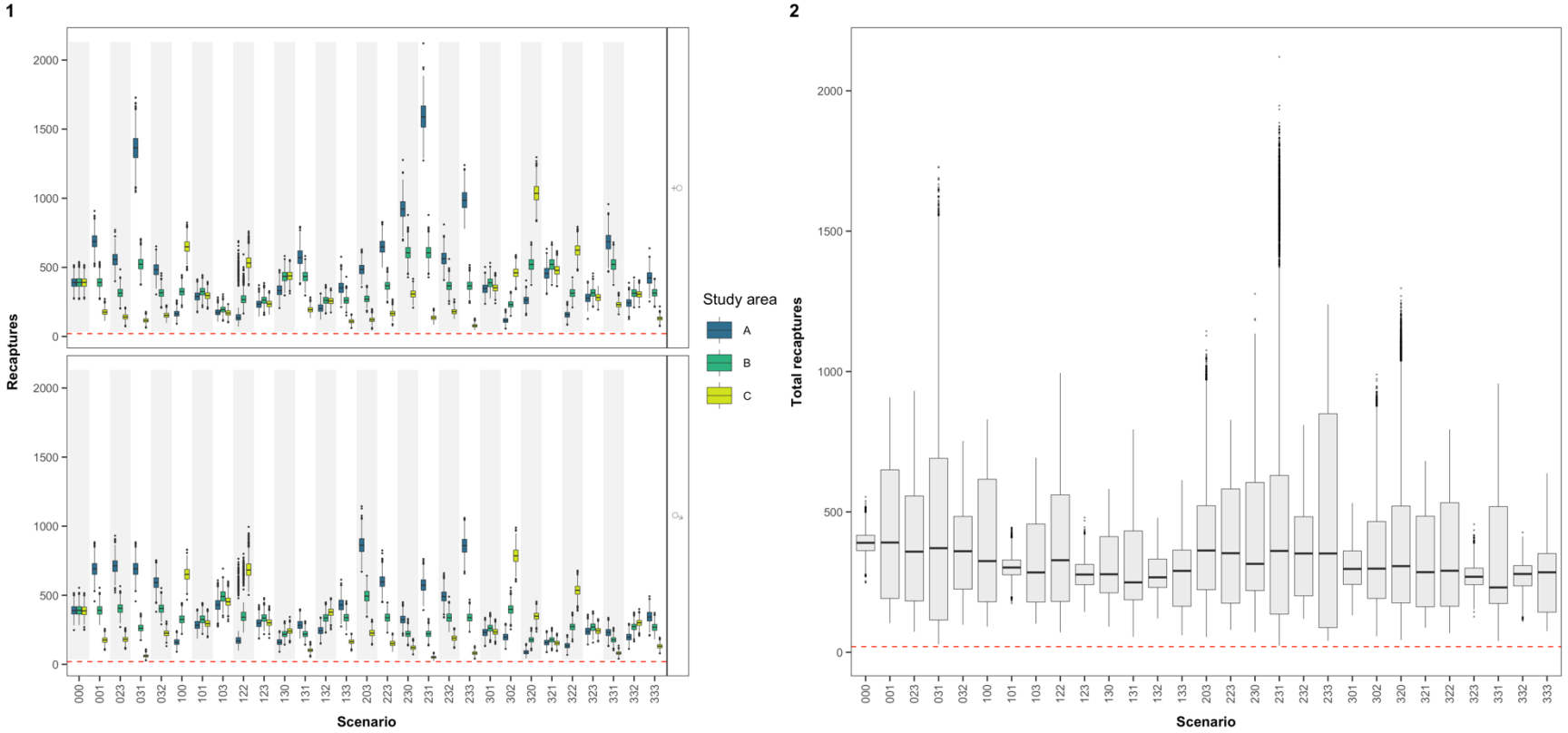

Figure A.2.1. Spatial recaptures of female (♀) and male (♂) black bears across sampling areas (A, B, C; figure1) and combined total spatial recaptures (figure 2). Scenario ID coded by variables corresponding to whether the parameters (D, g_0, σ) were constant (0) or vary by area (1), sex (2), or both sex and area (3). Coloured boxes represent the 25% to 75% percentiles, thick horizontal black lines the median; whiskers extend 1.5 times the interquartile range and black dots outside the boxes represent outliers. Red dashed horizonal line indicates the recommended minimum of 20 recaptures for SECR models.

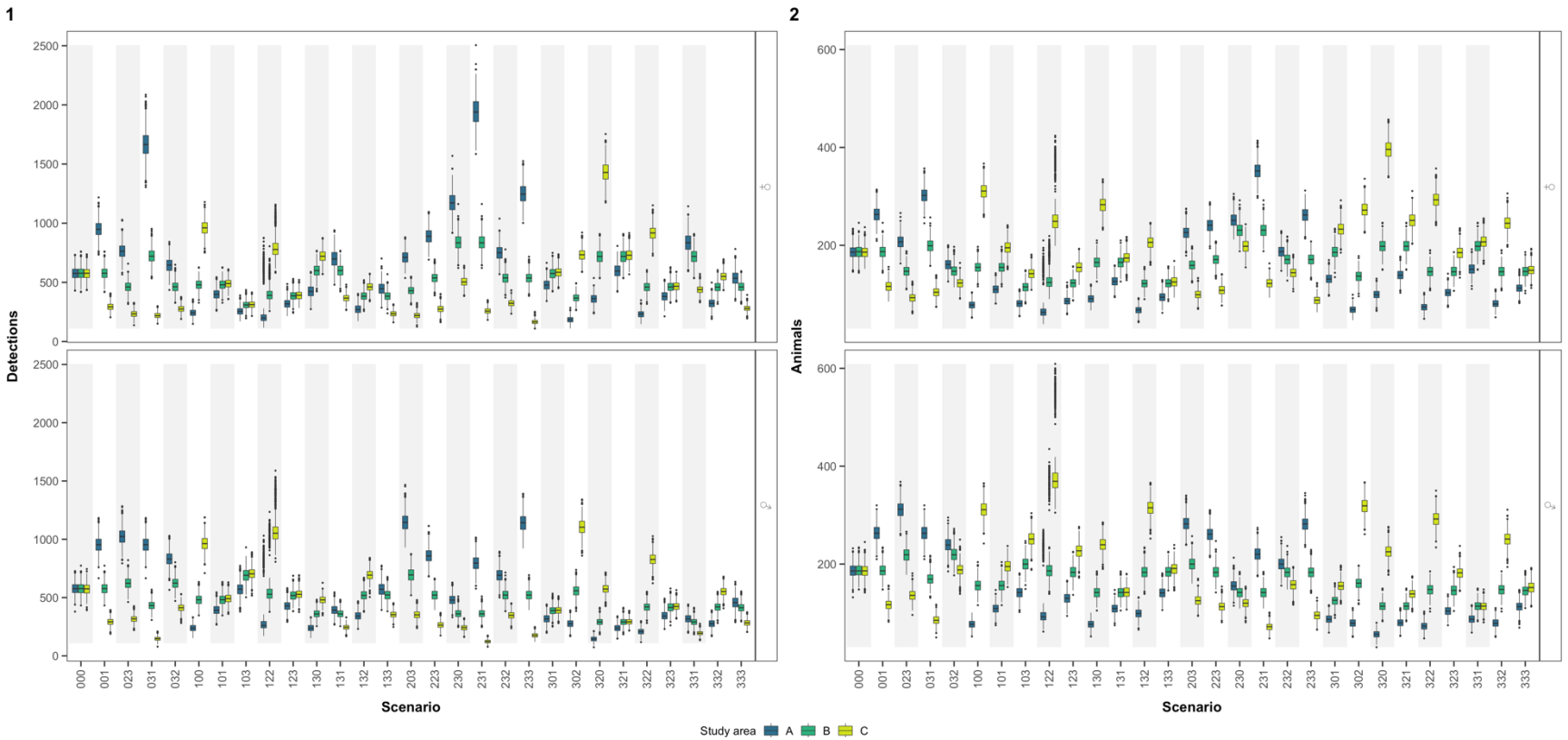

Figure A.2.2. Number of detections (figure 1) and individual female (♀) and male (♂) black bears (figure 2) across sampling areas (A, B, C). Scenario ID coded by variables corresponding to whether the parameters (D, g_0, σ) were constant (0) or varied by area (1), sex (2), or both sex and area (3). Coloured boxes represent the 25% to 75% percentiles, thick horizontal black lines the median; whiskers extend 1.5 times the interquartile range and black dots outside the boxes represent outliers.

A.3 Chapter 2 95% confidence interval coverage and mean percent relative bias

Table A.3.1. The mean 95% confidence interval (CI) coverage of simulated female and male black bear densities for the true data generating model (M_T) across study areas (A, B, C) for each scenario. Scenario ID coded by variables corresponding to whether the parameters (D, g_0, σ) were constant across areas and sexes (0), or varied by area (1), sex (2), or both sex and area (3). *K* is the number of parameters in M_T. Bold values represent values equal to or greater than the nominal CI coverage (95.0).

		Female			**Male**		
Scenario	***K***	**A**	**B**	**C**	**A**	**B**	**C**
000	3	94.9	94.9	94.9	94.9	94.9	94.9
001	5	**95.1**	**95.1**	**95.1**	**95.1**	**95.1**	**95.1**
023	7	**95.0**	**95.0**	**95.0**	**95.0**	**95.0**	**95.0**
031	8	**95.7**	**95.7**	**95.7**	**95.7**	**95.7**	**95.7**
032	7	**95.3**	**95.3**	**95.3**	**95.3**	**95.3**	**95.3**
100	5	**95.9**	94.2	**95.1**	**95.9**	94.2	**95.1**
101	7	**95.6**	94.3	**95.3**	**95.6**	94.3	**95.3**
103	8	**95.3**	**95.1**	**96.3**	**95.3**	**95.1**	**96.3**
122	7	**95.7**	94.6	93.7	**95.7**	94.6	93.7
123	9	**95.1**	**95.0**	**96.2**	**95.1**	**95.0**	**96.2**
130	8	**96.1**	**95.1**	**93.9**	**96.1**	**95.1**	93.9
131	10	**95.7**	94.5	**95.6**	**95.7**	94.5	**95.6**
132	9	**95.1**	**95.1**	94.9	**95.1**	**95.1**	94.9
133	11	**95.7**	**94.6**	**94.6**	**95.7**	94.6	94.6
203	7	94.2	94.2	94.2	94.0	94.0	94.0
223	8	94.4	94.4	94.4	93.8	93.8	93.8
230	7	94.7	94.7	94.7	93.0	93.0	93.0
231	9	**95.0**	**95.0**	**95.0**	93.3	93.3	93.3
232	8	**95.0**	**95.0**	**95.0**	94.1	94.1	94.1
233	10	94.5	94.5	94.5	93.4	93.4	93.4
301	8	94.8	**95.2**	**95.4**	**95.2**	**94.2**	**95.7**
302	7	94.6	94.3	94.6	94.3	94.5	**96.2**

Table A.3.1 (continued).

		Female			Male		
Scenario	***K***	**A**	**B**	**C**	**A**	**B**	**C**
320	7	**94.3**	**95.8**	**94.7**	**95.1**	94.7	**96.5**
321	9	94.5	**95.1**	**95.3**	**95.1**	**95**	**96.3**
322	8	**95.1**	94.6	94.5	94.8	**95.8**	**95.8**
323	10	**95.8**	**94.7**	**95.1**	**95.0**	**95.3**	**95.1**
331	11	**95.2**	**95.3**	**95.5**	**95.4**	94.1	**95.1**
332	10	94.7	**95.0**	94.1	94.5	93.7	**95.6**
333	12	94.9	94.4	94.4	93.9	94.6	93.8

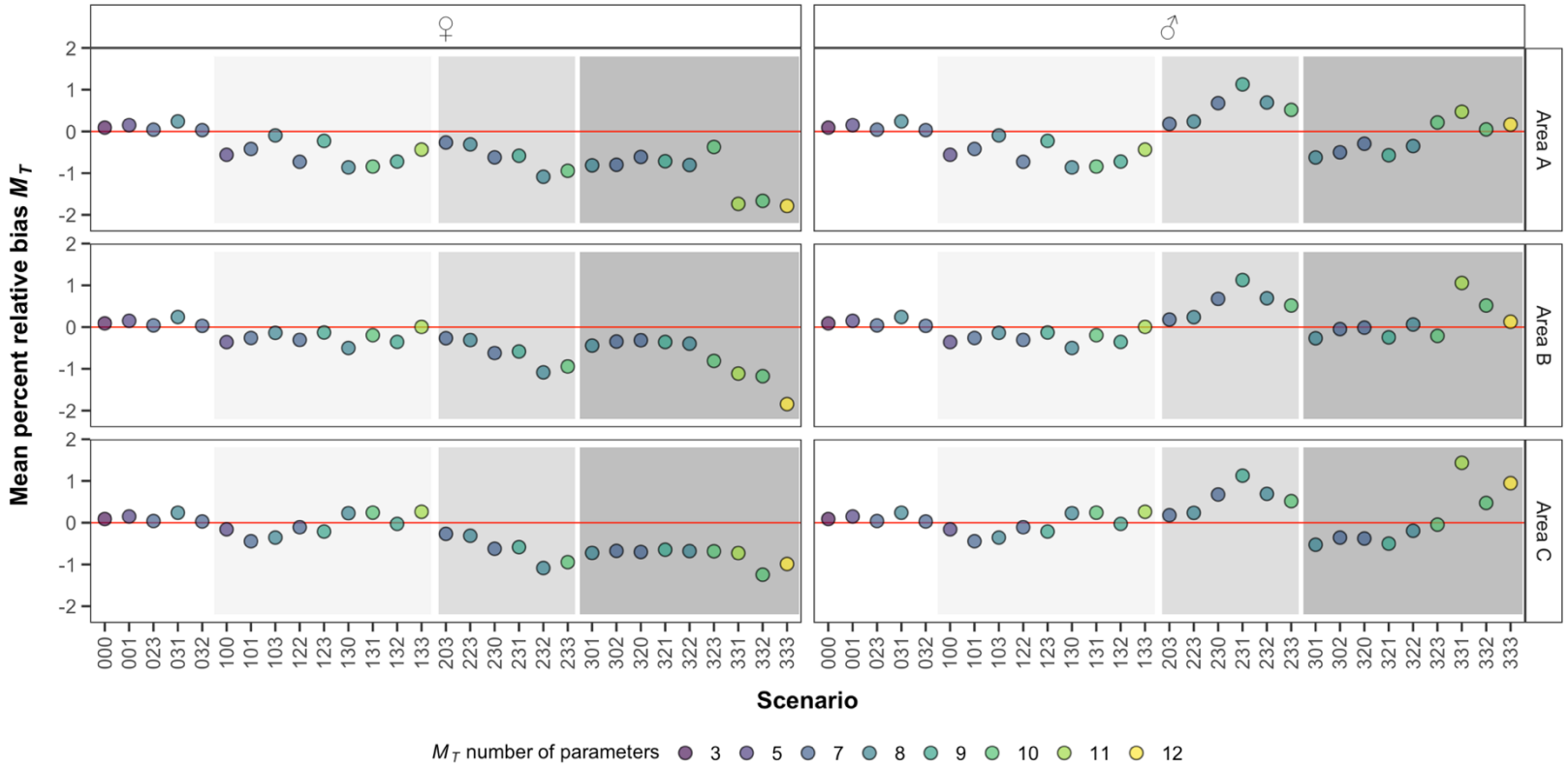

Figure A.3.1. Mean percent relative bias (PRB) of female (♀) and male (♂) black bear density estimates for the true data generating model (M_T) across study areas (A, B, C), for 1000 simulations of each scenario. Scenarios are coded by variables corresponding to whether the parameters (D, g_0, σ) were constant across areas and sexes (0), or varied by area (1), sex (2), or both sex and area (3). Red horizontal lines represent no bias. Background colors correspond to the four levels of variation in density: constant density (white), density varies by area (light gray), sex (medium gray), and both area and sex (dark gray). All scenarios fall within acceptable bias ($\leq$ 5% |MPRB|).

A.4 Chapter 2 comparison between interactive and additive models

For each of the 29 scenarios 1000 black bear populations were simulated and fit to 105 candidate models; this resulted in 3,045,000 models fit overall that required high computational costs and was prohibitively slow to summarize model outputs. Additive or interactive models forms with the same structure of covariates for each parameter (i.e., additive model D~area g_0~area+sex σ~sex; interactive model D~area g_0~area×sex σ~sex) exhibit similar patterns in density estimates across the sampling areas for both sexes (these patterns are summarized for scenario 333 in Figure S4 below; other scenarios display similar patterns). Because density estimates from interactive or additive model forms are similar (Figure A.4.1), including all candidate model forms with additive and interactive forms would not enhance the overall insight and conclusions drawn from this work. Therefore, to reduce high computational cost and simplify interpretation of results, we excluded candidate model forms where covariates on any one of the parameters (D, g_0, σ) included interactions between sex and area. This resulted in 48 candidate models with only additive effects being presented in the results and discussion.

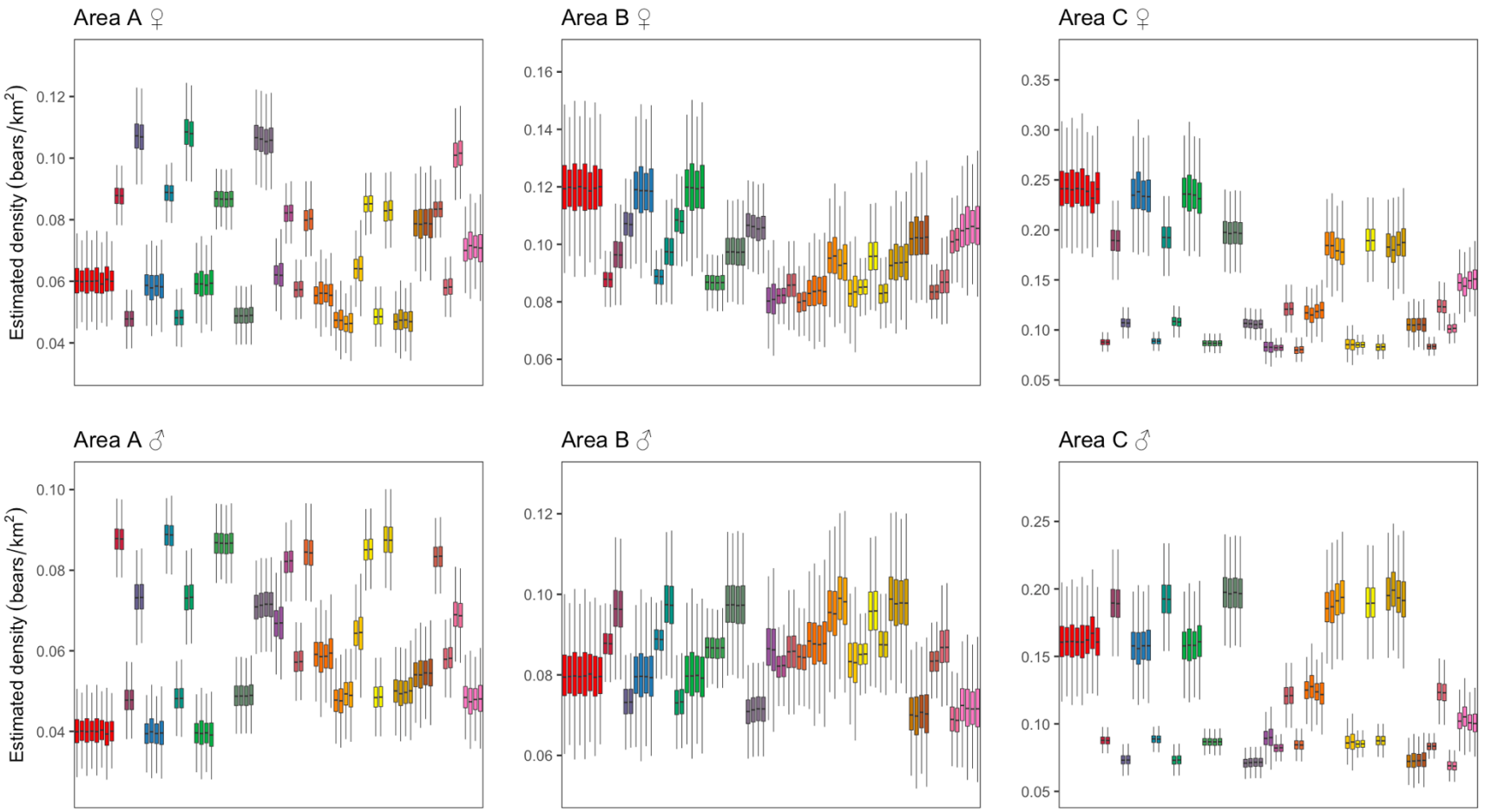

Figure A.4.1. For scenario 333 (D, g_0, σ vary by sex and area), female (♀) and male (♂) bear densities (bears/km^2) in three different sampling areas (A, B, C) from 82 different SECR candidate models forms fit to 1000 simulated populations with spatial and sex specific density (D), detection probability (g_0) and spatial scale (σ) parameters. Coloured boxes represent the 25% to 75% percentiles, thick horizontal black lines the median; whiskers extend 1.5 times the interquartile rang; outliers are excluded from the plots. The colour of boxes indicates model forms that have the same structure of covariates for each parameter, but either additive or interactive effects of sex and area. The approximate data generating model for this scenario is indicated by the eight red boxes on the far left of each panel. True densities in area A (0.06 and 0.04 bears/ km^2), area B (0.12 and 0.08 bears/km^2), and area C (0.24 and 0.16 bears/km^2) for female and male bears, respectively.

A.5 Chapter 2 most frequent SECR model forms for each scenario

Table A.5.1. The five most frequent top-ranked SECR models ($\Delta AIC_c = 0$), out of 1000 simulations, for each scenario. Columns represent the frequency the model form was ranked as the top model (*n*), number of parameters in the model (*K*), the minimum, maximum, and mean Akaike weight (w_i) and the mean percent relative bias (MPRB), mean coefficient of variation (MCV) and root-mean squared-error (RMSE) of male and female black bear densities (bears/km^2) across different sampling regions (A, B, C) for each model form. Italicized bold values indicate a |MPRB| greater than 5%. Model parameters D, g_0, σ are constant (.) or vary by area (a), sex (s) or the additive effect between the two (a+s). Bold text indicates the true data generating model (M_T) for each scenario. Scenarios are coded by variables corresponding to whether the three parameters (D, g_0, σ) are constant across areas and sexes (0), or vary by area (1), sex (2), or both sex and area (3). For some scenarios there were less than five models forms identified as the top-ranked model.

							Female								
				w_i			MPRB			MCV			RMSE		
Scenario	**Model**	***K***	***n***	**min**	**max**	**mean**	**A**	**B**	**C**	**A**	**B**	**C**	**A**	**B**	**C**
000	**D(.) g_0(.) σ(.)**	3	426	0.075	0.278	0.172	0.079	0.079	0.079	0.035	0.035	0.035	4.15E-03	4.15E-03	4.15E-03
000	D(s) g_0(.) σ(.)	4	78	0.071	0.289	0.168	-1.011	-1.011	-1.011	0.046	0.046	0.046	8.28E-03	8.28E-03	8.28E-03
000	D(.) g_0((s) σ(.)	4	69	0.083	0.247	0.147	0.707	0.707	0.707	0.035	0.035	0.035	4.37E-03	4.37E-03	4.37E-03
000	D(.) g_0(.) σ(s)	4	67	0.071	0.313	0.162	0.972	0.972	0.972	0.035	0.035	0.035	4.85E-03	4.85E-03	4.85E-03
000	D(.) g_0(.) σ(a)	5	60	0.064	0.3	0.158	0.317	0.317	0.317	0.035	0.035	0.035	4.15E-03	4.15E-03	4.15E-03
001	**D(.) g_0(.) σ(a)**	5	487	0.084	0.319	0.218	0.349	0.349	0.349	0.035	0.035	0.035	4.16E-03	4.16E-03	4.16E-03
001	D(s) g_0(.)σ(a)	6	110	0.097	0.384	0.211	-0.316	-0.316	-0.316	0.046	0.046	0.046	8.28E-03	8.28E-03	8.28E-03
001	D(.) g_0(.) σ(a+s)	6	78	0.117	0.352	0.207	0.225	0.225	0.225	0.035	0.035	0.035	3.77E-03	3.77E-03	3.77E-03
001	D(.) g_0(s) σ(a)	6	72	0.113	0.317	0.191	-0.003	-0.003	-0.003	0.035	0.035	0.035	4.38E-03	4.38E-03	4.38E-03
001	D(a) g_0(.) σ(a)	7	72	0.092	0.32	0.197	0.271	0.023	-0.620	0.050	0.061	0.081	8.05E-03	1.17E-02	1.61E-02
023	**D(.) g_0(s)σ(a+s)**	7	618	0.18	0.559	0.405	0.254	0.254	0.254	0.036	0.036	0.036	4.31E-03	4.31E-03	4.31E-03
023	D(a) g_0(s) σ(a+s)	9	117	0.205	0.591	0.375	0.559	0.282	-0.777	0.051	0.062	0.083	9.19E-03	1.10E-02	1.59E-02
023	D(.) g_0(a+s) σ(a+s)	9	112	0.18	0.586	0.368	0.197	0.197	0.197	0.036	0.036	0.036	4.50E-03	4.50E-03	4.50E-03
023	D(s) g_0(s) σ(a+s)	8	103	0.208	0.711	0.393	-0.083	-0.083	-0.083	0.055	0.055	0.055	9.93E-03	9.93E-03	9.93E-03

023	D(a+s) g_0(s) σ(a+s)	10	15	0.235	0.523	0.374	1.548	0.285	0.292	0.066	0.075	0.093	1.51E-02	1.62E-02	2.04E-02
031	**D(.) g_0(a+s) σ(a)**	8	585	0.188	0.468	0.354	0.376	0.376	0.376	0.035	0.035	0.035	4.13E-03	4.13E-03	4.13E-03
031	D(s) g_0(a+s) σ(a)	9	131	0.176	0.592	0.349	-2.200	-2.200	-2.200	0.045	0.045	0.045	7.71E-03	7.71E-03	7.71E-03
031	D(.) g_0(a+s) σ(a+s)	9	115	0.148	0.578	0.345	0.047	0.047	0.047	0.035	0.035	0.035	4.04E-03	4.04E-03	4.04E-03
031	D(a) g_0(a+s) σ(a)	10	99	0.176	0.516	0.323	-1.039	1.690	3.199	0.047	0.061	0.101	8.01E-03	1.09E-02	2.07E-02
031	D(s) g_0(a+s) σ(a+s)	10	32	0.188	0.754	0.366	-2.143	-2.143	-2.143	0.046	0.046	0.046	7.47E-03	7.47E-03	7.47E-03
032	**D(.) g_0(a+s) σ(s)**	7	618	0.168	0.558	0.412	0.173	0.173	0.173	0.036	0.036	0.036	4.31E-03	4.31E-03	4.31E-03
032	D(s) g_0(a+s) σ(s)	8	146	0.195	0.687	0.409	-2.790	-2.790	-2.790	0.057	0.057	0.057	1.09E-02	1.09E-02	1.09E-02
032	D(.) g_0(a+s) σ(a+s)	9	95	0.178	0.543	0.335	0.415	0.415	0.415	0.037	0.037	0.037	4.36E-03	4.36E-03	4.36E-03
032	D(a) g_0(a+s) σ(s)	9	80	0.227	0.583	0.351	-1.358	0.761	1.321	0.055	0.057	0.064	9.24E-03	1.03E-02	1.10E-02
032	D(a) g_0(a+s) σ(a+s)	11	25	0.163	0.702	0.344	-1.794	3.180	2.918	0.057	0.062	0.075	1.15E-02	1.11E-02	1.66E-02
100	**D(a) g_0(.) σ(.)**	5	512	0.08	0.324	0.217	0.311	0.014	-0.133	0.083	0.060	0.044	4.03E-03	6.16E-03	8.54E-03
100	D(a) g_0(.) σ(s)	6	83	0.107	0.383	0.207	0.669	0.168	-0.486	0.083	0.060	0.045	3.61E-03	6.58E-03	9.41E-03
100	D(a+s) g_0(.) σ(.)	6	77	0.108	0.405	0.207	0.240	-0.197	0.557	0.088	0.067	0.054	4.78E-03	8.25E-03	1.42E-02
100	D(a) g_0(.) σ(a)	7	77	0.085	0.317	0.183	0.417	0.021	-0.149	0.095	0.067	0.047	5.84E-03	8.04E-03	8.65E-03
100	D(a) g_0(s) σ(.)	6	75	0.112	0.32	0.2	0.888	0.191	0.843	0.082	0.060	0.044	4.17E-03	6.00E-03	9.78E-03
101	**D(a) g_0(.) σ(a)**	7	588	0.136	0.372	0.277	0.115	0.212	0.083	0.078	0.067	0.062	3.88E-03	6.88E-03	1.17E-02
101	D(a+s) g_0(.) σ(a)	8	94	0.145	0.431	0.256	0.694	-0.539	-1.483	0.085	0.075	0.071	5.10E-03	9.52E-03	1.82E-02
101	D(a) g_0(.) σ(a+s)	8	86	0.164	0.407	0.259	0.542	0.097	0.015	0.078	0.067	0.062	3.68E-03	6.84E-03	1.38E-02
101	D(a) g_0(s) σ(a)	8	78	0.131	0.391	0.236	0.632	0.976	-0.559	0.078	0.067	0.062	3.77E-03	6.73E-03	1.32E-02
101	D(a) g_0(a+s) σ(a)	10	47	0.161	0.493	0.277	0.219	0.300	1.322	0.078	0.066	0.062	3.73E-03	5.24E-03	1.30E-02
103	**D(a)g0(.)σ(a+s)**	8	671	0.19	0.513	0.411	0.510	0.248	-0.082	0.078	0.066	0.062	3.91E-03	6.58E-03	1.18E-02
103	D(a+s) g_0 (.) σ(a+s)	9	116	0.194	0.643	0.39	0.328	-0.454	-0.484	0.094	0.086	0.083	6.35E-03	1.21E-02	2.38E-02
103	D(a) g_0(s) σ(a+s)	9	111	0.238	0.599	0.386	0.975	0.476	0.260	0.078	0.066	0.062	3.43E-03	5.77E-03	1.24E-02
103	D(a) g_0(a+s) σ(a+s)	11	73	0.212	0.682	0.408	-0.698	1.332	-0.141	0.078	0.066	0.062	3.98E-03	6.30E-03	1.11E-02
103	D(a+s) g_0 (s) σ(a+s)	10	16	0.224	0.614	0.327	-0.514	-2.333	1.076	0.095	0.086	0.083	6.14E-03	1.13E-02	2.59E-02
122	**D(a) g_0(s) σ(s)**	7	551	0.187	0.561	0.406	0.705	0.495	0.407	0.083	0.061	0.045	4.01E-03	6.51E-03	9.26E-03
122	D(a+s) g_0(s) σ(s)	8	119	0.223	0.716	0.397	-1.276	-0.826	-0.146	0.094	0.074	0.062	5.64E-03	8.67E-03	1.83E-02

122	D(a) g_0(s) σ(a+s)	9	89	0.177	0.618	0.381	0.531	-0.965	0.235	0.098	0.069	0.048	6.48E-03	7.84E-03	1.04E-02
122	D(a) g_0(a+s) σ(s)	9	76	0.206	0.615	0.359	-0.133	-0.816	0.391	0.087	0.062	0.046	3.83E-03	6.36E-03	1.03E-02
122	D(a+s) g_0(a+s) σ(.)	9	64	0.989	1	1	***-10.075***	***-33.039***	***-53.378***	0.083	0.077	0.081	6.18E-03	3.34E-02	1.07E-01
123	**D(a) g_0(s) σ(a+s)**	9	740	0.277	0.644	0.525	0.472	0.419	0.255	0.080	0.068	0.064	4.05E-03	6.74E-03	1.25E-02
123	D(a+s) g_0(s) σ(a+s)	10	119	0.269	0.821	0.512	0.142	-0.022	0.201	0.093	0.083	0.079	5.54E-03	1.14E-02	2.07E-02
123	D(a) g_0(a+s) σ(a+s)	11	118	0.286	0.728	0.48	-0.285	0.202	-0.355	0.080	0.068	0.064	3.76E-03	6.56E-03	1.23E-02
123	D(a+s) g_0 (a+s) σ(a+s)	12	23	0.272	0.68	0.436	2.897	-0.095	0.366	0.092	0.083	0.079	5.55E-03	9.19E-03	2.21E-02
130	**D(a) g_0(a+s) σ(.)**	8	602	0.186	0.468	0.355	-0.332	-0.030	0.380	0.081	0.062	0.051	3.88E-03	6.32E-03	1.05E-02
130	D(a) g_0(a+s) σ(s)	9	115	0.211	0.605	0.347	0.034	-0.170	0.977	0.081	0.063	0.051	3.32E-03	6.69E-03	9.36E-03
130	D(a+s) g_0(a+s) σ(.)	9	109	0.189	0.57	0.349	-2.128	-2.130	-0.881	0.087	0.070	0.059	4.84E-03	8.38E-03	1.42E-02
130	D(a) g_0(a+s) σ(a)	10	97	0.204	0.499	0.327	0.650	0.292	1.663	0.087	0.067	0.057	4.58E-03	7.11E-03	1.40E-02
130	D(a+s) g_0(a+s) σ(s)	10	37	0.189	0.66	0.388	-4.981	-2.987	-1.601	0.089	0.071	0.061	5.28E-03	8.92E-03	1.65E-02
131	**D(a) g_0(a+s)σ(a)**	10	703	0.297	0.534	0.454	-0.301	0.082	0.749	0.073	0.067	0.078	3.52E-03	6.73E-03	1.56E-02
131	D(a+s) g_0(a+s) σ(a)	11	132	0.295	0.698	0.455	-4.155	-2.356	-2.002	0.081	0.075	0.084	5.05E-03	8.69E-03	1.85E-02
131	D(a) g_0(a+s) σ(a+s)	11	124	0.299	0.708	0.428	-0.052	0.361	0.821	0.073	0.067	0.078	3.35E-03	6.94E-03	1.60E-02
131	D(a+s) g_0(a+s) σ(a+s)	12	41	0.309	0.929	0.502	***-5.754***	-4.763	-2.720	0.082	0.076	0.085	5.30E-03	8.80E-03	1.84E-02
132	**D(a) g_0(a+s) σ(s)**	9	722	0.284	0.643	0.524	-0.098	-0.010	0.244	0.082	0.063	0.052	3.84E-03	6.44E-03	1.03E-02
132	D(a+s) g_0(a+s) σ(s)	10	152	0.287	0.815	0.515	-3.128	-2.201	-2.282	0.095	0.078	0.069	5.97E-03	9.67E-03	1.96E-02
132	D(a) g_0(a+s) σ(a+s)	11	105	0.278	0.722	0.463	0.531	0.246	0.980	0.088	0.069	0.058	4.83E-03	7.13E-03	1.42E-02
132	D(a+s) g_0(a+s) σ(a+s)	12	21	0.304	0.766	0.468	-4.233	***-5.483***	-2.679	0.101	0.083	0.075	6.64E-03	1.19E-02	2.48E-02
133	**D(a) g_0(a+s) σ(a+s)**	11	836	0.502	0.731	0.676	0.281	0.440	0.935	0.074	0.068	0.080	3.75E-03	7.18E-03	1.61E-02
133	D(a+s) g_0(a+s) σ(a+s)	12	164	0.503	0.996	0.687	***-5.984***	-4.455	-4.642	0.089	0.085	0.094	5.94E-03	1.11E-02	2.25E-02
203	**D(s) g_0(.) σ(a+s)**	7	666	0.217	0.615	0.471	-0.148	-0.148	-0.148	0.055	0.055	0.055	7.77E-03	7.77E-03	7.77E-03
203	D(s) g_0(s)σ(a+s)	8	123	0.189	0.681	0.432	-0.088	-0.088	-0.088	0.055	0.055	0.055	7.85E-03	7.85E-03	7.85E-03
203	D(a+s) g_0(.) σ(a+s)	9	99	0.214	0.63	0.393	1.286	0.540	0.070	0.066	0.075	0.092	1.15E-02	1.48E-02	1.88E-02
203	D(s) g_0(a+s) σ(a+s)	10	72	0.203	0.815	0.46	0.787	0.787	0.787	0.054	0.054	0.054	8.73E-03	8.73E-03	8.73E-03
203	D(a+s) g_0(s) σ(a+s)	10	25	0.267	0.527	0.373	0.637	0.489	2.733	0.066	0.075	0.093	1.58E-02	1.31E-02	1.90E-02
223	**D(s) g_0(s) σ(a+s)**	8	738	0.208	0.77	0.599	-0.115	-0.115	-0.115	0.051	0.051	0.051	7.40E-03	7.40E-03	7.40E-03

223	D(s) g_0(a+s) σ(a+s)	10	126	0.282	0.867	0.54	0.567	0.567	0.567	0.051	0.051	0.051	7.78E-03	7.78E-03	7.78E-03
223	D(a+s) g_0(s) σ(a+s)	10	111	0.301	0.857	0.536	0.532	-0.163	0.552	0.063	0.073	0.091	1.13E-02	1.35E-02	2.00E-02
223	D(a+s) g_0(a+s) σ(a+s)	12	25	0.299	0.887	0.481	-0.145	-3.055	-1.739	0.063	0.073	0.091	1.18E-02	1.45E-02	2.04E-02
230	**D(s) g_0(a+s) σ(.)**	7	645	0.148	0.56	0.404	-0.528	-0.528	-0.528	0.043	0.043	0.043	6.12E-03	6.12E-03	6.12E-03
230	D(s) g_0(a+s) σ(s)	8	110	0.197	0.731	0.382	-0.605	-0.605	-0.605	0.044	0.044	0.044	5.91E-03	5.91E-03	5.91E-03
230	D(a+s) g_0(a+s) σ(.)	9	93	0.2	0.574	0.349	-1.797	1.785	0.944	0.059	0.061	0.067	1.12E-02	1.22E-02	1.29E-02
230	D(s) g_0(a+s) σ(a)	9	82	0.193	0.567	0.344	-0.475	-0.475	-0.475	0.043	0.043	0.043	6.18E-03	6.18E-03	6.18E-03
230	D(a+s) g_0(a+s) σ(a)	11	26	0.196	0.702	0.345	-3.937	4.012	2.757	0.062	0.064	0.076	9.05E-03	1.41E-02	2.32E-02
231	**D(s) g_0(a+s) σ(a)**	9	720	0.249	0.643	0.512	-0.423	-0.423	-0.423	0.042	0.042	0.042	5.90E-03	5.90E-03	5.90E-03
231	D(s) g_0(a+s) σ(a+s)	10	147	0.274	0.857	0.514	-0.387	-0.387	-0.387	0.043	0.043	0.043	5.75E-03	5.75E-03	5.75E-03
231	D(a+s) g_0(a+s) σ(a)	11	112	0.218	0.726	0.47	-1.028	-1.423	4.801	0.053	0.065	0.101	1.02E-02	1.44E-02	2.16E-02
231	D(a+s) g_0(a+s) σ(a+s)	12	21	0.316	0.692	0.426	0.125	-2.187	***5.687***	0.053	0.066	0.102	1.06E-02	1.21E-02	2.24E-02
232	**D(s) g_0(a+s) σ(s)**	8	759	0.308	0.774	0.589	-0.859	-0.859	-0.859	0.052	0.052	0.052	7.05E-03	7.05E-03	7.05E-03
232	D(s) g_0(a+s) σ(a+s)	10	116	0.256	0.854	0.504	-0.430	-0.430	-0.430	0.052	0.052	0.052	6.97E-03	6.97E-03	6.97E-03
232	D(a+s) g_0(a+s) σ(s)	10	110	0.298	0.816	0.514	-1.343	0.084	-0.606	0.066	0.068	0.075	1.16E-02	1.24E-02	1.51E-02
232	D(a+s) g_0(a+s) σ(a+s)	12	12	0.38	0.927	0.545	-1.353	0.707	***5.026***	0.069	0.074	0.084	1.25E-02	1.97E-02	2.10E-02
232	D(.) g_0(a+s) σ(s)	7	2	0.312	0.334	0.323	***-16.324***	***-16.324***	***-16.324***	0.037	0.037	0.037	2.30E-02	2.30E-02	2.30E-02
233	**D(s) g_0(a+s) σ(a+s)**	10	865	0.431	0.88	0.767	-0.691	-0.691	-0.691	0.050	0.050	0.050	7.17E-03	7.17E-03	7.17E-03
233	D(a+s) g_0(a+s) σ(a+s)	12	134	0.408	0.994	0.719	0.111	-1.916	2.932	0.060	0.073	0.110	1.10E-02	1.43E-02	2.68E-02
233	D(.) g_0(a+s) σ(a+s)	9	1	0.457	0.457	0.457	***-23.148***	***-23.148***	***-23.148***	0.037	0.037	0.037	3.24E-02	3.24E-02	3.24E-02
301	**D(a+s) g_0(.) σ(a)**	8	693	0.221	0.515	0.41	-0.035	0.234	-0.063	0.083	0.072	0.068	4.85E-03	8.81E-03	1.65E-02
301	D(a+s) g_0(.) σ(a+s)	9	99	0.237	0.616	0.392	-0.306	0.064	-1.614	0.085	0.074	0.071	5.58E-03	9.83E-03	1.77E-02
301	D(a+s) g_0(s) σ(a)	9	94	0.244	0.597	0.367	-0.111	-0.274	0.083	0.083	0.073	0.068	5.37E-03	8.24E-03	1.72E-02
301	D(a+s) g_0(a+s) σ(a)	11	77	0.235	0.715	0.404	-0.634	-0.773	-0.699	0.084	0.073	0.068	5.66E-03	1.01E-02	1.62E-02
301	D(a+s) g_0(s) σ(a+s)	10	30	0.21	0.665	0.402	1.460	1.422	1.721	0.084	0.074	0.069	6.11E-03	8.11E-03	1.44E-02
302	**D(a+s) g_0(.) σ(s)**	7	676	0.237	0.615	0.477	-0.201	-0.039	-0.545	0.094	0.074	0.061	5.55E-03	8.88E-03	1.49E-02
302	D(a+s) g_0(s) σ(s)	8	112	0.229	0.625	0.412	0.833	-0.452	-0.405	0.094	0.074	0.062	6.10E-03	8.52E-03	1.68E-02
302	D(a+s) g_0(.) σ(a+s)	9	111	0.232	0.653	0.41	2.534	1.832	1.137	0.106	0.080	0.064	7.13E-03	1.11E-02	1.69E-02

302	D(a+s) g_0(a+s) σ(s)	10	64	0.237	0.808	0.463	1.851	0.376	0.896	0.097	0.075	0.062	5.48E-03	1.22E-02	1.51E-02
302	D(a+s) g_0(a+s) σ(a+s)	12	21	0.221	0.759	0.447	3.523	-0.922	1.518	0.105	0.081	0.064	9.15E-03	9.08E-03	1.51E-02
320	**D(a+s) g_0(s) σ(.)**	7	630	0.171	0.559	0.412	0.293	-0.159	-0.486	0.086	0.064	0.050	5.19E-03	7.51E-03	1.24E-02
320	D(a+s) g_0(s) σ(s)	8	120	0.192	0.71	0.412	0.408	0.026	-0.614	0.086	0.065	0.051	5.35E-03	7.07E-03	1.18E-02
320	D(a+s) g_0(a+s) σ(.)	9	99	0.187	0.589	0.382	0.268	0.783	0.104	0.088	0.065	0.050	5.09E-03	7.91E-03	1.03E-02
320	D(a+s) g_0(s) σ(a)	9	99	0.201	0.541	0.365	-0.403	1.295	-0.725	0.097	0.070	0.052	6.47E-03	9.63E-03	1.42E-02
320	D(a+s) g_0(a+s) σ(s)	10	20	0.227	0.509	0.37	0.937	-0.159	1.848	0.088	0.066	0.051	5.34E-03	1.15E-02	1.43E-02
321	**D(a+s) g_0(s) σ(a)**	9	710	0.306	0.644	0.525	0.128	0.219	-0.317	0.082	0.071	0.066	4.88E-03	8.27E-03	1.62E-02
321	D(a+s) g_0(s) σ(a+s)	10	160	0.263	0.834	0.503	-0.568	-0.350	-0.053	0.083	0.072	0.067	5.38E-03	8.93E-03	1.61E-02
321	D(a+s) g_0(a+s) σ(a)	11	114	0.273	0.726	0.467	-0.705	0.056	0.426	0.082	0.071	0.066	4.81E-03	9.01E-03	1.51E-02
321	D(a+s) g_0(a+s) σ(a+s)	12	16	0.29	0.851	0.484	2.232	1.707	-1.470	0.082	0.072	0.068	4.71E-03	1.01E-02	1.61E-02
322	**D(a+s) g_0(s) σ(s)**	8	755	0.321	0.773	0.602	0.124	0.142	-0.390	0.092	0.071	0.058	5.50E-03	8.20E-03	1.41E-02
322	D(a+s) g_0(a+s) σ(s)	10	119	0.317	0.86	0.528	0.400	-0.030	0.216	0.095	0.073	0.059	5.13E-03	1.05E-02	1.40E-02
322	D(a+s) g_0(s) σ(a+s)	10	100	0.295	0.825	0.521	2.118	-0.139	0.115	0.105	0.078	0.061	6.88E-03	1.07E-02	1.63E-02
322	D(a+s) g_0(a+s) σ(a+s)	12	26	0.323	0.943	0.526	0.045	-0.922	-1.199	0.106	0.078	0.061	8.52E-03	8.77E-03	1.47E-02
323	**D(a+s) g_0(s) σ(a+s)**	10	874	0.386	0.881	0.769	0.450	-0.060	-0.095	0.090	0.080	0.075	5.35E-03	9.51E-03	1.89E-02
323	D(a+s) g_0(a+s) σ(a+s)	12	125	0.48	0.996	0.702	0.226	-0.823	0.203	0.090	0.080	0.076	5.09E-03	9.60E-03	1.67E-02
323	D(a) g_0(s) σ(a+s)	9	1	0.364	0.364	0.364	***-8.580***	***-15.148***	***-21.046***	0.078	0.069	0.064	5.15E-03	1.82E-02	5.05E-02
331	**D(a+s) g_0(a+s) σ(a)**	11	842	0.453	0.731	0.673	-1.015	-0.586	-0.066	0.077	0.071	0.080	4.53E-03	8.52E-03	1.90E-02
331	D(a+s) g_0(a+s) σ(a+s)	12	156	0.376	0.997	0.666	-1.476	-0.477	-0.178	0.078	0.072	0.081	5.01E-03	8.57E-03	2.01E-02
331	D(a) g_0(a+s) σ(a+s)	11	2	0.339	0.624	0.482	***-19.775***	***-13.783***	***-7.847***	0.077	0.067	0.079	1.27E-02	1.68E-02	2.62E-02
332	**D(a+s) g_0(a+s) σ(s)**	10	866	0.328	0.881	0.77	-0.783	-0.507	-0.771	0.092	0.075	0.065	5.48E-03	9.00E-03	1.56E-02
332	D(a+s) g_0(a+s) σ(a+s)	12	133	0.494	0.997	0.698	-0.333	-1.752	0.043	0.098	0.079	0.070	6.51E-03	9.81E-03	1.91E-02
332	D(a) g_0(a+s) σ(s)	9	1	0.52	0.52	0.52	***-19.525***	***-14.319***	***-17.094***	0.084	0.064	0.053	1.17E-02	1.72E-02	4.10E-02
333	**D(a+s) g_0(a+s) σ(a+s)**	12	999	0.606	1	0.992	-1.047	-1.137	-0.149	0.085	0.080	0.091	5.01E-03	9.65E-03	2.19E-02
333	D(a) g_0(a+s) σ(a+s)	11	1	0.557	0.557	0.557	***-16.289***	***-29.778***	***-10.179***	0.075	0.073	0.079	9.77E-03	3.57E-02	2.44E-02

Table A.5.1 (continued).

							Male								
				w_i			RB			CV			RMSE		
Scenario	**Model**	***K***	***n***	**min**	**max**	**mean**	**A**	**B**	**C**	**A**	**B**	**C**	**A**	**B**	**C**
000	**D(.) g_0(.) σ(.)**	3	426	0.075	0.278	0.172	0.079	0.079	0.079	0.035	0.035	0.035	4.15E-03	4.15E-03	4.15E-03
000	D(s) g_0(.) σ(.)	4	78	0.071	0.289	0.168	0.445	0.445	0.445	0.046	0.046	0.046	9.09E-03	9.09E-03	9.09E-03
000	D(.) g_0(s) σ(.)	4	69	0.083	0.247	0.147	0.707	0.707	0.707	0.035	0.035	0.035	4.37E-03	4.37E-03	4.37E-03
000	D(.) g_0(.) σ(s)	4	67	0.071	0.313	0.162	0.972	0.972	0.972	0.035	0.035	0.035	4.85E-03	4.85E-03	4.85E-03
000	D(.) g_0(.) σ(a)	5	60	0.064	0.3	0.158	0.317	0.317	0.317	0.035	0.035	0.035	4.15E-03	4.15E-03	4.15E-03
001	**D(.) g_0(.) σ(a)**	5	487	0.084	0.319	0.218	0.349	0.349	0.349	0.035	0.035	0.035	4.16E-03	4.16E-03	4.16E-03
001	D(s) g_0(.)σ(a)	6	110	0.097	0.384	0.211	0.800	0.800	0.800	0.046	0.046	0.046	8.14E-03	8.14E-03	8.14E-03
001	D(.) g_0(.) σ(a+s)	6	78	0.117	0.352	0.207	0.225	0.225	0.225	0.035	0.035	0.035	3.77E-03	3.77E-03	3.77E-03
001	D(.) g_0(s) σ(a)	6	72	0.113	0.317	0.191	-0.003	-0.003	-0.003	0.035	0.035	0.035	4.38E-03	4.38E-03	4.38E-03
001	D(a) g_0(.) σ(a)	7	72	0.092	0.32	0.197	0.271	0.023	-0.620	0.050	0.061	0.081	8.05E-03	1.17E-02	1.61E-02
023	**D(.) g_0(s) σ(a+s)**	7	618	0.18	0.559	0.405	0.254	0.254	0.254	0.036	0.036	0.036	4.31E-03	4.31E-03	4.31E-03
023	D(a) g_0(s) σ(a+s)	9	117	0.205	0.591	0.375	0.559	0.282	-0.777	0.051	0.062	0.083	9.19E-03	1.10E-02	1.59E-02
023	D(.) g_0(a+s) σ(a+s)	9	112	0.18	0.586	0.368	0.197	0.197	0.197	0.036	0.036	0.036	4.50E-03	4.50E-03	4.50E-03
023	D(s) g_0(s) σ(a+s)	8	103	0.208	0.711	0.393	0.032	0.032	0.032	0.047	0.047	0.047	8.20E-03	8.20E-03	8.20E-03
023	D(a+s) g_0(s) σ(a+s)	10	15	0.235	0.523	0.374	0.341	-0.756	-1.072	0.060	0.070	0.089	9.43E-03	1.28E-02	1.54E-02
031	**D(.) g_0(a+s) σ(a)**	8	585	0.188	0.468	0.354	0.376	0.376	0.376	0.035	0.035	0.035	4.13E-03	4.13E-03	4.13E-03
031	D(s) g_0(a+s) σ(a)	9	131	0.176	0.592	0.349	4.228	4.228	4.228	0.048	0.048	0.048	9.04E-03	9.04E-03	9.04E-03
031	D(.) g_0(a+s) σ(a+s)	9	115	0.148	0.578	0.345	0.047	0.047	0.047	0.035	0.035	0.035	4.04E-03	4.04E-03	4.04E-03
031	D(a) g_0(a+s) σ(a)	10	99	0.176	0.516	0.323	-1.039	1.690	3.199	0.047	0.061	0.101	8.01E-03	1.09E-02	2.07E-02
031	D(s) g_0(a+s) σ(a+s)	10	32	0.188	0.754	0.366	3.608	3.608	3.608	0.053	0.053	0.053	1.17E-02	1.17E-02	1.17E-02
032	**D(.) g_0(a+s) σ(s)**	7	618	0.168	0.558	0.412	0.173	0.173	0.173	0.036	0.036	0.036	4.31E-03	4.31E-03	4.31E-03
032	D(s) g_0(a+s) σ(s)	8	146	0.195	0.687	0.409	2.277	2.277	2.277	0.048	0.048	0.048	8.06E-03	8.06E-03	8.06E-03

032	D(.) g_0(a+s) σ(a+s)	9	95	0.178	0.543	0.335	0.415	0.415	0.415	0.037	0.037	0.037	4.36E-03	4.36E-03	4.36E-03
032	D(a) g_0(a+s) σ(s)	9	80	0.227	0.583	0.351	-1.358	0.761	1.321	0.055	0.057	0.064	9.24E-03	1.03E-02	1.10E-02
032	D(a) g_0(a+s) σ(a+s)	11	25	0.163	0.702	0.344	-1.794	3.180	2.918	0.057	0.062	0.075	1.15E-02	1.11E-02	1.66E-02
100	**D(a) g_0(.) σ(.)**	5	512	0.08	0.324	0.217	0.311	0.014	-0.133	0.083	0.060	0.044	4.03E-03	6.16E-03	8.54E-03
100	D(a) g_0(.) σ(s)	6	83	0.107	0.383	0.207	0.669	0.168	-0.486	0.083	0.060	0.045	3.61E-03	6.58E-03	9.41E-03
100	D(a+s) g_0(.) σ(.)	6	77	0.108	0.405	0.207	0.283	-0.104	0.637	0.088	0.067	0.054	4.48E-03	8.28E-03	1.41E-02
100	D(a) g_0(.) σ(a)	7	77	0.085	0.317	0.183	0.417	0.021	-0.149	0.095	0.067	0.047	5.84E-03	8.04E-03	8.65E-03
100	D(a) g_0(s) σ(.)	6	75	0.112	0.32	0.2	0.888	0.191	0.843	0.082	0.060	0.044	4.17E-03	6.00E-03	9.78E-03
101	**D(a) g_0(.) σ(a)**	7	588	0.136	0.372	0.277	0.115	0.212	0.083	0.078	0.067	0.062	3.88E-03	6.88E-03	1.17E-02
101	D(a+s) g_0(.) σ(a)	8	94	0.145	0.431	0.256	1.274	0.054	-0.860	0.085	0.075	0.071	4.95E-03	9.03E-03	1.88E-02
101	D(a) g_0(.) σ(a+s)	8	86	0.164	0.407	0.259	0.542	0.097	0.015	0.078	0.067	0.062	3.68E-03	6.84E-03	1.38E-02
101	D(a) g_0(s) σ(a)	8	78	0.131	0.391	0.236	0.632	0.976	-0.559	0.078	0.067	0.062	3.77E-03	6.73E-03	1.32E-02
101	D(a) g_0(a+s) σ(a)	10	47	0.161	0.493	0.277	0.219	0.300	1.322	0.078	0.066	0.062	3.73E-03	5.24E-03	1.30E-02
103	**D(a) g_0(.) σ(a+s)**	8	671	0.19	0.513	0.411	0.510	0.248	-0.082	0.078	0.066	0.062	3.91E-03	6.58E-03	1.18E-02
103	D(a+s) g_0(.) σ(a+s)	9	116	0.194	0.643	0.39	1.115	0.324	0.200	0.083	0.072	0.068	4.67E-03	8.61E-03	1.40E-02
103	D(a) g_0(s) σ(a+s)	9	111	0.238	0.599	0.386	0.975	0.476	0.260	0.078	0.066	0.062	3.43E-03	5.77E-03	1.24E-02
103	D(a) g_0(a+s) σ(a+s)	11	73	0.212	0.682	0.408	-0.698	1.332	-0.141	0.078	0.066	0.062	3.98E-03	6.30E-03	1.11E-02
103	D(a+s) g_0(s) σ(a+s)	10	16	0.224	0.614	0.327	1.180	-0.684	2.426	0.083	0.073	0.067	5.50E-03	8.70E-03	1.42E-02
122	**D(a) g_0(s) σ(s)**	7	551	0.187	0.561	0.406	0.705	0.495	0.407	0.083	0.061	0.045	4.01E-03	6.51E-03	9.26E-03
122	D(a+s) g_0(s) σ(s)	8	119	0.223	0.716	0.397	-1.015	-0.382	0.165	0.090	0.069	0.055	4.66E-03	8.51E-03	1.45E-02
122	D(a) g_0(s) σ(a+s)	9	89	0.177	0.618	0.381	0.531	-0.965	0.235	0.098	0.069	0.048	6.48E-03	7.84E-03	1.04E-02
122	D(a) g_0(a+s) σ(s)	9	76	0.206	0.615	0.359	-0.133	-0.816	0.391	0.087	0.062	0.046	3.83E-03	6.36E-03	1.03E-02
122	D(a+s) g_0(a+s) σ(.)	9	64	0.989	1	1	***42.028***	***5.734***	***-26.413***	0.076	0.070	0.075	2.17E-02	9.39E-03	5.37E-02
123	**D(a) g_0(s) σ(a+s)**	9	740	0.277	0.644	0.525	0.472	0.419	0.255	0.080	0.068	0.064	4.05E-03	6.74E-03	1.25E-02
123	D(a+s) g_0(s) σ(a+s)	10	119	0.269	0.821	0.512	0.710	0.386	0.669	0.087	0.077	0.073	5.39E-03	9.60E-03	1.80E-02
123	D(a) g_0(a+s) σ(a+s)	11	118	0.286	0.728	0.48	-0.285	0.202	-0.355	0.080	0.068	0.064	3.76E-03	6.56E-03	1.23E-02
123	D(a+s) g_0(a+s) σ(a+s)	12	23	0.272	0.68	0.436	1.737	-1.075	-0.847	0.087	0.077	0.073	4.88E-03	9.22E-03	1.86E-02
130	**D(a) g_0(a+s) σ(.)**	8	602	0.186	0.468	0.355	-0.332	-0.030	0.380	0.081	0.062	0.051	3.88E-03	6.32E-03	1.05E-02

130	D(a) g_0(a+s) σ(s)	9	115	0.211	0.605	0.347	0.034	-0.170	0.977	0.081	0.063	0.051	3.32E-03	6.69E-03	9.36E-03
130	D(a+s) g_0(a+s) σ(.)	9	109	0.189	0.57	0.349	2.235	2.276	3.604	0.089	0.072	0.064	5.40E-03	1.01E-02	1.99E-02
130	D(a) g_0(a+s) σ(a)	10	97	0.204	0.499	0.327	0.650	0.292	1.663	0.087	0.067	0.057	4.58E-03	7.11E-03	1.40E-02
130	D(a+s) g_0(a+s) σ(s)	10	37	0.189	0.66	0.388	2.655	4.884	***6.403***	0.093	0.077	0.069	6.33E-03	1.32E-02	2.71E-02
131	**D(a) g_0(a+s) σ(a)**	10	703	0.297	0.534	0.454	-0.301	0.082	0.749	0.073	0.067	0.078	3.52E-03	6.73E-03	1.56E-02
131	D(a+s) g_0(a+s) σ(a)	11	132	0.295	0.698	0.455	3.582	***5.605***	***6.037***	0.082	0.078	0.090	5.33E-03	1.14E-02	2.55E-02
131	D(a) g_0(a+s) σ(a+s)	11	124	0.299	0.708	0.428	-0.052	0.361	0.821	0.073	0.067	0.078	3.35E-03	6.94E-03	1.60E-02
131	D(a+s) g_0(a+s) σ(a+s)	12	41	0.309	0.929	0.502	***7.543***	***9.176***	***11.090***	0.086	0.082	0.093	6.55E-03	1.64E-02	3.20E-02
132	**D(a) g_0(a+s) σ(s)**	9	722	0.284	0.643	0.524	-0.098	-0.010	0.244	0.082	0.063	0.052	3.84E-03	6.44E-03	1.03E-02
132	D(a+s) g_0(a+s) σ(s)	10	152	0.287	0.815	0.515	1.666	2.826	2.632	0.088	0.071	0.061	5.11E-03	9.91E-03	1.78E-02
132	D(a) g_0(a+s) σ(a+s)	11	105	0.278	0.722	0.463	0.531	0.246	0.980	0.088	0.069	0.058	4.83E-03	7.13E-03	1.42E-02
132	D(a+s) g_0(a+s) σ(a+s)	12	21	0.304	0.766	0.468	1.623	0.337	2.915	0.096	0.076	0.066	6.40E-03	1.08E-02	1.81E-02
133	**D(a) g_0(a+s) σ(a+s)**	11	836	0.502	0.731	0.676	0.281	0.440	0.935	0.074	0.068	0.080	3.75E-03	7.18E-03	1.61E-02
133	D(a+s) g_0(a+s) σ(a+s)	12	164	0.503	0.996	0.687	3.218	4.861	4.805	0.082	0.077	0.087	4.80E-03	9.90E-03	2.28E-02
203	**D(s) g_0(.) σ(a+s)**	7	666	0.217	0.615	0.471	0.311	0.311	0.311	0.047	0.047	0.047	4.89E-03	4.89E-03	4.89E-03
203	D(s) g_0(s) σ(a+s)	8	123	0.189	0.681	0.432	0.275	0.275	0.275	0.047	0.047	0.047	4.58E-03	4.58E-03	4.58E-03
203	D(a+s) g_0(.) σ(a+s)	9	99	0.214	0.63	0.393	1.618	0.830	0.368	0.060	0.070	0.087	8.25E-03	1.02E-02	1.33E-02
203	D(s) g_0(a+s) σ(a+s)	10	72	0.203	0.815	0.46	0.846	0.846	0.846	0.047	0.047	0.047	4.73E-03	4.73E-03	4.73E-03
203	D(a+s) g_0(s) σ(a+s)	10	25	0.267	0.527	0.373	-0.408	-0.372	1.870	0.060	0.070	0.088	9.83E-03	9.80E-03	1.39E-02
223	**D(s) g_0(s) σ(a+s)**	8	738	0.208	0.77	0.599	0.591	0.591	0.591	0.051	0.051	0.051	5.55E-03	5.55E-03	5.55E-03
223	D(s) g_0(a+s) σ(a+s)	10	126	0.282	0.867	0.54	0.596	0.596	0.596	0.051	0.051	0.051	4.91E-03	4.91E-03	4.91E-03
223	D(a+s) g_0(s) σ(a+s)	10	111	0.301	0.857	0.536	0.490	-0.217	0.411	0.064	0.073	0.092	8.63E-03	1.02E-02	1.40E-02
223	D(a+s) g_0(a+s) σ(a+s)	12	25	0.299	0.887	0.481	1.812	-0.984	0.097	0.064	0.073	0.092	7.94E-03	1.12E-02	1.38E-02
230	**D(s) g_0(a+s) σ(.)**	7	645	0.148	0.56	0.404	1.089	1.089	1.089	0.055	0.055	0.055	5.84E-03	5.84E-03	5.84E-03
230	D(s) g_0(a+s) σ(s)	8	110	0.197	0.731	0.382	2.669	2.669	2.669	0.061	0.061	0.061	7.71E-03	7.71E-03	7.71E-03
230	D(a+s) g_0(a+s) σ(.)	9	93	0.2	0.574	0.349	-1.933	1.574	0.843	0.067	0.070	0.077	9.29E-03	9.11E-03	1.06E-02
230	D(s) g_0(a+s) σ(a)	9	82	0.193	0.567	0.344	1.173	1.173	1.173	0.055	0.055	0.055	5.66E-03	5.66E-03	5.66E-03
230	D(a+s) g_0(a+s) σ(a)	11	26	0.196	0.702	0.345	-3.247	4.690	2.964	0.070	0.073	0.085	7.87E-03	1.09E-02	1.42E-02

231	**D(s) g_0(a+s) σ(a)**	9	720	0.249	0.643	0.512	1.403	1.403	1.403	0.053	0.053	0.053	5.85E-03	5.85E-03	5.85E-03
231	D(s) g_0(a+s) σ(a+s)	10	147	0.274	0.857	0.514	2.510	2.510	2.510	0.058	0.058	0.058	7.49E-03	7.49E-03	7.49E-03
231	D(a+s) g_0(a+s) σ(a)	11	112	0.218	0.726	0.47	1.202	0.654	***7.343***	0.061	0.073	0.108	8.03E-03	9.43E-03	1.83E-02
231	D(a+s) g_0(a+s) σ(a+s)	12	21	0.316	0.692	0.426	0.504	-1.934	***6.793***	0.066	0.078	0.112	8.93E-03	8.40E-03	2.12E-02
232	**D(s) g_0(a+s) σ(s)**	8	759	0.308	0.774	0.589	1.069	1.069	1.069	0.052	0.052	0.052	5.47E-03	5.47E-03	5.47E-03
232	D(s) g_0(a+s) σ(a+s)	10	116	0.256	0.854	0.504	0.887	0.887	0.887	0.053	0.053	0.053	6.18E-03	6.18E-03	6.18E-03
232	D(a+s) g_0(a+s) σ(s)	10	110	0.298	0.816	0.514	-0.194	1.213	0.509	0.066	0.069	0.076	8.55E-03	9.00E-03	1.08E-02
232	D(a+s) g_0(a+s) σ(a+s)	12	12	0.38	0.927	0.545	-1.406	0.222	***5.343***	0.070	0.074	0.084	7.98E-03	9.12E-03	1.71E-02
232	D(.) g_0(a+s) σ(s)	7	2	0.312	0.334	0.323	***17.147***	***17.147***	***17.147***	0.037	0.037	0.037	1.73E-02	1.73E-02	1.73E-02
233	**D(s) g_0(a+s) σ(a+s)**	10	865	0.431	0.88	0.767	0.844	0.844	0.844	0.051	0.051	0.051	5.30E-03	5.30E-03	5.30E-03
233	D(a+s) g_0(a+s) σ(a+s)	12	134	0.408	0.994	0.719	1.029	-1.105	3.791	0.060	0.073	0.111	8.79E-03	9.89E-03	1.93E-02
233	D(.) g_0(a+s) σ(a+s)	9	1	0.457	0.457	0.457	***7.593***	***7.593***	***7.593***	0.037	0.037	0.037	7.59E-03	7.59E-03	7.59E-03
301	**D(a+s) g_0(.) σ(a)**	8	693	0.221	0.515	0.41	0.156	0.446	0.100	0.088	0.078	0.074	3.44E-03	6.50E-03	1.12E-02
301	D(a+s) g_0(.) σ(a+s)	9	99	0.237	0.616	0.392	-0.036	0.290	-1.235	0.092	0.082	0.079	4.11E-03	6.92E-03	1.52E-02
301	D(a+s) g_0(s) σ(a)	9	94	0.244	0.597	0.367	0.349	0.164	0.519	0.089	0.079	0.075	3.70E-03	5.46E-03	1.15E-02
301	D(a+s) g_0(a+s) σ(a)	11	77	0.235	0.715	0.404	0.635	0.474	0.588	0.089	0.079	0.075	3.79E-03	6.57E-03	1.14E-02
301	D(a+s) g_0(s) σ(a+s)	10	30	0.21	0.665	0.402	0.414	0.560	0.814	0.091	0.082	0.078	4.77E-03	8.77E-03	1.64E-02
302	**D(a+s) g_0(.) σ(s)**	7	676	0.237	0.615	0.477	0.284	0.432	-0.105	0.091	0.069	0.056	3.64E-03	5.60E-03	8.32E-03
302	D(a+s) g_0(s) σ(s)	8	112	0.229	0.625	0.412	1.840	0.625	0.634	0.090	0.069	0.056	3.68E-03	5.31E-03	9.26E-03
302	D(a+s) g_0(.) σ(a+s)	9	111	0.232	0.653	0.41	1.701	0.993	0.309	0.103	0.076	0.059	4.42E-03	6.58E-03	9.31E-03
302	D(a+s) g_0(a+s) σ(s)	10	64	0.237	0.808	0.463	0.475	-1.210	-0.635	0.093	0.071	0.057	4.17E-03	7.33E-03	9.36E-03
302	D(a+s) g_0(a+s) σ(a+s)	12	21	0.221	0.759	0.447	2.439	-1.508	0.970	0.102	0.076	0.058	4.52E-03	6.54E-03	1.20E-02
320	**D(a+s) g_0(s) σ(.)**	7	630	0.171	0.559	0.412	0.707	0.265	-0.084	0.093	0.073	0.062	3.76E-03	5.91E-03	9.70E-03
320	D(a+s) g_0(s) σ(s)	8	120	0.192	0.71	0.412	1.601	1.373	0.646	0.097	0.079	0.068	4.26E-03	8.01E-03	1.36E-02
320	D(a+s) g_0(a+s) σ(.)	9	99	0.187	0.589	0.382	-0.493	-0.049	-0.647	0.096	0.074	0.062	3.73E-03	5.34E-03	9.74E-03
320	D(a+s) g_0(s) σ(a)	9	99	0.201	0.541	0.365	1.124	2.784	0.693	0.103	0.079	0.063	4.90E-03	7.37E-03	1.05E-02
320	D(a+s) g_0(a+s) σ(s)	10	20	0.227	0.509	0.37	1.178	-0.022	1.946	0.099	0.079	0.067	4.49E-03	8.65E-03	1.12E-02
321	**D(a+s) g_0 (s) σ(a)**	9	710	0.306	0.644	0.525	0.228	0.360	-0.235	0.091	0.081	0.078	3.55E-03	6.57E-03	1.17E-02

321	D(a+s) g_0 (s) σ(a+s)	10	160	0.263	0.834	0.503	1.286	1.633	1.932	0.096	0.087	0.084	4.29E-03	8.59E-03	1.65E-02
321	D(a+s) g_0 (a+s) σ(a)	11	114	0.273	0.726	0.467	-0.349	0.328	0.746	0.091	0.081	0.078	3.58E-03	5.94E-03	1.12E-02
321	D(a+s) g_0 (a+s) σ(a+s)	12	16	0.29	0.851	0.484	2.345	1.968	-1.265	0.096	0.088	0.085	5.08E-03	1.16E-02	1.99E-02
322	**D(a+s) g_0(s) σ(s)**	8	755	0.321	0.773	0.602	0.643	0.676	0.106	0.094	0.073	0.060	3.74E-03	5.86E-03	9.28E-03
322	D(a+s) g_0(a+s) σ(s)	10	119	0.317	0.86	0.528	0.635	0.105	0.380	0.096	0.074	0.061	3.84E-03	6.81E-03	9.90E-03
322	D(a+s) g_0(s) σ(a+s)	10	100	0.295	0.825	0.521	3.058	0.648	0.901	0.106	0.079	0.063	5.05E-03	6.75E-03	9.76E-03
322	D(a+s) g_0(a+s) σ(a+s)	12	26	0.323	0.943	0.526	0.173	-0.625	-0.821	0.108	0.080	0.063	4.94E-03	5.35E-03	1.05E-02
323	**D(a+s) g_0(s) σ(a+s)**	10	874	0.386	0.881	0.769	1.098	0.589	0.497	0.092	0.082	0.078	3.71E-03	6.73E-03	1.21E-02
323	D(a+s) g_0(a+s) σ(a+s)	12	125	0.48	0.996	0.702	0.641	-0.459	0.633	0.092	0.082	0.078	3.43E-03	5.98E-03	1.16E-02
323	D(a) g_0(s) σ(a+s)	9	1	0.364	0.364	0.364	***37.130***	***27.279***	***18.432***	0.078	0.069	0.064	1.49E-02	2.18E-02	2.95E-02
331	**D(a+s) g_0(a+s) σ(a)**	11	842	0.453	0.731	0.673	1.195	1.633	2.166	0.086	0.082	0.093	3.47E-03	6.70E-03	1.48E-02
331	D(a+s) g_0(a+s) σ(a+s)	12	156	0.376	0.997	0.666	1.475	2.726	2.925	0.092	0.088	0.098	4.22E-03	9.70E-03	1.94E-02
331	D(a) g_0(a+s) σ(a+s)	11	2	0.339	0.624	0.482	***20.337***	***29.325***	***38.229***	0.077	0.067	0.079	9.36E-03	2.36E-02	6.38E-02
332	**D(a+s) g_0(a+s) σ(s)**	10	866	0.328	0.881	0.77	0.777	1.062	0.764	0.093	0.076	0.067	3.78E-03	6.32E-03	1.04E-02
332	D(a+s) g_0(a+s) σ(a+s)	12	133	0.494	0.997	0.698	2.206	0.753	2.606	0.099	0.081	0.072	4.42E-03	6.28E-03	1.33E-02
332	D(a) g_0(a+s) σ(s)	9	1	0.52	0.52	0.52	***20.712***	***28.522***	***24.359***	0.084	0.064	0.053	8.29E-03	2.28E-02	3.90E-02
333	**D(a+s) g_0(a+s) σ(a+s)**	12	999	0.606	1	0.992	0.919	0.813	1.835	0.087	0.082	0.093	3.53E-03	6.70E-03	1.57E-02
333	D(a) g_0(a+s) σ(a+s)	11	1	0.557	0.557	0.557	***25.566***	***5.333***	***34.732***	0.075	0.073	0.079	1.02E-02	4.27E-03	5.56E-02

Appendix B: MNRF black bear DNA capture-recapture summary

Black bear DNA capture-recapture datasets are available on Dryad: Howe, Eric. 2021. Spatially explicit genetic capture-recapture data from black bears in Ontario, Canada, 2017-2019. Dryad, Dataset, https://doi.org/10.5061/dryad.7wm37pvtz.

Table B.1. Summary of capture statistics from DNA population monitoring from 78 study areas across Ontario, Canada. Statistics calculated by study area and sex (female [♀] and male [♂]) and include the number of barbed wire hair corrals in each area (traps), how many of these corrals were visited (traps used), number of traps visited (traps visited), number of detections (detections; excluding multiple detections of the same individual at the same trap and occasion), number of unique individuals detected (individuals) and the number of re-captured individuals (re-captures). Across all study areas, there were five sampling occasions (exception of Shirley Lake Road in 2019 with 7 sampling occasions). Males[1] or female[2] study areas datasets excluded from analysis because of insufficient data (< 20 recaptures) or data quality concerns[4]. Repeated traplines sampled across multiple years[3].

Year	Study area	Traps	Traps used		Traps visited		Detections		Individuals		Re-captures	
			♀	♂	♀	♂	♀	♂	♀	♂	♀	♂
2017	325 Road	40	22	29	37	66	42	89	18	30	24	59
2017	700 Road[1]	40	21	17	50	27	60	35	19	16	41	19
2017	81 Road	41	38	41	121	124	165	185	31	36	134	149
2019	Anaconda	40	23	33	63	114	80	186	20	44	60	142
2018	Beauty Lake Road	40	25	25	59	53	69	74	19	25	50	49
2019	Black Creek Road	40	15	19	28	48	32	65	12	20	20	45
2019	Bogie & Clyde[1]	40	25	19	50	29	67	33	26	17	41	16
2019	Boreal	40	28	27	59	52	74	60	33	33	41	27
2017	Borland	40	26	26	65	56	70	75	11	21	59	54
2018	Caithness	40	26	29	54	58	64	81	17	21	47	60
2018	Camp1Road	41	28	31	61	74	74	143	25	39	49	104
2019	Cardiff Anstruther[1,2]	40	18	19	29	30	39	37	23	22	16	15
2018	Cargill	40	22	29	43	58	50	78	25	36	25	42
2019	Carp Road[2]	40	22	23	30	44	33	52	15	18	18	34
2017	CCGP	40	40	38	120	121	155	164	32	29	123	135
2018	Cedar Narrows	40	33	31	99	85	135	118	38	37	97	81
2018	Century Road	40	26	30	51	81	64	112	27	40	37	72

2017	Crib Road	40	38	38	130	107	156	159	30	39	126	120
2018	Deer Lake Road	40	28	29	59	56	72	83	22	29	50	54
2018	Detour	40	27	24	59	66	83	110	19	18	64	92
2019	Dorion	40	22	20	47	36	56	41	15	18	41	23
2018	Fred Flat	40	18	25	36	47	39	57	13	20	26	37
2018	Fushimi	40	30	29	57	70	66	107	22	29	44	78
2017	Garden Lake Road	41	27	38	63	123	73	220	18	53	55	167
2018	GargMijnSand	40	24	28	54	68	65	105	14	21	51	84
2017	Gibson Lake Road	40	29	20	78	45	94	66	31	22	63	44
2017	Goldfield	40	25	32	57	72	64	101	23	30	41	71
2017	Grassy	40	26	33	65	74	85	111	21	30	64	81
2019	Grimsthorpe[2]	40	18	26	29	48	34	56	21	29	13	27
2019	Highway 631	40	19	21	43	39	69	52	20	22	49	30
2017	Hwy 651	40	23	31	49	67	57	79	16	23	41	56
2018	Inglis Lake Road	40	26	37	60	87	76	118	16	36	60	82
2019	Killarney	40	21	27	44	63	60	84	22	28	38	56
2019	Lampson	41	29	34	90	91	130	141	29	35	101	106
2017	Larder Raven[1,2]	40	14	11	21	14	23	15	14	9	9	6
2019	Line 74[1,2]	34	5	5	7	7	7	7	5	3	2	4
2019	Line 75[1,2]	27	7	6	13	9	15	10	10	9	5	1
2018	Longlegged	40	27	39	71	102	85	161	26	56	59	105
2018	Marlborough Limerick[1,2]	41	5	4	5	4	5	4	4	4	1	0
2018	Massey Tote[2]	41	15	21	21	30	24	33	13	11	11	22
2019	Mayburn	40	25	27	61	74	73	118	22	37	51	81
2019	McClure Herschel[1,2]	40	6	16	7	20	7	22	7	15	0	7
2017	McConnell	40	24	25	44	53	49	69	24	29	25	40
2018	Menet Brent	40	28	30	60	70	77	113	36	45	41	68
2017	Munro	41	13	21	29	58	36	89	16	29	20	60
2019	NORT Road[2]	40	17	22	27	37	27	46	8	22	19	24
2018	Oates[4]	40	32	32	75	78	111	104	23	30	88	74
2019	Ogoki	40	37	40	115	166	141	344	27	51	114	293
2017	Opeepeesway	40	22	35	36	81	36	106	13	29	23	77
2018	Opeongo Line[1,2]	45	11	15	19	21	22	22	10	15	12	7

2017	Pardo	40	28	27	58	64	65	81	31	30	34	51
2019	Phillip Creek	40	27	34	63	80	82	114	23	29	59	85
2019	Pickerel	40	30	26	70	52	91	64	39	31	52	33
2018	Pineridge	40	19	25	42	55	46	86	16	36	30	50
2017	Portelance Road	40	22	27	43	66	45	99	22	35	23	64
2018	Red Squirrel[1]	40	27	20	58	26	68	26	23	19	45	7
2019	Road 600	41	25	31	72	71	98	91	19	21	79	70
2018	Robinson Lake	40	15	16	25	29	31	37	11	16	20	21
2018	Round Lake[1,2]	40	14	21	23	37	29	43	17	27	12	16
2019	Sand English	40	34	33	97	89	150	148	52	59	98	89
2019	Shaw Road[1]	40	24	16	56	26	67	28	17	18	50	10
2018	Shirley Lake Road[3]	40	24	30	52	58	59	82	22	37	37	45
2019	Shirley Lake Road[3]	40	36	31	67	71	111	131	26	35	85	96
2017	South EMU Road	40	23	23	59	52	71	66	24	25	47	41
2017	Sowden[3]	40	23	26	49	58	64	84	17	23	47	61
2019	Sowden[3]	40	30	38	91	106	133	175	19	30	114	145
2018	Sowden[3]	44	27	33	76	98	93	147	16	32	77	115
2018	Translimit	40	36	34	90	84	127	124	28	30	99	94
2019	Trout Lake	40	25	21	47	42	53	47	25	20	28	27
2018	Turtle River Road	40	23	29	49	60	67	72	28	34	39	38
2019	Two Island Lake[1,2]	42	16	13	27	21	36	23	18	15	18	8
2018	Vermilion River Road	40	32	37	82	125	93	214	24	50	69	164
2017	Watabeag	40	24	17	57	33	67	41	20	18	47	23
2018	Wenasaga	40	19	30	53	96	65	186	13	36	52	150
2018	Wenebegon	40	24	28	44	60	46	87	17	29	29	58
2019	WestEnd	50	27	27	53	48	64	59	30	36	34	23
2018	Whitman Dam	40	28	26	78	70	93	97	18	19	75	78
2018	Winter Lake[3]	40	24	24	42	49	44	57	20	31	24	26
2019	Winter Lake[3]	40	23	27	38	63	44	88	19	33	25	55
2018	WMU 54 Line[1,2]	40	16	21	28	33	34	43	15	25	19	18
2019	WMU 62[1,2]	40	13	16	24	21	30	23	13	15	17	8
2018	WMU 50 Parry Sound[1,2]	42	11	23	25	35	28	44	13	26	15	18

Appendix C: Chapter 3

C.1 Chapter 3 summary of spatial covariate data sources

Table C.1.1. Spatial covariates used for SECR density model including names, descriptions, sources of datasets, original resolution (Res.; pixel size), unit of time over which the original datasets were available (time), and units of processed layers. Covariates were quantified using the approximate circular area used by female and male black bear (radius of 4480m and 8290m, respectively). All covariates are continuous, and the processed resolution of all layers was set at 500m x 500m, except for NDVI and human settlement that were set to 1km x 1km and 10m x 10m, respectively.

Covariates		Description	Source	Res.	Time	Unit
NDVI		The average of the normalized difference vegetation index (NDVI) from the last week of June to the first week of August from 1989 to 2019.	CCAP[1]	1 km	Weekly	NA
Land cover	Agriculture	Percentage of area dominated by annual crops, perennial grasses for grazing, woody crops. Does not include grasslands used for light to moderate grazing.	NALCMS[2]	30 m	2015	%
	Deciduous	Percentage of area where tree crown cover is comprised of ≥75% deciduous species generally greater than 3m tall.	NALCMS[2]	30 m	2015	%
	Coniferous	Percentage of area where tree crown cover is comprised of ≥75% coniferous species generally greater than 3m tall.	NALCMS[2]	30 m	2015	%
	Mixed	Percentage of area where neither coniferous nor deciduous species occupy ≥75% tree crown cover. Species co-dominant.	NALCMS[2]	30 m	2015	%
Human	Road density	Density of all roads (freeway, highway, collector, arterial, local, ramps, resource and recreation) in km roads/km^2.	NRN[3]	NA	2021	km/km^2
	Human settlement	Build-up area density. Represented by the built-up (density of buildings) probability (1-100) in each pixel.	GHS[4]	10 m	2018	%

[1] Crop Condition Assessment Program (CCAP), advanced very high-resolution radiometer (AVHRR) corrected representation of the normalized difference vegetation index (Statistics Canada, 2021)

[2] 2015 Land cover of North America at 30 meters. North American land change monitoring system (NALCMS; NALCMS, 2020).

[3] Canada national road network (NRN; Statistics Canada, 2022)

[4] Global human settlement [GHS] built-up grid (Corbane et al. 2020)

C.2 Chapter 3 normalized difference vegetation index

NDVI values were calculated for Ontario's peak growing season (June 30 - August 1) and averaged across 1989-2019, using data obtained from Crop Condition Assessment Program Advanced Very High-Resolution Radiometer (AVHRR) satellite images. A temporally static NDVI layer was used as we were interested in the long-term and more generalizable vegetation productivity across the landscape. Across the study area, higher NDVI values corresponded to mixed and deciduous forests (Appendix C Section 2). For both the landscape analysis (see Appendix C Section 3) and pooled analysis we ran univariate and multivariate SECR models (for the latter see Appendix C Section 4) using the two-stage approach outlined in the main text.

NDVI displayed a significant negative relationship with black bear densities for the pooled and landscape analyses (Appendix C Section 3 and Section 4), opposite to what we would predict if density was correlated with vegetation productivity. NDVI has been shown to be a proxy for grizzly bear vegetation diet (Mowat et al. 2013) and positively correlated with black bear habitat selection (Duquette et al. 2017; Loosen et al. 2018) and distribution (Gantchoff et al. 2019). In our study, the strong negative association of NDVI with density could, in part, be explained by disturbed areas (roads, clear-cuts, gravel borrow pits) and regenerating clear-cuts acting as important foraging areas in the boreal forest because these areas contain spring foods including green vegetation (clover, common dandelion, hawkweed; Romin et al. 2013) but have lower NDVI values. This pattern could also be explained by our measure of NDVI being confounded by forest cover and type. For the pooled analyses, out of the forest types in our study area, in the boreal, NDVI was positively correlated with mixed forests and in the GLSL deciduous (Appendix C Section 5). Thus, the broadscale patterns of NDVI may be most reflective of the forest type patterns, which had significant negative associations with density and bears could

be responding to broad forest types more so than productivity per se. Moreover, while our NDVI functioned as a coarse proxy for general vegetation productivity available to bears during the growing season, it does not reflect spring and early summer foods including insects and ungulates (Poulin et al. 2003, Romain et al. 2013). Our findings align with Nielsen et al. (2017) who report a negative association between NDVI and grizzly bear abundance and suggest that NDVI may be a poor measure of grizzly bear resources in some study areas. Therefore, while NDVI may be a poor measure of the absolute abundance or quality of foods during sampling, the aim of this covariate was to characterize bear density as a function of general productivity and clearly bears across study areas are distributed in areas with lower broad scale productivity during this time. This suggest that primary productivity is either not a good proxy for bear foods during the spring, or that bears are focused on behaviors other than foraging. Collectively our findings highlight the challenges of drawing conclusions from large-scale covariates like NDVI that are confounded by other processes and patterns.

Table C.2.1. β parameter estimates, standard errors (SE) and 95% confidence intervals (lower [LCL] and upper [UCL] confidence intervals) of univariate SECR density models with NDVI as a density covariate fit to female and male black bear capture-recapture datasets in the Great Lakes – St Lawrence (GLSL) and boreal forest regions (Rowe 1972), Ontario, Canada, from 2017–2019.

	β estimate [a]	SE	LCL	UCL
Female GLSL	-0.315	0.049	-0.411	-0.218
Male GLSL	-0.271	0.044	-0.357	-0.185
Female Boreal	-0.161	0.037	-0.235	-0.088
Male Boreal	-0.171	0.028	-0.225	-0.117

[a] Baseline density on the log scale is reference category; all covariates standardized (mean = 0, standard deviation = 1) such that the beta parameter estimate indicates the change in the standard deviation of the baseline density (bears/hectare) on the log scale for one unit change in the standard deviation of the covariates value.

C.3 Chapter 3 study area level analysis summary

We used a two-stage modeling approach, fitting models to the same datasets as described in the main text. In the first stage we created three candidate detection models where density was held constant and the baseline encounter probability g_0 varied as a function of two behavioural responses: a global, permanent change in behaviour after initial capture (*b*) and a trap-specific, permanent change in behavior after initial capture (*bk*). While seasonal variation may influence black bears detectability and home range, a covariate for time of sampling was not included because preliminary runs of highly parameterized detection models failed to converge due to data sparsity. AIC_c was used to evaluate the relative strength of support for each of the competing detection models (Hurvitch and Tsai 1989, Burnham and Anderson 2002). In the second stage, the most parsimonious detection model was then used in the subsequent runs of the density model which included spatial covariates (identical to the covariates detailed in the main text, except for NDVI and percent agriculture landcover were included). Ideally, we intended to fit global models including additive effects of some or all covariates but such models were overparametrized for the sparse datasets and prone to overfitting and convergence issues. We reduced the candidate model set to less complicated univariate models. However, for some study areas unreasonably large standard errors of the β estimates suggested overparameterization (Grueber et al. 2011). To exclude such models the precision of β parameter estimates was assessed using coefficient of variation (CV = SE / β estimate) and all univariate models with $|CV| > 1$ were excluded.

Summary of AIC_c model selection criterion for SECR detection by sex and study area are presented in Table C.3.2. For both sexes, the most frequent top-ranked detection model included a trap-specific behavioural response (*bk*), followed by the model with a global behavioural response (*b*; Table C.3.3). A total of 340 univariate density models from 63 study areas successfully converged

(Table C.3.4). Models that failed to converge and all crop models were excluded from the subsequent results and discussion, with all crop models dropped because only five models successfully converged.

Across all model forms there was some degree of positive and negative association between β parameter estimates and density that varied spatially across the province. The proportion of successfully converged models by direction and significances for each model form is summarized in Figure C.3.1. Across model forms the strength of the β parameter estimates, as indicated by the magnitude of the β parameter estimates, varied (Figure C.3.2). Because masks for each covariate were scaled for each study area and sex, we present unstandardized β estimates in Figure C.3.2 to allow for comparison of covariate values across study areas by sex; this does not allow for comparison across different covariates as scales differ.

Table C.3.2. Summary of AIC_c model selection criterion for stage one of the SECR detection models fitted to black bear capture-recapture surveys from 65 study area in Ontario, Canada from 2017–2019. *K* denotes the number of parameters; LL the log likelihood; W_i the AIC_c weight. Detection covariates includes general (*b*) and a trap-specific (*bk*) learned behavioural response. Bold text indicates detection models parameters used in stage two of model fitting.

		Female						Male					
Study area	**Year**	**Model**	***K***	**LL**	**AIC_c**	**$\triangle AIC_c$**	***W_i***	**Model**	***K***	**LL**	**AICc**	**$\triangle AIC_c$**	***W_i***
325Rd	2017	**D~1 g0~bk sigma~1**	4	-133.4	278.0	0.0	0.9	**D~1 g0~bk sigma~1**	4	-284.3	578.3	0.0	1.0
	2017	D~1 g0~b sigma~1	4	-136.0	283.1	5.2	0.1	D~1 g0~b sigma~1	4	-296.7	602.9	24.6	0.0
	2017	D~1 g0~1 sigma~1	3	-145.3	298.3	20.3	0.0	D~1 g0~1 sigma~1	3	-300.5	607.8	29.6	0.0
700Rd	2017	**D~1 g0~bk sigma~1**	4	-161.3	333.5	0.0	1.0						
	2017	D~1 g0~b sigma~1	4	-165.1	341.1	7.6	0.0						
	2017	D~1 g0~1 sigma~1	3	-176.3	360.3	26.8	0.0						
81Rd	2017	**D~1 g0~bk sigma~1**	4	-352.3	714.1	0.0	1.0	**D~1 g0~bk sigma~1**	4	-556.7	1122.7	0.0	1.0
	2017	D~1 g0~b sigma~1	4	-372.4	754.3	40.2	0.0	D~1 g0~b sigma~1	4	-575.0	1159.3	36.6	0.0
	2017	D~1 g0~1 sigma~1	3	-378.5	764.0	49.8	0.0	D~1 g0~1 sigma~1	3	-587.7	1182.1	59.5	0.0
Anaconda	2019	**D~1 g0~b sigma~1**	4	-200.6	411.9	0.0	0.5	**D~1 g0~bk sigma~1**	4	-549.2	1107.3	0.0	1.0
	2019	D~1 g0~bk sigma~1	4	-200.8	412.2	0.3	0.5	D~1 g0~b sigma~1	4	-557.2	1123.4	16.1	0.0
	2019	D~1 g0~1 sigma~1	3	-208.0	423.5	11.6	0.0	D~1 g0~1 sigma~1	3	-560.3	1127.2	19.9	0.0
Beauty Lake Road	2018	**D~1 g0~bk sigma~1**	4	-182.7	376.2	0.0	1.0	**D~1 g0~bk sigma~1**	4	-245.9	501.8	0.0	1.0
	2018	D~1 g0~b sigma~1	4	-199.4	409.6	33.4	0.0	D~1 g0~b sigma~1	4	-257.3	524.7	22.9	0.0
	2018	D~1 g0~1 sigma~1	3	-207.3	422.2	46.0	0.0	D~1 g0~1 sigma~1	3	-268.7	544.5	42.7	0.0
Black Creek Rd	2019	**D~1 g0~bk sigma~1**	4	-96.2	206.2	0.0	1.0	**D~1 g0~bk sigma~1**	4	-214.6	439.8	0.0	0.6
	2019	D~1 g0~b sigma~1	4	-101.8	217.3	11.1	0.0	D~1 g0~b sigma~1	4	-215.0	440.6	0.8	0.4
	2019	D~1 g0~1 sigma~1	3	-105.3	219.6	13.4	0.0	D~1 g0~1 sigma~1	3	-223.5	454.5	14.7	0.0
Bogie and Clyde	2019	**D~1 g0~b sigma~1**	4	-191.9	393.7	0.0	0.9						
	2019	D~1 g0~bk sigma~1	4	-194.5	398.9	5.2	0.1						
	2019	D~1 g0~1 sigma~1	3	-202.0	411.2	17.5	0.0						
Boreal	2019	**D~1 g0~bk sigma~1**	4	-224.8	458.9	0.0	1.0	**D~1 g0~bk sigma~1**	4	-207.0	423.4	0.0	1.0
	2019	D~1 g0~b sigma~1	4	-238.7	486.9	28.0	0.0	D~1 g0~1 sigma~1	3	-211.5	429.9	6.5	0.0

	2019	D~1 g0~1 sigma~1	3	-240.2	487.2	28.2	0.0	D~1 g0~b sigma~1	4	-211.5	432.4	9.1	0.0
Borland	2017	**D~1 g0~b sigma~1**	4	-138.5	291.6	0.0	0.7	**D~1 g0~b sigma~1**	4	-238.3	487.1	0.0	0.9
	2017	D~1 g0~bk sigma~1	4	-139.3	293.2	1.6	0.3	D~1 g0~bk sigma~1	4	-241.0	492.4	5.3	0.1
	2017	D~1 g0~1 sigma~1	3	-147.2	303.9	12.3	0.0	D~1 g0~1 sigma~1	3	-243.6	494.5	7.4	0.0
Caithness	2018	**D~1 g0~bk sigma~1**	4	-179.0	369.3	0.0	1.0	**D~1 g0~bk sigma~1**	4	-262.0	534.6	0.0	0.8
	2018	D~1 g0~b sigma~1	4	-182.3	376.0	6.8	0.0	D~1 g0~b sigma~1	4	-263.7	537.9	3.4	0.2
	2018	D~1 g0~1 sigma~1	3	-188.3	384.4	15.2	0.0	D~1 g0~1 sigma~1	3	-269.2	545.8	11.2	0.0
Camp1Road	2018	**D~1 g0~bk sigma~1**	4	-204.5	419.0	0.0	1.0	**D~1 g0~bk sigma~1**	4	-484.8	978.8	0.0	1.0
	2018	D~1 g0~b sigma~1	4	-210.8	431.5	12.5	0.0	D~1 g0~b sigma~1	4	-490.8	990.8	12.1	0.0
	2018	D~1 g0~1 sigma~1	3	-227.9	462.9	43.9	0.0	D~1 g0~1 sigma~1	3	-493.5	993.6	14.8	0.0
Cargill	2018	**D~1 g0~bk sigma~1**	4	-151.9	313.8	0.0	1.0	**D~1 g0~bk sigma~1**	4	-277.7	564.6	0.0	1.0
	2018	D~1 g0~b sigma~1	4	-155.1	320.1	6.3	0.0	D~1 g0~1 sigma~1	3	-286.2	579.2	14.6	0.0
	2018	D~1 g0~1 sigma~1	3	-158.9	324.9	11.1	0.0	D~1 g0~b sigma~1	4	-285.9	581.1	16.5	0.0
CarpRd	2019							D~1 g0~bk sigma~1	4	-197.1	405.2	0.0	1.0
	2019							D~1 g0~b sigma~1	4	-210.3	431.6	26.4	0.0
	2019							D~1 g0~1 sigma~1	3	-212.6	432.9	27.6	0.0
CCGP	2017	**D~1 g0~bk sigma~1**	4	-371.2	751.8	0.0	1.0	**D~1 g0~b sigma~1**	4	-438.9	887.5	0.0	1.0
	2017	D~1 g0~1 sigma~1	3	-376.3	759.5	7.6	0.0	D~1 g0~bk sigma~1	4	-442.4	894.5	7.1	0.0
	2017	D~1 g0~b sigma~1	4	-375.3	760.1	8.3	0.0	D~1 g0~1 sigma~1	3	-453.5	914.0	26.5	0.0
Cedar Narrows	2018	**D~1 g0~bk sigma~1**	4	-262.0	533.1	0.0	1.0	**D~1 g0~bk sigma~1**	4	-357.9	725.0	0.0	1.0
	2018	D~1 g0~b sigma~1	4	-272.8	554.8	21.6	0.0	D~1 g0~1 sigma~1	3	-382.4	771.5	46.5	0.0
	2018	D~1 g0~1 sigma~1	3	-282.1	570.8	37.7	0.0	D~1 g0~b sigma~1	4	-382.1	773.4	48.3	0.0
Century Road	2018	**D~1 g0~bk sigma~1**	4	-187.3	384.5	0.0	1.0	**D~1 g0~bk sigma~1**	4	-331.7	672.5	0.0	1.0
	2018	D~1 g0~b sigma~1	4	-190.9	391.7	7.2	0.0	D~1 g0~b sigma~1	4	-361.5	732.2	59.7	0.0
	2018	D~1 g0~1 sigma~1	3	-194.9	396.9	12.4	0.0	D~1 g0~1 sigma~1	3	-363.3	733.3	60.8	0.0
Crib Road	2017	**D~1 g0~bk sigma~1**	4	-316.8	643.1	0.0	1.0	**D~1 g0~bk sigma~1**	4	-520.2	1049.5	0.0	1.0
	2017	D~1 g0~b sigma~1	4	-321.9	653.3	10.2	0.0	D~1 g0~b sigma~1	4	-525.5	1060.2	10.7	0.0
	2017	D~1 g0~1 sigma~1	3	-324.0	654.9	11.8	0.0	D~1 g0~1 sigma~1	3	-533.6	1073.9	24.4	0.0
Deer Lake Road	2018	**D~1 g0~bk sigma~1**	4	-193.2	396.7	0.0	1.0	**D~1 g0~bk sigma~1**	4	-278.8	567.2	0.0	1.0
	2018	D~1 g0~b sigma~1	4	-209.5	429.4	32.7	0.0	D~1 g0~b sigma~1	4	-284.6	578.9	11.7	0.0
	2018	D~1 g0~1 sigma~1	3	-221.5	450.3	53.6	0.0	D~1 g0~1 sigma~1	3	-293.4	593.8	26.6	0.0

Detour	2018	**D~1 g0~bk sigma~1**	4	-216.5	443.8	0.0	0.8	**D~1 g0~bk sigma~1**	4	-288.3	587.7	0.0	1.0
	2018	D~1 g0~b sigma~1	4	-217.9	446.7	2.9	0.2	D~1 g0~b sigma~1	4	-291.9	594.9	7.2	0.0
	2018	D~1 g0~1 sigma~1	3	-228.1	463.7	19.9	0.0	D~1 g0~1 sigma~1	3	-306.5	620.7	33.0	0.0
Dorion	2019	**D~1 g0~bk sigma~1**	4	-142.1	296.1	0.0	1.0	**D~1 g0~bk sigma~1**	4	-141.0	293.0	0.0	1.0
	2019	D~1 g0~b sigma~1	4	-148.2	308.4	12.3	0.0	D~1 g0~b sigma~1	4	-145.3	301.7	8.7	0.0
	2019	D~1 g0~1 sigma~1	3	-159.6	327.4	31.2	0.0	D~1 g0~1 sigma~1	3	-153.8	315.4	22.4	0.0
FredFlat	2018	**D~1 g0~bk sigma~1**	4	-120.8	254.6	0.0	1.0	**D~1 g0~bk sigma~1**	4	-192.7	396.1	0.0	1.0
	2018	D~1 g0~1 sigma~1	3	-128.3	265.2	10.6	0.0	D~1 g0~1 sigma~1	3	-201.4	410.3	14.2	0.0
	2018	D~1 g0~b sigma~1	4	-126.9	266.7	12.1	0.0	D~1 g0~b sigma~1	4	-201.4	413.5	17.4	0.0
Fushimi	2018	**D~1 g0~1 sigma~1**	3	-189.9	387.2	0.0	0.7	**D~1 g0~bk sigma~1**	4	-341.3	692.2	0.0	0.6
	2018	D~1 g0~b sigma~1	4	-189.9	390.2	3.0	0.2	D~1 g0~b sigma~1	4	-341.6	692.9	0.8	0.4
	2018	D~1 g0~bk sigma~1	4	-189.9	390.2	3.0	0.2	D~1 g0~1 sigma~1	3	-348.6	704.2	12.1	0.0
Garden Lk Rd	2017	**D~1 g0~bk sigma~1**	4	-172.5	356.0	0.0	0.9	**D~1 g0~bk sigma~1**	4	-597.2	1203.3	0.0	1.0
	2017	D~1 g0~b sigma~1	4	-174.7	360.5	4.5	0.1	D~1 g0~b sigma~1	4	-610.6	1230.1	26.8	0.0
	2017	D~1 g0~1 sigma~1	3	-179.6	366.8	10.8	0.0	D~1 g0~1 sigma~1	3	-622.3	1251.1	47.8	0.0
Garg Mijn Sand	2018	**D~1 g0~bk sigma~1**	4	-165.0	342.4	0.0	0.9	**D~1 g0~bk sigma~1**	4	-386.9	784.3	0.0	0.9
	2018	D~1 g0~b sigma~1	4	-167.2	346.8	4.4	0.1	D~1 g0~b sigma~1	4	-389.6	789.7	5.4	0.1
	2018	D~1 g0~1 sigma~1	3	-181.0	370.5	28.1	0.0	D~1 g0~1 sigma~1	3	-397.7	802.9	18.6	0.0
Gibson Lake Rd	2017	**D~1 g0~bk sigma~1**	4	-223.7	457.0	0.0	0.6	**D~1 g0~bk sigma~1**	4	-236.7	483.7	0.0	1.0
	2017	D~1 g0~b sigma~1	4	-224.2	458.0	1.0	0.4	D~1 g0~b sigma~1	4	-246.5	503.4	19.7	0.0
	2017	D~1 g0~1 sigma~1	3	-237.9	482.6	25.6	0.0	D~1 g0~1 sigma~1	3	-251.7	510.8	27.1	0.0
Goldfield Road	2017	**D~1 g0~bk sigma~1**	4	-181.7	373.6	0.0	1.0	**D~1 g0~bk sigma~1**	4	-309.0	627.6	0.0	0.9
	2017	D~1 g0~b sigma~1	4	-189.8	389.8	16.1	0.0	D~1 g0~b sigma~1	4	-311.8	633.1	5.6	0.1
	2017	D~1 g0~1 sigma~1	3	-194.0	395.3	21.7	0.0	D~1 g0~1 sigma~1	3	-330.9	668.7	41.1	0.0
Grassy	2017	**D~1 g0~bk sigma~1**	4	-222.5	455.5	0.0	0.9	**D~1 g0~bk sigma~1**	4	-339.7	688.9	0.0	0.9
	2017	D~1 g0~b sigma~1	4	-225.2	460.9	5.4	0.1	D~1 g0~b sigma~1	4	-341.6	692.8	3.9	0.1
	2017	D~1 g0~1 sigma~1	3	-240.6	488.6	33.2	0.0	D~1 g0~1 sigma~1	3	-360.0	726.8	37.9	0.0
Grimsthorpe	2019	**D~1 g0~b sigma~1**						**D~1 g0~bk sigma~1**	4	-190.1	389.8	0.0	1.0
	2019	**D~1 g0~bk sigma~1**						D~1 g0~1 sigma~1	3	-195.5	397.9	8.1	0.0
	2019	D~1 g0~1 sigma~1						D~1 g0~b sigma~1	4	-194.5	398.6	8.9	0.0
Highway 631	2019	**D~1 g0~bk sigma~1**	4	-188.7	388.1	0.0	0.5	**D~1 g0~bk sigma~1**	4	-177.7	365.8	0.0	1.0

	2019	D~1 g0~b sigma~1	4	-188.8	388.3	0.2	0.4	D~1 g0~b sigma~1	4	-183.1	376.5	10.7	0.0
	2019	D~1 g0~1 sigma~1	3	-191.7	391.0	2.8	0.1	D~1 g0~1 sigma~1	3	-187.4	382.2	16.4	0.0
	2017	D~1 g0~bk sigma~1	4	-153.8	319.2	0.0	1.0	D~1 g0~bk sigma~1	4	-245.2	500.6	0.0	1.0
	2017	D~1 g0~b sigma~1	4	-164.9	341.4	22.2	0.0	D~1 g0~b sigma~1	4	-262.8	535.9	35.3	0.0
	2017	D~1 g0~1 sigma~1	3	-173.3	354.5	35.3	0.0	D~1 g0~1 sigma~1	3	-268.9	545.0	44.4	0.0
Inglis Lake Road	2018	**D~1 g0~bk sigma~1**	4	-209.4	430.4	0.0	1.0	**D~1 g0~bk sigma~1**	4	-406.5	822.4	0.0	1.0
	2018	D~1 g0~b sigma~1	4	-226.2	464.0	33.6	0.0	D~1 g0~b sigma~1	4	-416.3	841.8	19.4	0.0
	2018	D~1 g0~1 sigma~1	3	-238.2	484.4	54.0	0.0	D~1 g0~1 sigma~1	3	-417.9	842.6	20.2	0.0
Killarney	2019	**D~1 g0~bk sigma~1**	4	-163.6	337.5	0.0	0.6	**D~1 g0~bk sigma~1**	4	-263.5	536.8	0.0	1.0
	2019	D~1 g0~b sigma~1	4	-164.1	338.6	1.0	0.4	D~1 g0~b sigma~1	4	-274.5	558.7	21.9	0.0
	2019	D~1 g0~1 sigma~1	3	-171.6	350.6	13.0	0.0	D~1 g0~1 sigma~1	3	-286.6	580.2	43.4	0.0
Lampson	2019	**D~1 g0~bk sigma~1**	4	-322.7	655.2	0.0	1.0	**D~1 g0~bk sigma~1**	4	-418.9	847.2	0.0	1.0
	2019	D~1 g0~b sigma~1	4	-371.0	751.7	96.5	0.0	D~1 g0~b sigma~1	4	-439.6	888.6	41.4	0.0
	2019	D~1 g0~1 sigma~1	3	-386.3	779.5	124.3	0.0	D~1 g0~1 sigma~1	3	-441.4	889.6	42.3	0.0
Longlegged	2018	**D~1 g0~bk sigma~1**	4	-229.2	468.3	0.0	1.0	**D~1 g0~bk sigma~1**	4	-526.1	1061.0	0.0	0.9
	2018	D~1 g0~b sigma~1	4	-236.5	482.8	14.5	0.0	D~1 g0~b sigma~1	4	-529.0	1066.9	5.9	0.1
	2018	D~1 g0~1 sigma~1	3	-238.0	483.0	14.7	0.0	D~1 g0~1 sigma~1	3	-533.3	1073.0	12.0	0.0
Massey Tote	2018	D~1 g0~b sigma~1						D~1 g0~1 sigma~1	3	-123.2	255.9	0.0	0.9
	2018	D~1 g0~bk sigma~1						**D~1 g0~bk sigma~1**	4	-123.1	260.9	5.0	0.1
	2018	**D~1 g0~1 sigma~1**						D~1 g0~b sigma~1	4	-123.2	261.1	5.2	0.1
Mayburn	2019	**D~1 g0~bk sigma~1**	4	-198.0	406.4	0.0	1.0	**D~1 g0~bk sigma~1**	4	-361.8	732.8	0.0	1.0
	2019	D~1 g0~b sigma~1	4	-200.9	412.3	5.9	0.0	D~1 g0~b sigma~1	4	-378.0	765.3	32.5	0.0
	2019	D~1 g0~1 sigma~1	3	-209.1	425.6	19.2	0.0	D~1 g0~1 sigma~1	3	-383.7	774.0	41.3	0.0
McConnell	2017	**D~1 g0~bk sigma~1**	4	-161.4	332.9	0.0	0.8	**D~1 g0~bk sigma~1**	4	-225.7	461.2	0.0	1.0
	2017	D~1 g0~1 sigma~1	3	-164.3	335.9	3.0	0.2	D~1 g0~b sigma~1	4	-237.7	485.0	23.8	0.0
	2017	D~1 g0~b sigma~1	4	-164.0	338.1	5.1	0.1	D~1 g0~1 sigma~1	3	-240.4	487.7	26.5	0.0
Menet Brent	2018	D~1 g0~bk sigma~1	4	-216.6	442.4	0.0	0.9	D~1 g0~bk sigma~1	4	-376.4	761.7	0.0	0.8
	2018	D~1 g0~b sigma~1	4	-219.5	448.3	5.9	0.1	D~1 g0~b sigma~1	4	-377.8	764.5	2.8	0.2
	2018	D~1 g0~1 sigma~1	3	-226.2	459.1	16.7	0.0	D~1 g0~1 sigma~1	3	-380.9	768.4	6.7	0.0
Munro Tower	2017	**D~1 g0~b sigma~1**	4	-107.4	226.5	0.0	0.7	**D~1 g0~bk sigma~1**	4	-279.1	567.9	0.0	1.0
	2017	D~1 g0~bk sigma~1	4	-108.4	228.4	2.0	0.3	D~1 g0~b sigma~1	4	-289.4	588.5	20.5	0.0

	2017	D~1 g0~1 sigma~1	3	-114.2	236.4	9.9	0.0	D~1 g0~1 sigma~1	3	-291.3	589.5	21.6	0.0
NORT Road	2019							**D~1 g0~bk sigma~1**	4	-172.0	354.4	0.0	0.8
	2019							D~1 g0~1 sigma~1	3	-175.5	358.3	3.8	0.1
	2019							D~1 g0~b sigma~1	4	-175.3	360.9	6.5	0.0
Ogoki	2019	**D~1 g0~bk sigma~1**	4	-308.0	625.7	0.0	0.5	**D~1 g0~bk sigma~1**	4	-897.7	1804.3	0.0	1.0
	2019	D~1 g0~1 sigma~1	3	-309.5	626.0	0.3	0.4	D~1 g0~1 sigma~1	3	-908.5	1823.6	19.3	0.0
	2019	D~1 g0~b sigma~1	4	-309.5	628.8	3.1	0.1	D~1 g0~b sigma~1	4	-907.9	1824.6	20.3	0.0
Opeepeesway	2017	**D~1 g0~b sigma~1**	4	-116.2	245.4	0.0	0.4	**D~1 g0~bk sigma~1**	4	-369.9	749.5	0.0	1.0
	2017	D~1 g0~bk sigma~1	4	-116.2	245.4	0.1	0.4	D~1 g0~b sigma~1	4	-376.2	762.0	12.5	0.0
	2017	D~1 g0~1 sigma~1	3	-119.5	247.7	2.3	0.1	D~1 g0~1 sigma~1	3	-378.1	763.3	13.8	0.0
Pardo	2017	**D~1 g0~b sigma~1**	4	-183.4	376.4	0.0	0.6	**D~1 g0~bk sigma~1**	4	-252.3	514.2	0.0	1.0
	2017	D~1 g0~bk sigma~1	4	-184.1	377.8	1.4	0.3	D~1 g0~1 sigma~1	3	-260.1	527.1	12.9	0.0
	2017	D~1 g0~1 sigma~1	3	-186.1	379.1	2.8	0.1	D~1 g0~b sigma~1	4	-259.2	528.0	13.9	0.0
Phillip Creek	2019	**D~1 g0~b sigma~1**	4	-221.5	453.2	0.0	1.0	**D~1 g0~bk sigma~1**	4	-354.8	719.3	0.0	1.0
	2019	D~1 g0~bk sigma~1	4	-228.4	466.9	13.7	0.0	D~1 g0~b sigma~1	4	-358.0	725.6	6.3	0.0
	2019	D~1 g0~1 sigma~1	3	-237.6	482.4	29.2	0.0	D~1 g0~1 sigma~1	3	-363.9	734.8	15.5	0.0
Pickerel	2019	**D~1 g0~bk sigma~1**	4	-247.4	504.1	0.0	1.0	**D~1 g0~bk sigma~1**	4	-220.0	449.5	0.0	1.0
	2019	D~1 g0~b sigma~1	4	-254.1	517.3	13.2	0.0	D~1 g0~b sigma~1	4	-228.4	466.4	16.9	0.0
	2019	D~1 g0~1 sigma~1	3	-257.2	521.2	17.1	0.0	D~1 g0~1 sigma~1	3	-230.5	468.0	18.4	0.0
Pineridge	2018	**D~1 g0~bk sigma~1**	4	-139.0	289.7	0.0	1.0	**D~1 g0~bk sigma~1**	4	-285.3	579.9	0.0	1.0
	2018	D~1 g0~b sigma~1	4	-142.4	296.4	6.7	0.0	D~1 g0~b sigma~1	4	-294.5	598.4	18.5	0.0
	2018	D~1 g0~1 sigma~1	3	-147.7	303.3	13.6	0.0	D~1 g0~1 sigma~1	3	-301.3	609.4	29.5	0.0
Portelance	2017	**D~1 g0~bk sigma~1**	4	-156.9	324.2	0.0	1.0	**D~1 g0~bk sigma~1**	4	-319.3	647.9	0.0	1.0
	2017	D~1 g0~1 sigma~1	3	-164.8	337.0	12.8	0.0	D~1 g0~b sigma~1	4	-343.3	696.0	48.1	0.0
	2017	D~1 g0~b sigma~1	4	-164.5	339.3	15.1	0.0	D~1 g0~1 sigma~1	3	-345.5	697.7	49.8	0.0
RedSquirrel	2018	**D~1 g0~bk sigma~1**	4	-208.9	428.0	0.0	1.0						
	2018	D~1 g0~b sigma~1	4	-220.0	450.3	22.2	0.0						
	2018	D~1 g0~1 sigma~1	3	-224.7	456.6	28.6	0.0						
Road600	2019	**D~1 g0~bk sigma~1**	4	-207.9	426.6	0.0	1.0	**D~1 g0~bk sigma~1**	4	-313.9	638.3	0.0	1.0
	2019	D~1 g0~b sigma~1	4	-229.9	470.7	44.1	0.0	D~1 g0~b sigma~1	4	-319.8	650.0	11.7	0.0
	2019	D~1 g0~1 sigma~1	3	-242.1	491.7	65.1	0.0	D~1 g0~1 sigma~1	3	-325.8	659.1	20.8	0.0

Robinson Lake	2018	**D~1 g0~bk sigma~1**	4	-109.5	233.8	0.0	1.0	**D~1 g0~b sigma~1**	4	-132.5	276.6	0.0	0.5
	2018	D~1 g0~b sigma~1	4	-112.8	240.2	6.4	0.0	D~1 g0~bk sigma~1	4	-132.6	276.9	0.2	0.5
	2018	D~1 g0~1 sigma~1	3	-117.1	243.6	9.8	0.0	D~1 g0~1 sigma~1	3	-138.9	285.7	9.1	0.0
Sand English	2019	**D~1 g0~bk sigma~1**	4	-349.5	707.8	0.0	1.0	**D~1 g0~bk sigma~1**	4	-422.6	853.8	0.0	1.0
	2019	D~1 g0~b sigma~1	4	-365.3	739.5	31.7	0.0	D~1 g0~b sigma~1	4	-453.9	916.5	62.6	0.0
	2019	D~1 g0~1 sigma~1	3	-375.5	757.5	49.7	0.0	D~1 g0~1 sigma~1	3	-468.5	943.5	89.6	0.0
Shaw Rd	2019	**D~1 g0~bk sigma~1**	4	-191.9	395.1	0.0	1.0						
	2019	D~1 g0~b sigma~1	4	-195.0	401.4	6.3	0.0						
	2019	D~1 g0~1 sigma~1	3	-201.2	410.3	15.3	0.0						
Shirley Lake Rd	2019	**D~1 g0~b sigma~1**	4	-255.3	520.4	0.0	1.0	**D~1 g0~bk sigma~1**	4	-375.0	759.3	0.0	1.0
	2019	D~1 g0~bk sigma~1	4	-259.3	528.6	8.1	0.0	D~1 g0~b sigma~1	4	-390.6	790.5	31.2	0.0
	2019	D~1 g0~1 sigma~1	3	-279.1	565.3	44.9	0.0	D~1 g0~1 sigma~1	3	-401.8	810.4	51.1	0.0
South EMU	2017	**D~1 g0~bk sigma~1**	4	-209.5	429.0	0.0	1.0	**D~1 g0~bk sigma~1**	4	-214.0	438.1	0.0	1.0
	2017	D~1 g0~b sigma~1	4	-218.2	446.5	17.4	0.0	D~1 g0~1 sigma~1	3	-231.8	470.7	32.6	0.0
	2017	D~1 g0~1 sigma~1	3	-220.2	447.6	18.6	0.0	D~1 g0~b sigma~1	4	-231.0	471.9	33.8	0.0
Sowden	2019	**D~1 g0~bk sigma~1**	4	-337.2	685.2	0.0	1.0	**D~1 g0~b sigma~1**	4	-474.4	958.5	0.0	1.0
	2019	D~1 g0~b sigma~1	4	-362.4	735.7	50.5	0.0	D~1 g0~bk sigma~1	4	-483.6	976.7	18.3	0.0
	2019	D~1 g0~1 sigma~1	3	-378.5	764.6	79.4	0.0	D~1 g0~1 sigma~1	3	-497.8	1002.6	44.1	0.0
Translimit	2018	**D~1 g0~bk sigma~1**	4	-321.1	652.0	0.0	1.0	**D~1 g0~bk sigma~1**	4	-416.4	842.5	0.0	1.0
	2018	D~1 g0~b sigma~1	4	-328.0	665.7	13.7	0.0	D~1 g0~b sigma~1	4	-426.7	862.9	20.4	0.0
	2018	D~1 g0~1 sigma~1	3	-341.5	690.0	37.9	0.0	D~1 g0~1 sigma~1	3	-438.1	883.2	40.7	0.0
Trout Lake	2019	**D~1 g0~bk sigma~1**	4	-158.9	327.8	0.0	1.0	**D~1 g0~bk sigma~1**	4	-176.6	363.9	0.0	0.9
	2019	D~1 g0~b sigma~1	4	-163.1	336.2	8.4	0.0	D~1 g0~1 sigma~1	3	-180.8	369.1	5.2	0.1
	2019	D~1 g0~1 sigma~1	3	-166.7	340.6	12.8	0.0	D~1 g0~b sigma~1	4	-180.5	371.7	7.8	0.0
Turtle River Road	2018	D~1 g0~bk sigma~1	4	-183.1	375.9	0.0	1.0	**D~1 g0~bk sigma~1**	4	-234.3	478.1	0.0	1.0
	2018	**D~1 g0~b sigma~1**	4	-199.8	409.3	33.4	0.0	D~1 g0~b sigma~1	4	-241.8	492.9	14.8	0.0
	2018	D~1 g0~1 sigma~1	3	-213.5	434.0	58.1	0.0	D~1 g0~1 sigma~1	3	-249.7	506.2	28.2	0.0
Vermilion River Road	2018	**D~1 g0~bk sigma~1**	4	-241.8	493.8	0.0	1.0	**D~1 g0~bk sigma~1**	4	-636.5	1282.0	0.0	1.0
	2018	D~1 g0~b sigma~1	4	-251.1	512.3	18.5	0.0	D~1 g0~b sigma~1	4	-650.9	1310.6	28.6	0.0
	2018	D~1 g0~1 sigma~1	3	-255.4	517.9	24.1	0.0	D~1 g0~1 sigma~1	3	-659.0	1324.5	42.5	0.0

Watabeag	2017	D~1 g0~bk sigma~1	4	-177.4	365.5	0.0	0.7	**D~1 g0~bk sigma~1**	4	-137.3	285.7	0.0	1.0
	2017	**D~1 g0~b sigma~1**	4	-178.4	367.5	2.1	0.3	D~1 g0~b sigma~1	4	-142.4	295.8	10.1	0.0
	2017	D~1 g0~1 sigma~1	3	-182.6	372.7	7.2	0.0	D~1 g0~1 sigma~1	3	-147.6	302.8	17.1	0.0
Wenasaga	2018	**D~1 g0~bk sigma~1**	4	-168.2	349.3	0.0	1.0	**D~1 g0~bk sigma~1**	4	-490.5	990.2	0.0	1.0
	2018	D~1 g0~1 sigma~1	3	-174.8	358.2	8.9	0.0	D~1 g0~b sigma~1	4	-494.0	997.4	7.2	0.0
	2018	D~1 g0~b sigma~1	4	-174.2	361.4	12.1	0.0	D~1 g0~1 sigma~1	3	-498.3	1003.3	13.1	0.0
Wenebegon	2018	**D~1 g0~bk sigma~1**	4	-133.8	278.9	0.0	1.0	**D~1 g0~bk sigma~1**	4	-289.5	588.6	0.0	1.0
	2018	D~1 g0~b sigma~1	4	-139.3	290.0	11.1	0.0	D~1 g0~b sigma~1	4	-293.4	596.5	7.9	0.0
	2018	D~1 g0~1 sigma~1	3	-147.7	303.3	24.4	0.0	D~1 g0~1 sigma~1	3	-298.0	602.9	14.3	0.0
West End	2019	**D~1 g0~bk sigma~1**	4	-193.8	397.2	0.0	1.0	**D~1 g0~bk sigma~1**	4	-218.3	445.9	0.0	1.0
	2019	D~1 g0~b sigma~1	4	-208.4	426.4	29.2	0.0	D~1 g0~b sigma~1	4	-230.3	469.8	23.9	0.0
	2019	D~1 g0~1 sigma~1	3	-213.2	433.3	36.1	0.0	D~1 g0~1 sigma~1	3	-237.5	481.7	35.8	0.0
Whitman Dam	2018	**D~1 g0~bk sigma~1**	4	-231.5	474.0	0.0	1.0	**D~1 g0~bk sigma~1**	4	-318.8	648.5	0.0	1.0
	2018	D~1 g0~b sigma~1	4	-270.2	551.5	77.5	0.0	D~1 g0~b sigma~1	4	-325.4	661.7	13.3	0.0
	2018	D~1 g0~1 sigma~1	3	-282.8	573.4	99.4	0.0	D~1 g0~1 sigma~1	3	-334.1	675.9	27.4	0.0
Winter Lake	2019	**D~1 g0~b sigma~1**	4	-146.3	303.4	0.0	0.8	**D~1 g0~bk sigma~1**	4	-262.1	533.6	0.0	1.0
	2019	D~1 g0~bk sigma~1	4	-147.6	306.1	2.7	0.2	D~1 g0~b sigma~1	4	-269.6	548.6	15.0	0.0
	2019	D~1 g0~1 sigma~1	3	-152.5	312.7	9.3	0.0	D~1 g0~1 sigma~1	3	-276.5	559.8	26.1	0.0

Table C.3.3 Summary of the AIC_c minimizing model for SECR detection models for stage 1 fit to 122 black bear capture-recapture datasets (61 female; 61 male) collected from 65 study areas in Ontario, Canada between 2017–2019. Columns represent the number (*N*) and percent of total datasets where each model form was identified as the AIC_c minimizing model. Detection covariates includes general (*b*) and a trap-specific (*bk*) behavioural response. "." Indicates parameter held constant.

	Female		**Male**		**Combined**	
SECR model	***N***	**%**	***N***	**%**	***N***	**%**
D(.) g_0 (*bk*) σ(.)	48	78.7	57	93.4	105	86.1
D(.) g_0 (*b*) σ(.)	12	19.7	4	6.6	16	13.1
D(.) g_0 (.) σ(.)	1	1.6	0	0.0	1	0.8

Table C.3.4. Number of successfully converged univariate SECR model by form, fit to black bear spatial capture-recapture data collected across 65 study areas in Ontario Canada from 2017–2019.

Sex	**Univariate density model form[1]**						**Combined**
	Human	Road	NDVI	Coniferous forest	Deciduous forest	Mixed forest	
Female	19	20	30	28	31	21	149
Male	31	42	28	31	28	31	191

[1] Covariate that the density (D) parameter varies by

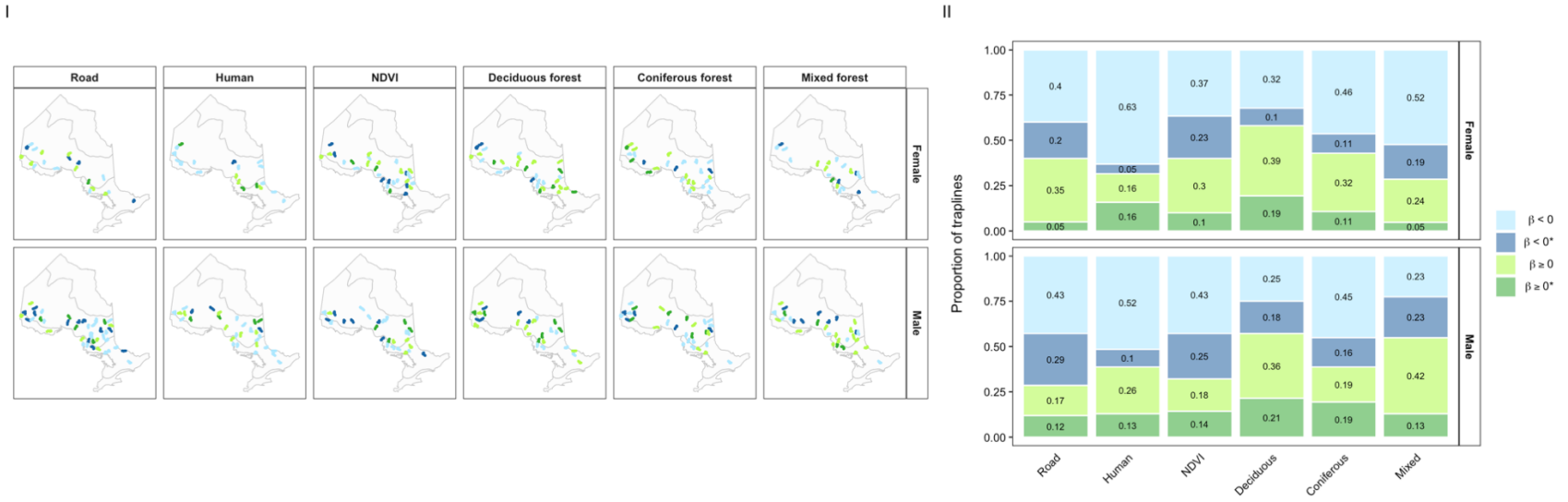

Figure C.3.1. Summary of the direction of β parameter estimates from univariate SECR models fit to 65 study areas in Ontario from 2017–2019. Covariates on density model include normalized difference vegetation index (NDVI), percent forest types (coniferous, deciduous, mixed), human settlement density (human) and road density (road). Figure I displays the direction of β estimates across study areas; at this scale coloured lines represents study areas. Figure II displays the proportion of successfully fit models by the β parameter direction and significance; green and blue shades indicate a positive and negative direction of effect respectively, and asterisks (*) indicates significant effect (95% confidence intervals do not include 0).

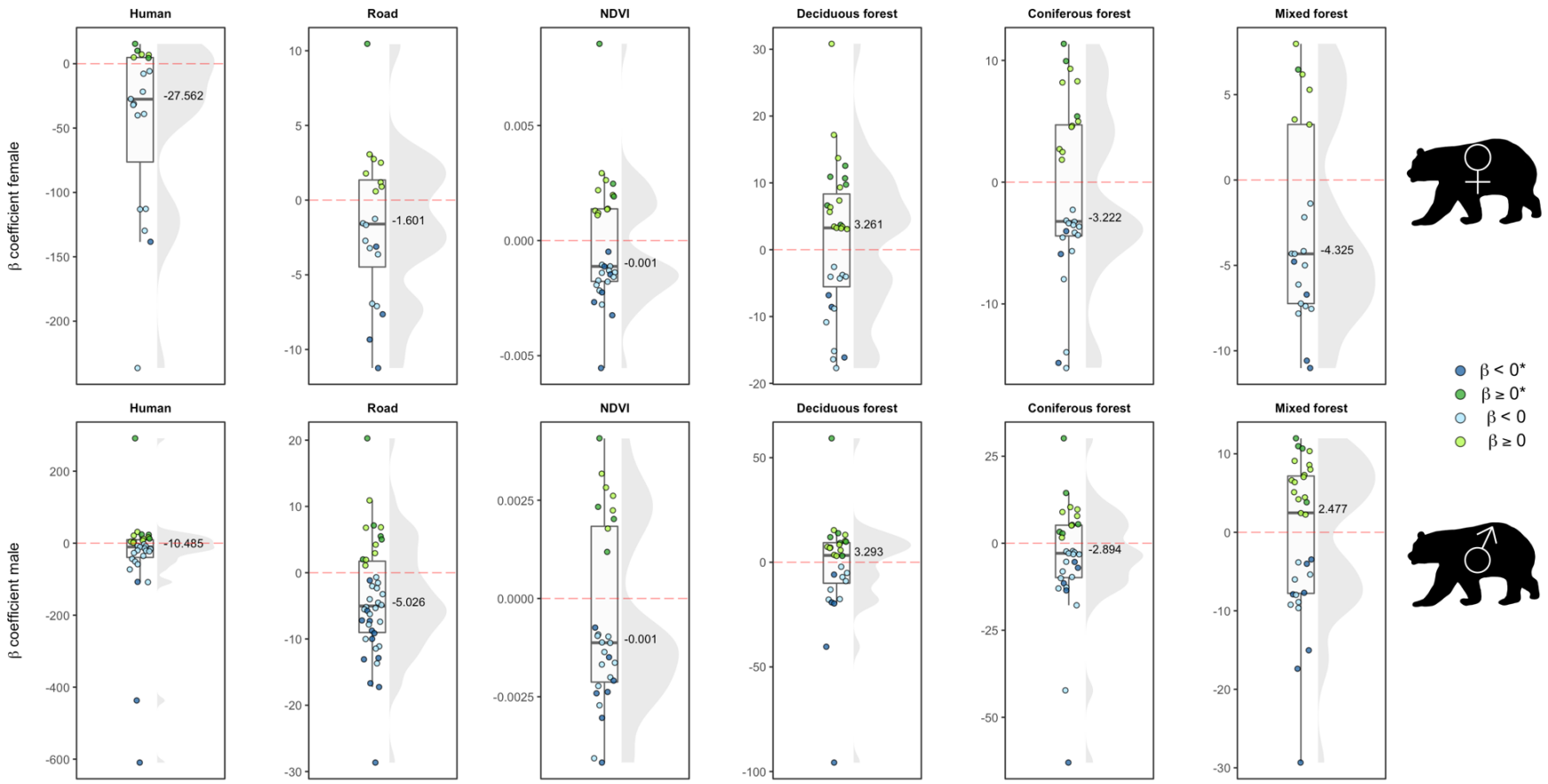

Figure C.3.2. Log-scale effect size (β parameter estimates) of female (♀) and male (♂) univariate models with density covariates including normalized difference vegetation index (NDVI), percent forest types (coniferous, deciduous, mixed), human settlement density (human) and road density (road). β estimates unstandardized to allow for comparison of effects within a covariate across study areas. The effect size indicates the change in the baseline density (bears/hectare) on the log scale for one unit change in the covariates value. Green and blue shades indicate a positive and negative direction of effect respectively, and asterisks (*) indicates significant effect (95% confidence intervals do not include 0). Thick gray horizontal line within boxplots and text represents the median of β estimates and dashed red horizontal line indicates no effect of covariates on density.

C. 4 Chapter 3 pooled analysis multivariate models and comparison to univariate models

Log-scale effect size (β parameter estimates) of two global SECR multivariate models (Table C.4.1) fit to female and male black bear populations in the GLSL and boreal forests regions of Ontario, Canada, from 2017–2019. Multivariate models not included in second analysis because of multicollinearity between covariates and challenges assessing model convergence. Despite this, the direction and magnitude of β parameter estimates in the univariate models are generally comparable to the multivariate models.

Table C.4.1. Stage 1 and 2 for multivariate SECR models. Detection model includes covariates for behavioural response where capture provides net increase or decrease in subsequent capture probability by detector (*bk*) and sampling occasion (*t)*. Density model covariates represent hypothesis of bottom-up (productivity and forest type) and top-down (anthropogenic effects) and includes normalized difference vegetation index (NDVI), percent forest types (coniferous forest [con_F] and deciduous forest [dec_F]), percent agriculture land cover (CROP), human settlement density (HS) and road density (RD). "." indicates that model parameter held constant.

Modeling stage	**Detection model**			**Density model**	
	Hypothesis	**g_0**	**σ**	**Hypothesis**	**D**
Female Boreal Male Boreal Male GLSL	Sampling occasion and trap-specific response	g_0 (*bk*)	σ (*t*)	Anthropogenic effects and productivity	D(*NDVI + HS + RD + CROP)*
				Anthropogenic effects and forest type	D(*con_F + dec_F + HS + RD + CROP)*
Female GLSL	Trap-specific response	g_0 (*bk*)	σ (.)	Anthropogenic effects and productivity	D(*NDVI + HS + RD + CROP)*
				Anthropogenic effects and forest type	D(*con_F + dec_F + HS + RD + CROP)*

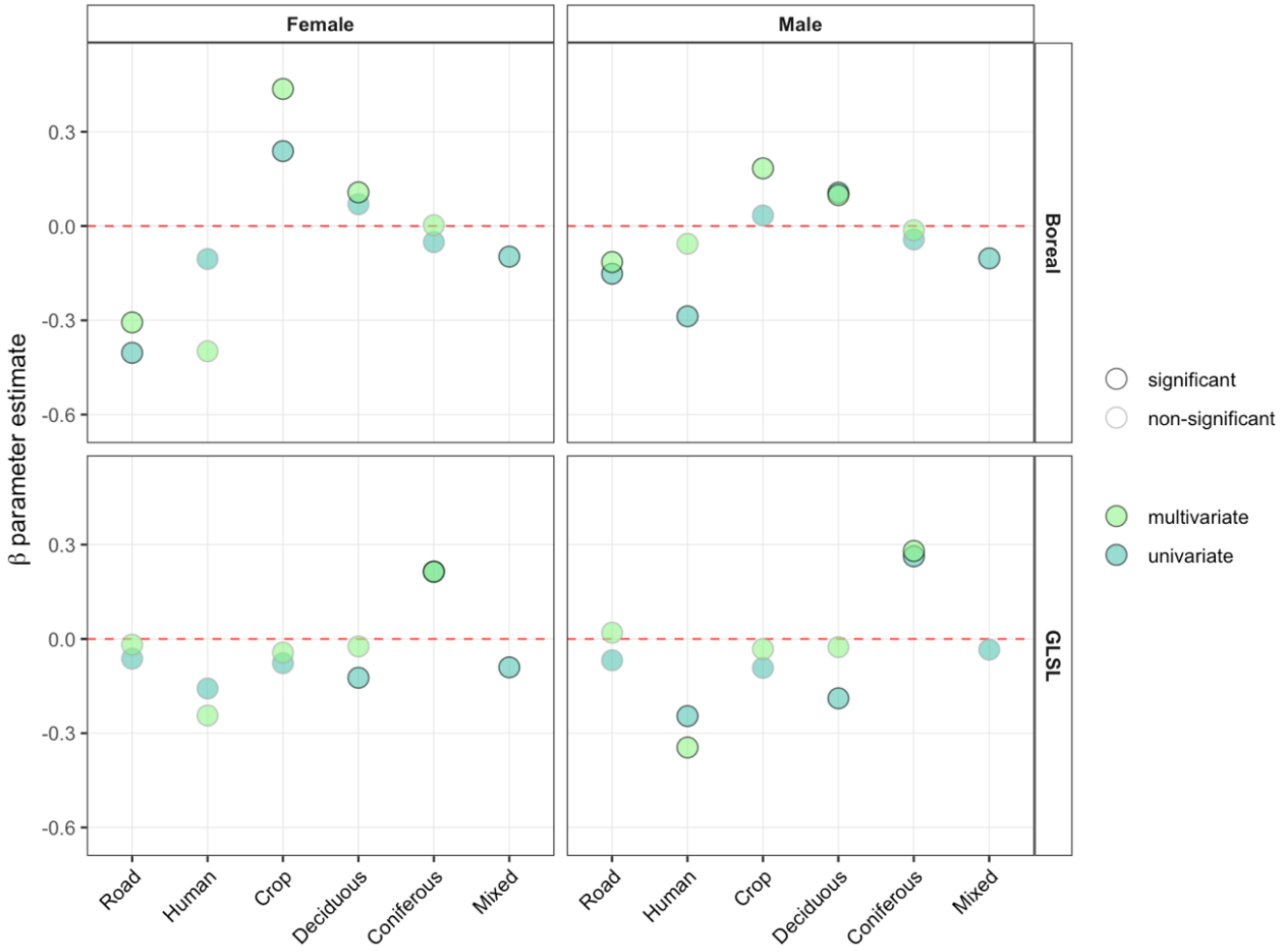

Figure C.4.1. Log-scale effect size (β parameter estimates) of six univariate models with density covariates including percent forest types (coniferous, deciduous, mixed), percent crop, human settlement density (human) and road density (road) and one global multivariate model (D ~ road + human + coniferous + deciduous + crop). β estimates standardized to allow for covariate comparison within study area by sex. The effect size indicates the change in the baseline density (bears/hectare) on the log scale for one unit change in the covariates value. Black outlines around circles indicate significant effect (95% confidence intervals do not include 0) and dashed red horizontal line indicates no effect of predictor on density.

C. 5 Chapter 3 pooled analysis detection model selection criteria and density correlation coefficients

Table C.5.1. Summary of AIC_c model selection criterion for stage one fit to four black bear capture-recapture datasets from 65 study area in Ontario, Canada from 2017-2019. *K* denotes the number of parameters; LL the log likelihood; W_i the AIC_c weight. Detection covariates includes a trap-specific (*bk*) learned behavioural response and sampling occasion (*t)*. Bold text indicates detection model parameters used in stage two of density model fitting.

Dataset	Model form	*K*	LL	AIC_c	$\triangle AIC_c$	W_i
Female GLSL[1]	**D(1) g_0(bk) σ(1)**	**4**	**-4183.40**	**8374.89**	**0.00**	**0.66**
	D(1) g_0(bk) σ(t)	9	-4178.91	8376.19	1.30	0.34
	D(1) g_0(1) σ(t)	8	-4440.31	8896.91	522.02	0.00
	D(1) g_0 (1) σ(1)	3	-4524.77	9055.59	680.70	0.00
Female Boreal	**D(1) g_0(bk) σ(t)**	**8**	**-9222.82**	**18461.81**	**0.00**	**1.00**
	D(1) g_0(bk) σ(1)	4	-9272.98	18554.00	92.20	0.00
	D(1) g_0(1) σ(t)	7	-9606.49	19227.10	765.29	0.00
	D(1) g_0(1) σ(1)	3	-9861.32	19728.66	1266.85	0.00
Male GLSL[1]	**D(1) g_0(bk) σ(t)**	**9**	**-5358.23**	**10734.80**	**0.00**	**1.00**
	D(1) g_0(bk) σ(1)	4	-5386.90	10781.88	47.08	0.00
	D(1) g_0 (1) σ(t)	8	-5592.12	11200.51	465.71	0.00
	D(1) g0(1) σ(1)	3	-5685.31	11376.67	641.87	0.00
Male Boreal	**D(1) g_0(bk) σ(t)**	**8**	**-15889.20**	**31794.50**	**0.00**	**1.00**
	D(1) g_0(bk) σ(1)	4	-15922.05	31852.12	57.62	0.00
	D(1) g_0(1) σ(t)	7	-16309.19	32632.47	837.97	0.00
	D(1) g_0(1) σ(1)	3	-16470.24	32946.49	1151.99	0.00

[1] addition parameter in GLSL datasets fit to models with *t* covariate because one study area sampled over additional occasions

Table C.5.2. Pearson's correlation coefficients for covariates used in SECR models for male and female black bears. Correlations calculated from mask points (x,y) pooled across all study areas included in the SECR model. Covariates includes normalized difference vegetation index (NDVI), percent forest types (coniferous, deciduous, mixed), percent agriculture land cover (crop), human settlement density (human) and road density (road). Bold values $| r | \geq 0.7$.

Covariates		**Boreal**		**GLSL**	
		Female	**Male**	**Female**	**Male**
NDVI	human	0.07	0.14	0.03	0.07
NDVI	road	0.13	0.17	0.24	0.29
human	road	0.44	0.43	0.27	0.25
NDVI	crop	0.16	0.18	0.14	0.13
human	crop	0.29	0.35	0.18	0.12
road	crop	0.34	0.39	0.20	0.17
NDVI	coniferous	-0.48	-0.53	-0.28	-0.27
human	coniferous	-0.10	-0.14	-0.03	0.01
road	coniferous	-0.26	-0.32	-0.14	-0.13
crop	coniferous	-0.14	-0.16	-0.17	-0.16
NDVI	deciduous	0.21	0.18	0.37	0.41
human	deciduous	0.06	0.11	0.15	0.19
road	deciduous	0.16	0.21	0.12	0.21
crop	deciduous	0.23	0.28	0.19	0.22
coniferous	deciduous	-0.51	-0.52	-0.49	-0.49
NDVI	mixed	0.69	**0.75**	0.27	0.21
human	mixed	-0.01	0.03	-0.29	-0.31
road	mixed	0.02	0.09	-0.04	-0.13
crop	mixed	-0.10	-0.07	-0.37	-0.40
coniferous	mixed	-0.60	-0.67	-0.11	-0.01
deciduous	mixed	-0.07	-0.04	-0.55	-0.63

Appendix D: Chapter 4

D.1 Chapter 4 spatial covariates

Table D.1.1 Spatial covariates including names, descriptions, sources of datasets, original resolution (pixel size), unit of time over which original datasets were available, and units of processed layers. Processed resolution of all raster layers set at 1km x 1km.

Covariate	Description	Source	Resolution	Time scale	Units
Deciduous forest	Percentage of area where tree crown cover is comprised of ≥75% deciduous species generally greater than 3m tall.	NALCMS[1]	30 x 30m	2015	%
Coniferous Forest	Percentage of area where tree crown cover is comprised of ≥75% coniferous species generally greater than 3m tall.	NALCMS[1]	30 x 30m	2015	%
Road density	Density of all roads (freeway, highway, collector, arterial, local, resource and recreation) in km roads/km^2.	NRN[2]	NA	2021	km/km^2
Human influence index	Includes nine global data layers covering human population density, human land use and infrastructure (built-up areas, nighttime lights, land use/land cover) and human access (coastlines, roads, railways, navigable rivers).	HII[3]	1 x 1km	1995 – 2004	0 (no human presence) – 64 (max human presence)
Harvest density	Average number of bears harvested annually per km^2 in each WMU from the previous 7 years of sampling.	MNRF[4]	NA	2018 – 2010[5]	bears harvested/ km^2

[1] 2015 Land cover of North America at 30 meters. North American land change monitoring system (NALCMS; NALCMS, 2020).

[2] Canada national road network (NRN; Statistics Canada, 2022)

[3] Global human influence index [HII] dataset (WCS and CIESIN 2005)

[4] calculated from hunter-reported harvest. The Ministry of Natural Resources and Forestry (MNRF) reports harvest annually through surveys mailed to licensed hunters. Includes harvest from fall hunt and, when applicable, spring hunt.

[5] because study areas were sampled across three different years, harvest density was averaged across the previous seven years from the year of sampling (i.e., for study areas sampled in 2019, harvest was averaged from 2012-2018).

D. 2 Chapter 4 approximating the buffer size

The buffer used to quantify spatial covariates was delignated based on raw movement data collected from the MNRF capture-recapture datasets. The maximum distance between any two detections was calculated for each animal caught more than once across 77 study areas and provides an approximation of animals observed range length. For study areas sampled over multiple years, only datasets from the first year were included. To examine how our spatial covariates varied by extent we initially developed three buffer widths based on the median, 62.5% and 75% quantiles of the observed range length for each sex (Figure D.2.1; Table D.2.1). While it is likely that black bears are exhibit non-circular home ranges, we treated the observed range length as the diameter of a bear's circular home range to meet SECR detection model assumption of a circular home range. These buffer values collaborate with past radio-collar studies of female black bears adjacent to the Chapeau Crown Game Preserve in the boreal forest of Ontario, 1992-1998. Estimate of the spring 95% conditional home range utilization distribution (CUDs) of female black bear in the area ranges between 12.84 – 20.23 km^2 (4.04 – 5.06 km circular home range diameter; Howe, *unpublished*) that varied by age and if females were encumbered or not. We did not include a buffer width using the 95% percentile because these values represented large movements that are uncommon during the study period (Table D.2.1). All covariates displayed high correlation across buffer widths (range r= 0.95 – 1*;* mean r = 0.99*;* Table D.2.2). Therefore, we selected to use the 75% quantile buffer of 4430m and 8740m for females and males respectively because these values were most similar to the Ontario radio-collar data (Howe, *unpublished)* and we expected range lengths to slightly underestimate home range circles.

Table D.2.1. Quantiles of observed range length of each animal (maximum distance between any two detections of an animal) from female and male black bear capture-recapture data collected across 77 study sites in Ontario, Canada from 2017-2019[1]. Estimated circular home ranges calculated using observed range length as circle diameter.

Quartile	Observed range length (km)		Estimated circular home range (km²)	
	Female	Male	Female	Male
50%	2.90	5.30	6.61	22.08
62.5%	3.19	6.87	7.97	37.02
75%	4.43	8.74	15.40	60.06
95%	8.82	16.01	61.10	201.26

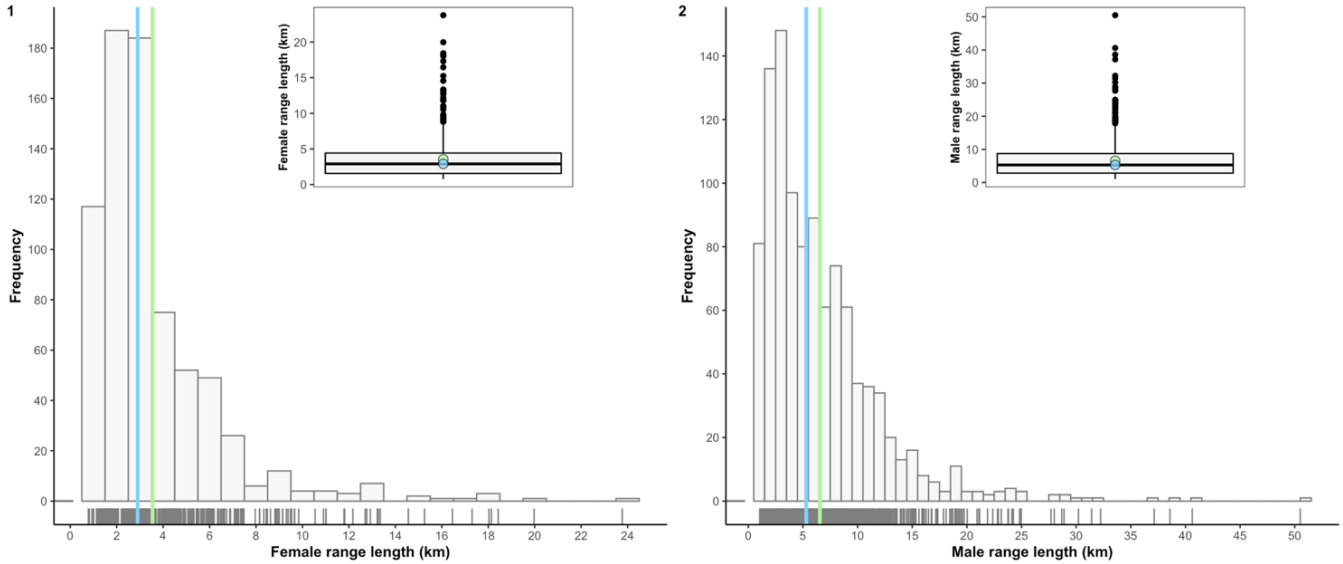

Figure D.2.1. Observed range length of each animal (maximum distance between any two detections) from black bear capture-recapture data collected across 77 study sites in Ontario, Canada from 2017-2019. Data represents female and male bears caught more than once. Vertical lines represent mean (green) and median (blue). For inset plots, whiskers extend 1.5 times the interquartile range from the boxes; coloured circles within boxes represent mean (green) and median (blue); black line within box represents median; black circle outside box represent outliers.

Table D.2.2. Pearson's correlation coefficients (*r)* of spatial covariates quantified across three different buffer sizes for male and female black bears in 77 study. Covariates includes percent forest types (coniferous, deciduous, mixed), percent agriculture land cover (crop), road density (road), mean and median human influence index (HII), and average harvest density (harvest). All covariates continuous except for average harvest density that has a discrete value for each study area.

Female			**Male**		
Covariates (buffer width in m)		***r***	**Covariate (buffer width in m)**		***r***
road (2900)	road (3190)	1.00	road (5300)	road (6870)	0.99
road (2900)	road (4430)	0.98	road (5300)	road (8740)	0.98
road (3190)	road (4430)	0.99	road (6870)	road (8740)	0.99
mean HII (2900)	mean HII (3190)	1.00	mean HII (5300)	mean HII (6870)	0.99
mean HII (2900)	mean HII (4430)	0.99	mean HII (5300)	mean HII (8740)	0.95
mean HII (3190)	mean HII (4430)	0.99	mean HII (6870)	mean HII (8740)	0.98
median HII (2900)	median HII (3190)	0.99	median HII (2900)	median HII (3190)	0.99
median HII (2900)	median HII (4430)	0.96	median HII (2900)	median HII (4430)	0.96
median HII (3190)	median HII (4430)	0.97	median HII (3190)	median HII (4430)	0.97
coniferous (2900)	coniferous (3190)	1.00	coniferous (5300)	coniferous (6870)	1.00
coniferous (2900)	coniferous (4430)	0.99	coniferous (5300)	coniferous (8740)	0.99
coniferous (3190)	coniferous (4430)	1.00	coniferous (6870)	coniferous (8740)	1.00
crop (2900)	crop (3190)	1.00	crop (5300)	crop (6870)	1.00
crop (2900)	crop (4430)	1.00	crop (5300)	crop (8740)	0.99
crop (3190)	crop (4430)	1.00	crop (6870)	crop (8740)	1.00
deciduous (2900)	deciduous (3190)	1.00	deciduous (5300)	deciduous (6870)	1.00
deciduous (2900)	deciduous (4430)	0.99	deciduous (5300)	deciduous (8740)	0.99
deciduous (3190)	deciduous (4430)	1.00	deciduous (6870)	deciduous (8740)	1.00
mixed (2900)	mixed (3190)	1.00	mixed (5300)	mixed (6870)	1.00
mixed (2900)	mixed (4430)	0.99	mixed (5300)	mixed (8740)	0.99
mixed (3190)	mixed (4430)	1.00	mixed (6870)	mixed (8740)	1.00
shrb grass (2900)	shrb grass (3190)	1.00	shrb grass (5300)	shrb grass (6870)	0.99

shrb grass (2900)	shrb grass (4430)	0.98	shrb grass (5300)	shrb grass (8740)	0.98
shrb grass (3190)	shrb grass (4430)	0.98	shrb grass (6870)	shrb grass (8740)	0.99
harvest (2900)	harvest (3190)	1.00	harvest (5300)	harvest (6870)	1.00
harvest (2900)	harvest (4430)	1.00	harvest (5300)	harvest (8740)	1.00
harvest (3190)	harvest (4430)	1.00	harvest (6870)	harvest (8740)	1.00

D. 3 Pearson's correlation coefficients density spatial covariates

Table D.3.1 Pearson's correlation coefficients for pooled and forest region (boreal and Great – Lakes St Lawrence [GLSL]) model covariates including percent forest types (coniferous, deciduous), road density (road), median human influence index (HII), and average harvest density (harvest). For each study area covariates were quantified across a 4430m m buffer and 8740m m buffer surrounding the arrays of detectors for male and females, respectively. Bold values $| r | \geq 0.7$

		Pooled models		**Forest region models**			
		Female	**Male**	**Female GLSL**	**Male GLSL**	**Female boreal**	**Male boreal**
road	HII	0.13	0.29	0.28	0.46	-0.16	-0.10
road	coniferous	-0.32	-0.34	-0.22	-0.16	-0.11	-0.19
HII	coniferous	-0.15	-0.21	0.15	0.25	-0.13	-0.15
road	deciduous	0.32	0.44	0.09	0.27	0.02	0.05
HII	deciduous	0.09	0.26	0.08	0.23	-0.14	-0.04
coniferous	deciduous	-0.54	-0.56	-0.54	-0.45	-0.36	-0.43
road	harvest	0.10	0.22	-0.02	0.14	-0.07	0.01
HII	harvest	0.44	0.45	0.69	0.59	0.29	0.29
coniferous	harvest	-0.36	-0.48	0.20	0.13	-0.38	-0.51
deciduous	harvest	0.41	0.49	0.11	0.20	0.33	0.45

D. 4 Point estimation of black bear densities

We conducted a SECR analysis with three years of genetic capture-recapture detection data to estimate female and male black bear density at each study area. We fit sex specific SECR models to 122 datasets from 65 of the study areas in a likelihood framework using the R package 'secr' (Efford 2020a). For study areas sampled across multiple years we only retained datasets from the first year of sampling. We defined the state space, excluding permeant waterbodies as non-bear habitat, for each study area as a 1km resolution raster that extended 20km around all traps and verified that using a 1km grid point spacing had negligible effects on density estimates. We used the function 'suggest.buffer' to verify that 20km was an appropriate buffer width; if a larger buffer was suggested this value was used. For the detection model we allowed g_0 to vary as a function of a trap-specific response (*bk)* and σ by sampling occasion (*t*) and linear time trend over occasions (*T*). We were not interested in examining spatial factors shaping density and therefore used a simple state model assuming constant density that was formulated as a homogeneous Poisson point process. Models were fit using a half-normal detection function and maximizing the conditional likelihood for proximity detectors and density was derived as a parameter using the Horvitz-Thompson-like estimator (see Efford et al. 2009). β parameter coefficient estimates and their standard errors (SE) were visually inspected for unreasonably large values that could indicate overparameterization or non-identifiability (Gimenez et al. 2011, O'Brien and Kinnaird 2011). We compared the fit of converged candidate models using AIC_c (Hurvitch and Tsai 1989, Burnham and Anderson 2002) and used the top ranked model to estimate density.

D. 5 Chapter 4 comparison of SECR candidate models for pooled datasets

Table D.5.1. Summary of AIC_c model selection criterion for SECR models fitted to female and male black bear capture-recapture surveys from 65 study area in Ontario, Canada from 2017–2019. *K* denotes the number of parameters; LL the log likelihood; W_i the AIC_c weight. Detection covariates includes trap-specific (*bk*) learned behavioural response, linear time trend (*T*), and forest region (*for_reg*). Density covariates include harvest density (*harvest*), road density (*road*), human influence index (*HII*), and percent coniferous and deciduous forests (*con_F*, *dec_F*); "." indicates parameter held constant.

Sex	Model form	*K*	LL	AIC_c	ΔAIC_c	W_i
Female	D(*road* + *HII* + *harvest* + *dec_F* + *con_F*) g_0(*bk*) σ(*for_reg*+ *T*)	11	-13296.20	26614.60	0.00	1.00
	D(*road* + *HII* + *harvest* + *dec_F* + *con_F*) g_0(*bk*) σ(*T*)	10	-13321.72	26663.61	49.01	0.00
	D(*road* + *HII* + *harvest* + *dec_F* + *con_F*) g_0(*bk*) σ(*For_reg*)	10	-13324.00	26668.17	53.57	0.00
	D(*road* + *HII* + *harvest* + *dec_F* + *con_F*) g_0(*bk*) σ(.)	9	-13349.91	26717.94	103.35	0.00
	D(*road* + *HII* + *harvest* + *dec_F* + *con_F*) g_0(.) σ(*For_reg* + *T*)	10	-13873.64	27767.44	1152.84	0.00
	D(*road* + *HII* + *harvest* + *dec_F* + *con_F*) g_0(.) σ(*T*)	9	-13933.73	27885.58	1270.98	0.00
	D(*road* + *HII* + *harvest* + *dec_F* + *con_F*) g_0(.) σ(*For_reg*)	9	-14183.64	28385.41	1770.81	0.00
	D(*road* + *HII* + *harvest* + *dec_F* + *con_F*) g_0(.) σ(.)	8	-14243.21	28502.53	1887.93	0.00
Male	D(*road* + *HII* + *harvest* + *dec_F* + *con_F*) g_0(*bk*) σ(*For_reg* + *T*)	11	-21065.71	42153.56	0.00	1.00
	D(*road* + *HII* + *harvest* + *dec_F* + *con_F*) g_0(*bk*) σ(*T*)	10	-21073.27	42166.65	13.09	0.00
	D(*road* + *HII* + *harvest* + *dec_F* + *con_F*) g_0(*bk*) σ(*For_reg*)	10	-21110.94	42242.00	88.44	0.00
	D(*road* + *HII* + *harvest* + *dec_F* + *con_F*) g_0(*bk*) σ(.)	9	-21117.77	42253.64	100.08	0.00
	D(*road* + *HII* + *harvest* + *dec_F* + *con_F*) g_0(.) σ(*For_reg* + *T*)	10	-21676.39	43372.90	1219.34	0.00
	D(*road* + *HII* + *harvest* + *dec_F* + *con_F*) g_0(.) σ(*T*)	9	-21689.27	43396.64	1243.08	0.00
	D(*road* + *HII* + *harvest* + *dec_F* + *con_F*) g_0(.) σ(*For_reg*)	9	-21891.15	43800.40	1646.84	0.00
	D(*road* + *HII* + *harvest* + *dec_F* + *con_F*) g_0(.) σ(1)	8	-21900.87	43817.82	1664.26	0.00

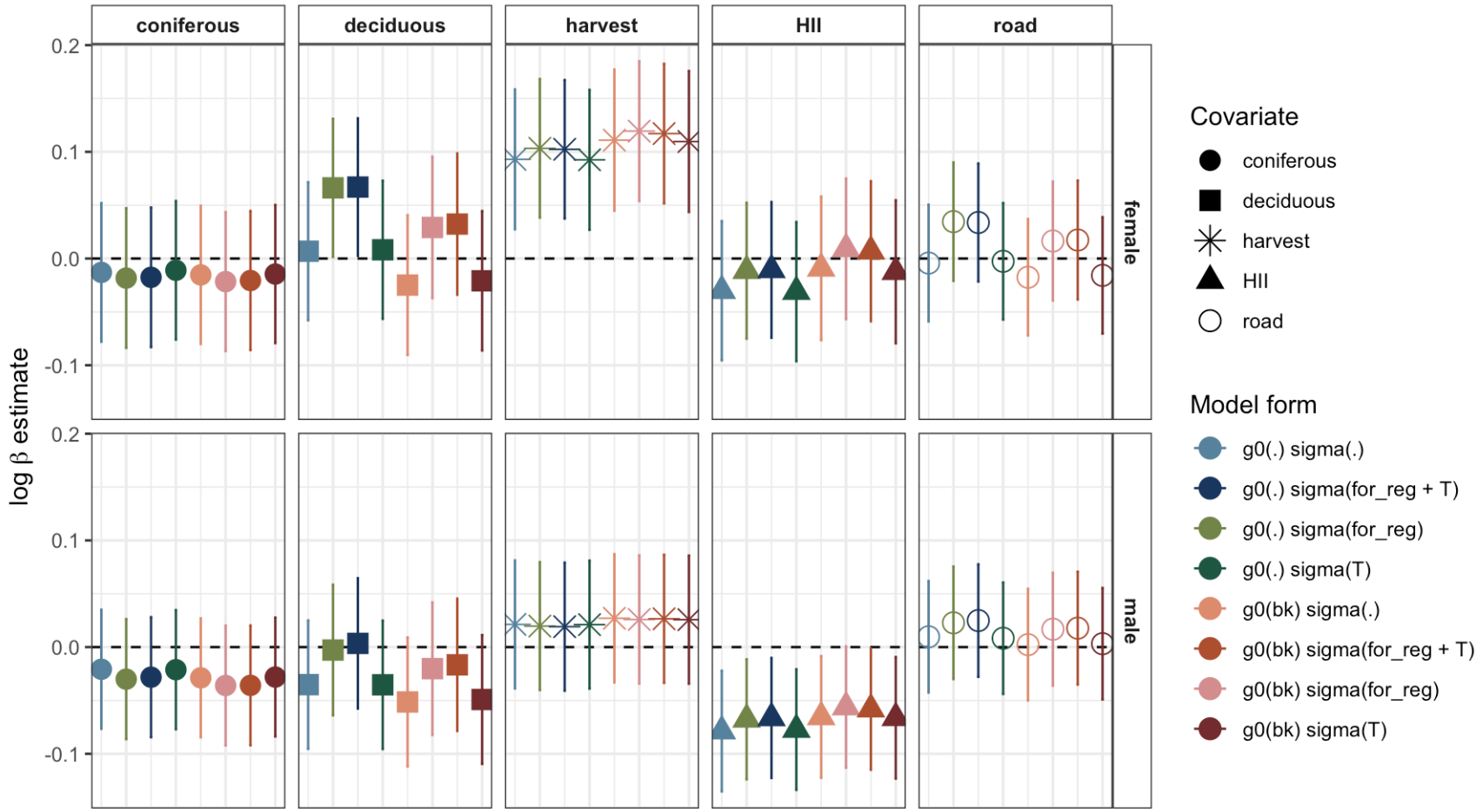

Figure D.5.1. Log-scale effect size (β parameter estimates) of female and male candidate SECR models with density covariates including percent forest types (coniferous, deciduous), human influence index (HII), road density (road) and harvest density (harvest). β estimates standardized to allow for covariate comparison within sex. The effect size indicates the change in the baseline density (bears/hectare) on the log scale for one unit change in the covariates value. Vertical lines indicate 95% confidence intervals and dashed black horizontal lines no effect of a covariate on density. Baseline detection probability g0 varies by trap-specific (*bk*) learned behavioural response and spatial scale parameter sigma by linear time trend (*T*) and forest region (*for_reg*); "." indicates parameter held constant.

D. 6 Chapter 4 Ontario black bear harvest summary

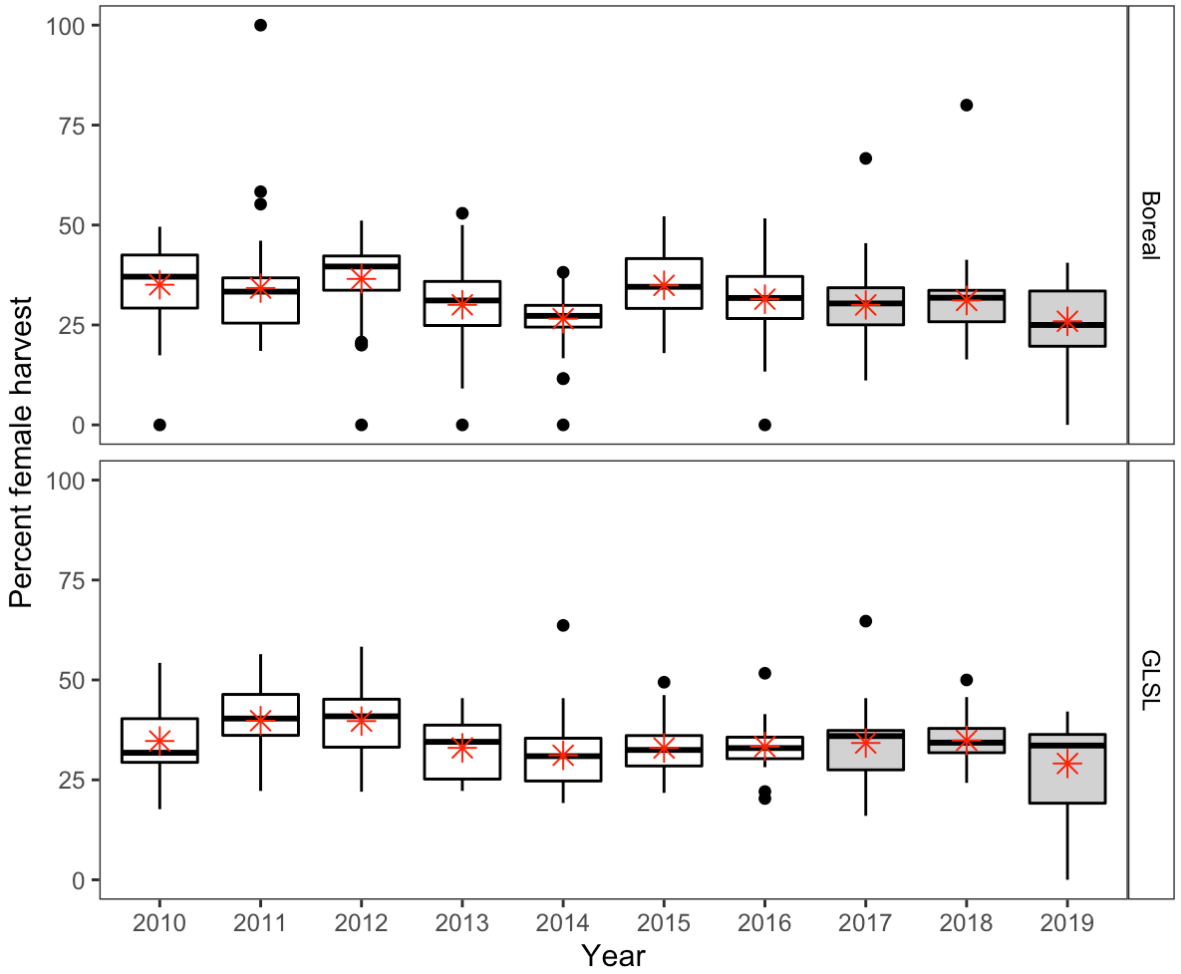

Figure D.6.1 Percent female harvest across 65 WMU in the boreal and Great Lakes – St Lawrence (GLSL) in Ontario Canada, from 2010-2019. Years of MNRF black bear surveys indicated by gray shading in boxes and seven years prior by white boxes. Thick horizontal black lines and red stars in the boxes indicate the median and mean, respectively, and black dots represent outliers.